The Impact of Assimilable Organic Carbon on Biological Fouling of Reverse Osmosis Membranes in Seawater Desalination

A Thesis

Submitted to the Faculty

of

Drexel University

by

Lauren A. Weinrich

in partial fulfillment of the

requirements for the degree

of

Doctor of Philosophy

February 2015

DEDICATION

Dedicated to Robert L. Weinrich, Sr. (August 14, 1937 – April 30, 2014) who declined a career in chemical engineering to happily spend his life as a talented German baker, devoted husband, and loving father. His strength and wisdom lives on. Thank you for the life lessons and instilling in me the character and confidence to meet any challenge.

ACKNOWLEDGEMENTS

I am extremely grateful to my advisor Dr. Charles N. Haas for facilitating my personal and professional goal that this degree represents. I am honored that he provided the support in this academic pursuit; his depth of knowledge and vision added tremendous value to this project and my experience as his advisee. I thank my committee for expanding my academic interests into relevant industry experience in environmental engineering, sustainable treatment, and scientific applications. To my committee: Dr. Haas, Dr. Mark LeChevallier, Dr. Patrick Gurian, Dr. Mira Olson, and Dr. Sabrina Spatari, thank you guiding my studies in the classroom and in the water industry for the benefit of my future pursuits to overcome water scarcity challenges and maintain focus on environmental sustainability and scientific integrity. I also thank my supervisors Drs. Mark LeChevallier and Orren Schneider for mentoring me and the entire I&ES group for their encouragement. Dr. Eugenio Giraldo introduced the idea that pursuing my doctorate and working did not have to be mutually exclusive, and I am glad for the recommendation.

I am indebted to the teams at American Water-Acciona Agua LLC, West Basin Municipal Water District and Hydranautics for providing data and facilitating sample collection. I am extremely gracious for the assistance and hospitality of Susan MacPherson, Aleix Martorell Cebrián, Jon Sandler and staff, Robin Gagnon, and Chris Owen during my months of work in Tampa. Thank you to Marina Kreminskaya (American Water) for her laboratory support in Delran and Ed Basgall (Drexel University) for sharing his microscopy expertise.

I thank my family, fiancé, and friends for their unwavering support through the good times with fun and laughter and the inevitable dreadful ones. The ebb and flow of life is more fun in the company of my loved ones. Thank you for being there, and thank you for being a friend.

This project was funded as an unsolicited proposal by the Water Reuse Research Foundation. I am grateful to the Foundation and the project advisory committee that assisted in providing the industry perspective for the successful completion of this project.

TABLE OF CONTENTS

LIST OF TABLES

LIST OF FIGURES

ABSTRACT

The Impact of Assimilable Organic Carbon on Biological Fouling of Reverse Osmosis Membranes in Seawater Desalination
Lauren A. Weinrich

Biological fouling is neither well understood nor consistently prevented and continues to be a challenging problem in seawater reverse osmosis (SWRO) desalination. Biofouling occurs from bacterial proliferation and leads to operations and water quality challenges. Despite use of biocides (i.e., disinfectants) to control microbial growth, biofouling has not been well-managed in the seawater desalination industry. This project used a biological assay, the assimilable organic carbon (AOC) test to evaluate pretreatment effects on the nutrient supply. The AOC test provided a useful surrogate measurement for the biodegradability or biofouling potential of RO feed water. Biofouling observed in full scale and in controlled conditions at the bench- and pilot-scale resulted in correlations between AOC and operational effects, such as increased differential pressure and decreased permeate flux through the membrane. Increased differential pressure was associated with RO membrane biological fouling when the median AOC was 50 µg/L during pilot testing. In a comparison test using 30 and 1000 µg/L AOC, fouling was detected on more portions of the membrane when AOC was higher. Biofilm and bacterial deposits were apparent from scanning electron microscope imaging and biomass measurements using ATP. Chemicals used in seawater RO plants such as antiscaling, cleaning, and dechlorinating agents increased AOC, and therefore the biodegradability of the seawater. AOC was also a byproduct of reactions with commonly used disinfectants, such as chlorine, chlorine dioxide and ozone. AOC was increased by 70% in seawater with 1 mg/L humic acid and a chlorine dose of 0.5 mg/L Cl_2. Increases in biodegradability and AOC were often not mirrored by a the total organic carbon (TOC) measurement; TOC varied less than 3%. TOC is not an informative tool for the plant

operators to predict biofouling potential, which is problematic because it is often the only organic carbon parameter used in SWRO monitoring. Polyphosphonates and polymer-based antiscalants increased AOC less than 30 µg/L; however, phosphate-based antiscalants increased AOC levels nearly 100 µg/L. Depending on the active chemical or inherent impurities, antiscalants may increase biofouling potential of the RO feed despite the targeted application for controlling inorganic fouling. Better operational practices such as removing the chlorine residual prior to dosing the antiscalant would alleviate the adverse effect of AOC byproduct production. TOC removal efficiency is typically very poor and the pretreatment impacts on AOC levels should be controlled in SWRO plants that experience biological fouling problems on the RO membranes. Besides creating more effective organic carbon removal, minor pretreatment configurations and monitoring programs in the plants are recommended to help control AOC levels in the RO feed.

CHAPTER 1: BACKGROUND AND LITERATURE REVIEW

Desalination using seawater reverse osmosis membranes (SWRO) is a sustainable solution for meeting drinking water supply needs and this application continues to expand globally. However, SWRO still faces expensive challenges from membrane fouling. Of the various types of fouling, biological growth and deposition of bacteria on the reverse osmosis (RO) membranes (i.e., biological fouling) continues to be difficult to prevent or control. SWRO biological fouling results in high operating expenses and inhibits efficient treatment. In preparing the approach to research how to reduce or control fouling, evidence from a review of the literature and the desalination industry's experience pointed to the necessity of having a tool that provides predictive capability for biological fouling.

1.1 Background

A literature review for assessing the recent development of measurement and modeling techniques for reducing reverse osmosis membrane fouling has been published (Weinrich et al., 2013). Portions of that review are presented to describe the current science for predicting and mitigating biological fouling (biofouling) and reinforce the lack of effective control mechanisms to accommodate the industry's need. SWRO biofouling is widely regarded as a critical area that requires additional research in the seawater desalination industry. Biofouling, caused by microbial growth on membranes, is not well managed. Industry personnel and researchers reported that an essential need exists for better biodegradable organic matter (BOM) monitoring and measurement tools to predict fouling (Voutchkov 2010; Amy et al. 2011; Veerapaneni et al. 2011). Some advances in fouling prediction using data modeling show promise although the testing has not been conducted in membrane applications for seawater desalination. Advanced computing capability and complex modeling approaches for fouling prediction have time and cost limitations that may be inhibiting factors.

1.2 Desalination

In the United States, two-thirds of desalination capacity is used for municipal water supply (Carter 2011). Desalination is on the rise and the United States is currently leading in the number of desalination projects that are planned or in construction. The rise in desalination was forecast from the current level of 2,324 million gallons per day (MGD) of contracted desalination capacity up to 3,434 MGD by 2016 in the United States (Gasson et al. 2010). Desalination applications include thermal and membrane processes. Globally, seawater is desalinated using thermal distillation or crystallization but these are often energy intensive and more expensive than reverse osmosis (RO). In the United States, 96% of desalinated water is produced by RO (Drew 2010). Although SWRO membrane desalination can be a costly alternative to freshwater sources for drinking water, advances in membrane technology and performance, market demand, and energy recovery have driven costs down in the past few decades (WateReuse Association 2011).

1.3 Reverse Osmosis

Reverse osmosis membrane separation is designed to remove ions and produce pure water. The most common configuration of RO membranes used for desalination are flat sheet membranes that are wound in a spiral ("spiral wound") encased in fiberglass tubes. Typically these are connected in series in pressure vessels and configured in an array. Figure 1 shows the configuration of a spiral wound RO membrane element.

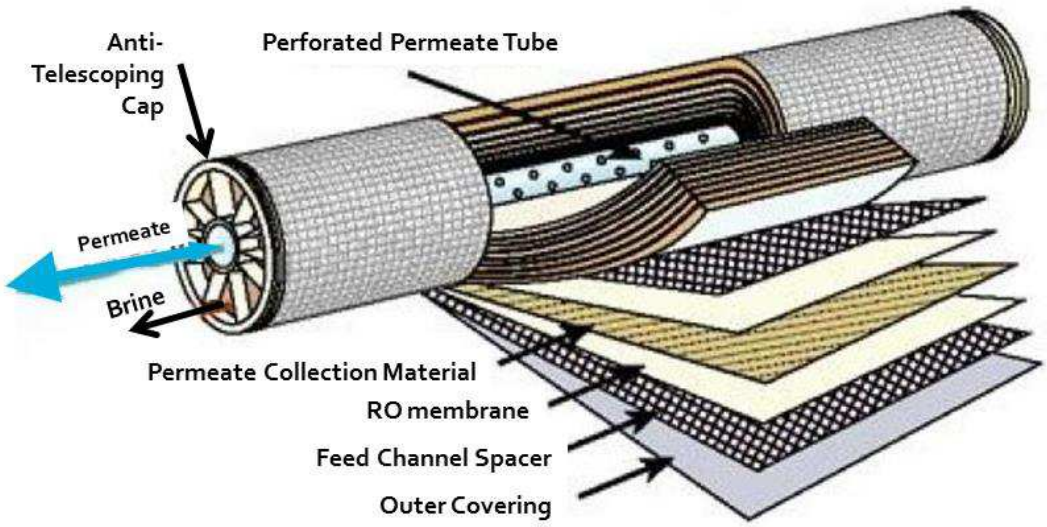

Figure 1 Spiral Wound Reverse Osmosis Membrane (Lenntech 2014). Seawater enters one side, on the opposite end RO permeate and brine are collected in separate streams.

Reverse osmosis membranes are semipermeable with pore size < 0.001 µm and are capable of removing total dissolved solids from high ionic strength water, e.g. seawater. Pretreatment assists in reducing the contaminants that enter the RO feed. Treatment upstream of RO membranes is designed to remove competing substances to protect the RO membranes from fouling caused by particles, inorganic salts, and organic compounds. Seawater RO plants are typically operated to produce a constant amount of permeate through the membranes, i.e., flux. Flux is the volume of water produced through an area of membrane surface over a unit of time, e.g. liters per square meter per hour or gallons per square foot per day. Driving pressure is applied to the RO feed to overcome the osmotic pressure of the salt water and produce fresh water; seawater RO plants typically operate in the range of 800 – 1000 psi. As the membranes become fouled by the accumulation of contaminants on the membrane surface or in the membrane pores, higher pressures are applied in order to compensate for the impeded flow through the membrane. High pressure pumps are responsible for a significant portion of energy usage in SWRO.

Therefore increased energy demand and associated operational costs are a direct result of RO membrane fouling. In addition, other operation and maintenance (O&M) costs are incurred from chemical usage, cleaning frequency, and membrane replacement to address reversible and irreversible fouling on RO membranes. Prediction, prevention, and removal of fouling continue to pose an expensive challenge. This project reinforces the need to address shortcomings in desalination O&M and optimize the SWRO process.

1.4 Membrane Fouling

Membrane fouling results from the accumulation of materials on, in, or near the membrane (Taylor & Weisner 1999). The result of this accumulation has long been recognized as a major problem for RO facilities because it can result in a decline in water production over time for constant pressure operations or an increase in required feed pressures (Zhu & Elimelech 1995). Because fouling issues lead to a significant economic burden on membrane plants, the future of desalination is partly driven by the economic viability of membranes and their application, including low pressure and RO membranes. Therefore, a successful future for membrane applications will be realized by having a clear understanding of fouling mechanisms and developing essential tools for quantification and prevention. Fouling is generally documented as one of four types: scaling from precipitation of sparingly soluble salts, plugging caused by deposition of particulate matter, adsorption of organic matter, and biological fouling from the growth of microorganisms on membrane surfaces (Zhu & Elimelech 1995; Duranceau 2007).

Solution chemistry, hydrodynamic conditions, and membrane properties are the major drivers of membrane fouling. Membrane fouling may be further classified as to whether it is reversible or irreversible. Reversible fouling is caused by physical separation mechanisms that induce cake formation, deposition of particles, and plugging of pores (Hilal et al. 2006). Irreversible fouling occurs when dissolved compounds interact with the membrane material and cannot be removed by chemical or physical cleaning.

1.4.1 Inorganic Salt Precipitation

The precipitation of sparingly soluble salts onto the membrane surface occurs as dissolved materials increase in concentration on the feed side of the membrane, until the point at which the solubility of the salt is exceeded in the reject water, or brine, and precipitation occurs. Also known as scaling, this type of fouling occurs only in high pressure membranes such as nanofiltration and RO. Low pressure membrane separation by microfiltration (MF) and ultrafiltration (UF) does not concentrate salts in the reject stream and therefore scaling does not occur. Scaling is often attributed to precipitation of the polyvalent cations (calcium, magnesium, barium, and strontium) and anions (silicate, sulfate, carbonate, and phosphate). Typically, scaling is mitigated with chemical and physical pretreatment (Yang et al. 2009). Chemical pretreatment of inorganic scaling caused by calcium salt precipitates can be managed with pH adjustment or antiscalant addition (Pontié et al. 2005). However, impure mineral acids often used as antiscalants have been shown to contain BOM (Amy et al. 2011) that can promote biological fouling (Vrouwenvelder et al. 2000; Vrouwenvelder & Van Der Kooij 2001).

Chemicals are added prior to membrane separation to reduce the precipitation of sparingly soluble salts. Antiscalant chemicals in RO applications typically contain two or more phosphonate groups, called polyphosphonates. The ability of a chemical to reduce scale formation is related to its chemical structure, molecular weight, active functional groups, and solution pH (Shih et al. 2004). Molecular weight is reported to range from 1,000 to 3,500 and typically consist of polycarboxylates, polyacrylates, polyphosphonates, and polyphosphates. Phosphonates contain a carbon-phosphorus bond that must be broken for microbial metabolism, and bacterial degradation pathways have been studied in naturally occurring phosphonates. With the increasing use of artificial phosphonates in industry and their natural occurrence in the environment, phosphate-containing chemicals provide an essential nutrient supply. In addition, the presence of

phosphate in waste streams and concentrates has impacts in areas of discharge that may be associated with algal blooms. Companies are developing environmentally friendly antiscalants to avoid this issue, some of which are free of phosphates (Musale et al. 2011). Antiscalants and mineral acids have been shown to increase biofouling potential (Vrouwenvelder et al. 2000; Weinrich et al. 2011), and impurities contained in the treatment chemicals are also potential nutrient sources. Many of the chemical suppliers reserve proprietary rights to the chemical composition of the antiscalants, and therefore specific chemical formulations are not disclosed. Material Safety and Data Sheets (MSDS) lack Chemical Abstract Service (CAS) numbers and only provide general information. For example, the MSDS for VITEC® 5100 NSF (Avista Technologies, San Marcos, CA), an antiscalant used at a brackish water desalination plant, provides 'phosphonic acid derivative compound' as part of the mixture. This lack of transparency makes it challenging to predict the biodegradability and potential for biological fouling. It should be noted that under a new program by the Occupational Safety and Health Administration's (OSHA) Hazard Communication Standard, the United States will be aligned with the Globally Harmonized System of Classification and Labeling of Chemicals (GHS). This will impact the way chemicals are labeled and the MSDS will be rebranded as Safety Data Sheets. However, at the time of this research chemical distributors still ship products labeled under the old system until December 1, 2015. Prior desalination configurations used sodium hexametaphosphate (SHMP) as an antiscalant, but it is no longer used because SHMP was shown to be a food source for bacteria and resulted in biofouling (Alawadhi 1997; Voutchkov 2010). A commonly reported antiscalant in the cooling water industry is 2-phosphonobutane-1,2,4-tricarboxylic acid (PBTC) and it has been extensively examined on a molecular level (Demadis et al. 2005). PBTC contains phosphate and carboxylic acid functional groups, which are common in other antiscalant chemicals and important nutrient reserves for bacterial growth. Pathways for cleaving the carbon-phosphate bond present in these chemicals have been investigated (Huang et al. 2005) and

bacteria contain specific genes capable of this degradation, including some *Vibrio* species. The genus *Vibrio* contains biofilm-forming species that have been detected on a biologically-fouled SWRO membrane (Zhang et al. 2011). Biofouling potential, measured using the bioluminescence assimilable organic carbon (AOC) test and the marine organism *Vibrio harveyi*, increased in samples collected after antiscalant addition at the Fujairah desalination plant (Schneider et al. 2011; Weinrich et al. 2011). The antiscalant application was low at 0.5 mg/L. In general, antiscalant degradation and assimilation by bacteria in seawater matrices has not been clearly elucidated. Other phosphonate chemicals include amino trimethylene phosphonic acid (ATMP), 1-hydroxy ethylidene-1,1-diphosphonic acid (HEDP), and proprietary phosphino succinic oligomers. For HEDP and PBTC, 0.5–2% of the chemical composition may include phosphoric acid and phosphorous acid. Other common classes of antiscalant chemicals include polycarboxylates, polyacrylates, and organic acids. Citric acid used in SWRO pretreatment was shown to be an assimilable food source for *Vibrio harveyi* used in the AOC test (Weinrich et al. 2011).

Mitigating the occurrence of scaling and inorganic fouling without creating conditions that may exacerbate biological growth is emerging as a crucial area for managing efficient SWRO operation. Chemical addition during pretreatment requires additional chemistry and microbiology research to address a collective approach to reducing fouling potential. Ultimately the nutrients available for microbial growth should be controlled to minimize biological fouling. Understanding and preventing such secondary effects requires research specifically targeted for SWRO design and processes.

1.4.2 Colloidal or Particulate Fouling

Particulate fouling occurs as water permeates through membranes that contain suspended materials. Particles have been recently categorized as either suspended or colloidal (Voutchkov 2010). Particle sizes less than 1 μm are considered 'colloids', but 90% of 'suspended' particulate foulants in SWRO are >1 μm (Voutchkov 2010). Suspended foulants may include organic and inorganic particles in seawater, for example plankton, silt, and other fine debris. Filtration of the seawater prior to the RO membranes can efficiently remove suspended materials. Colloidal particles are naturally occurring inorganic and organic compounds and range in size from 0.001 to 1 μm. These materials are concentrated during physical membrane separation and since they may not pass through with the concentrate, then fouling and a subsequent decline in flux occurs. Colloid materials may either deposit within the membrane pores (known as pore blocking) or form a cake as suspended particles accumulate. SWRO manufacturers recommend that membrane feed turbidity is < 0.1 NTU, silt density index (SDI_{15}) < 4, and zeta potential > - 30 microvolts (mV) to avoid colloidal fouling (Voutchkov 2010). From measurements made in the North Atlantic and Northwest Pacific oceans, small colloids ranging in size from 0.005 to 0.200 μm are identified as the most abundant particles in seawater and concentrations were nearly 10^9 particles per milliliter (Wells & Goldberg 1993). A recent publication by Tang et al. (2011) provides a comprehensive review of the existing literature related to mechanisms and factors controlling this type of fouling in wastewater and freshwaters.

Colloid dynamics vary greatly in seawater and aggregate formation has been observed. Aggregate formation may occur either by reaction-limited colloid aggregation (RLCA) or by diffusion-limited colloid aggregation. RLCA formations have more condensed structures and distribution occurs in both near-shore and offshore environments (Wells & Goldberg 1993). In addition, biopolymers have been found in colloidal aggregates. Literature reviews suggest one of

the results of aggregation to be that organic matter is packaged which increases biodegradability of carbon in the water column. Colloids from the Santa Monica basin (California) also share similarities to soil-derived fulvic acids as determined through transmission electron micrographs (Wells & Goldberg 1991). The granular size of 0.002 to 0.005 μm determined in these studies corresponds to ~10 kDa which is in the range for dissolved organic carbon (DOC) fractions measured in seawater. Molecular weights (MW) of proteins, amino acids, sugars, and other biopolymers range from 0.2 to 200 kDa. NF and RO are generally best ranked for removal of similarly sized chemicals. It should be noted that in addition to naturally occurring colloids, there are also anthropogenic colloid sources such as petroleum derivatives. Influences at the intake from storm drains and urban runoff, wastewater treatment plant discharge, or point source pollution from ships in port areas introduce anthropogenic colloids.

1.4.3 Organic Fouling

Organic fouling was reported to be most common in SWRO desalination (Veerpaneni et al. 2011) and 40% of RO permeability decline is attributed to a combination of organic and biological fouling. These two types are interrelated because of the inherent relationship between organic matter directly responsible for fouling of the membrane, and the hypothesis that organic matter present in RO feed provides substrate for biological growth. Dissolved organic carbon (DOC) has been investigated for its inherent content that is responsible for membrane fouling and characterized by molecular weight (MW) or size (in nanometers). Analytical capabilities for measuring organic matter in a water sample is discussed in section 1.5.1 and reminds the reader that defining the fractions of organic carbon responsible for fouling are at best operational definitions given the available analytical measurement techniques. Traditional approaches for predicting organic fouling potential include DOC, UV absorbance, and color; however, fouling rates do not correlate with these parameters (Amy et al. 2011). Organic matter in seawater was

reported to be 24% high MW DOC (1–100 nm) and about 75% low MW DOC (<1 nm); the other 1% was identified as particulate organic carbon (Benner et al. 1997). Given that RO membrane pores are < 0.001 μm, high molecular weight DOC and particulates would be retained by the RO membrane, since they would be too large for removal in upstream pretreatment such as ultrafiltration (UF) or microfiltration (MF). UF and MF membranes pore sizes are from 0.01 to 0.05 and 0.1 to 0.5 μm, respectively. Studies have shown that UF membranes do not achieve significant removal of marine natural organic matter (Tansakul et al. 2010). Opportunities exist for either breaking NOM down into smaller fractions that can be removed by biological pretreatment, or some other combination of organic absorption and removal. These approaches are discussed in more detail following bench-scale investigations presented in this study.

1.4.4 Biological Fouling

Biological fouling (biofouling) is neither well understood nor consistently prevented and continues to be a challenge in SWRO membrane separation processes (Griebe & Flemming 1998; Vrouwenvelder et al. 2000; Vrouwenvelder & Van Der Kooij 2001; Pang et al. 2005; Kumar et al. 2006). The growth of microorganisms into a biofilm on the membrane surface adds to the expense of SWRO treatment. Decreasing permeate flux, increasing pressure drops in the RO modules, increasing salt passage, and irreversible damage to the RO membrane are all issues associated with biofouling. Bacterial communities in the biofilms release extracellular polymeric substances (EPS) which provide an area for additional bacteria to proliferate. EPS present in the biofilm (composed of EPS and bacteria) account for 50 to 90% of the biofilm total organic carbon (TOC) (Matin et al 2011). Other naturally-occurring or anthropogenic biopolymers can contribute to biofouling, as well as assimilable organic carbon (AOC) provides a food source that enables bacteria to proliferate. Chemicals introduced into the treatment process, such as impure acids, phosphate-based scale inhibitors, and oxidants may also exacerbate biofouling. The research

presented in this dissertation was designed to address the hypothesis that oxidative reactions between disinfectants and DOC may be similar to that of drinking water treatment. Primary oxidation during drinking water treatment through the application of ozone changes the structure of NOM into smaller, polar, oxygenated compounds (von Gunten 2003). Van Der Kooij (1986) showed that AOC concentrations increased in water samples treated with increasing chlorine doses. In a similar study, Hambsch & Werner (1993) reported higher biodegradability of humic substances after chlorination. LeChevallier et al. (1992) reported that chlorination can increase AOC levels depending on the point of chlorine application. These effects have been extensively investigated in surface and groundwater matrices used for drinking water, but the effects of disinfection with specific regard to production of BOM is largely unknown in seawater and brackish water matrices used for RO desalination.

Red tides are highly destructive events that can occur when red-pigmented marine algae rapidly increase in concentration, called an algae bloom. Blooms can severely increase turbidity of seawater; however, the release of organic material, algogenic organic matter (AOM), is also a major concern. Dinoflagellates are generally recognized as most frequently responsible for marine algal blooms. *Karenia brevis* and *Noctiluca scintillans* are examples of algae that occur in seawater and are associated with red tides, and *Auerococcus anophagefferens* is associated with brown tides (Edzwald & Haarhoff 2011). An algal bloom may have algae counts that range from 10^3 to 10^6 #/mL; typical concentrations are less than 10^3 #/mL.

Transmembrane pressure and hydrodynamic shear forces can cause algal cell lysis and lead to release of intracellular organic matter (IOM) in RO treatment, thereby increasing soluble and highly biodegradable AOM (Ladner et al. 2010). AOM is composed of acids, proteins, simple sugars, anionic polymers, negatively charged and neutral polysaccharides (Edzwald & Haarhoff 2011). AOM provides a rich substrate for bacterial growth, thereby exacerbating membrane

biofouling (Ladner et al. 2010). In general, harmful algal blooms are being increasingly recognized for their often detrimental impacts on RO desalination facilities. Future research is needed to anticipate and mitigate the impacts of algal blooms in geographic regions for RO facility design and operational efficiency (Caron et al. 2010).

1.5 Biological Fouling Prediction

Seawater desalination facilities commonly measure silt density index (SDI) or a similar but slightly more advanced modified fouling index (MFI) to meet RO manufacturer requirements and use the data for tracking fouling. These tests predict particulate fouling; they are based on plugging of a 0.45-micron (μm) membrane over a defined time interval (often 15 min). However, these test conditions are not predictive of either organic adsorption or biological growth. The potential for mineral scaling of calcium carbonate to occur may be predicted using Langelier Saturation Index (LSI) and the Stiff and Davis Index (Voutchkov 2010). Mineral scaling is fairly easy to manage and there are sufficient indexes for measuring the potential; however, management with antiscalants or impure acids should be carefully chosen as these solutions have been shown to introduce nutrients available for microbial growth and proliferation. The most common or promising techniques for measuring organic carbon and biodegradable carbon in seawater are discussed in the following section as they relate to the prediction of biofouling potential.

1.5.1 Organic Carbon Quantification

Obtaining the most appropriate measurement to represent the biodegradability of RO feed water is a challenge; available techniques such as total and dissolved organic carbon and UV absorbance have been used with little success for predicting biofouling potential. Combustion (Standard Method 5310 B) and chemical oxidation (SM 5310 C) techniques (APHA 2005) measure the particulate and dissolved or suspended organic carbon, collectively referred to as

TOC (Figure 2). Alternatively, the sample may be filtered through 0.2 – 0.7 µm pore size filters and the organic carbon in the filtrate would be operationally defined as dissolved organic carbon (DOC). Although DOC is more useful in water treatment to describe the carbon that would pass through microfiltration or ultrafiltration pretreatment, the results still lack specificity for the biodegradable fraction. The biodegradable fraction of TOC which is easily assimilated is operationally defined as AOC and is described later in this section.

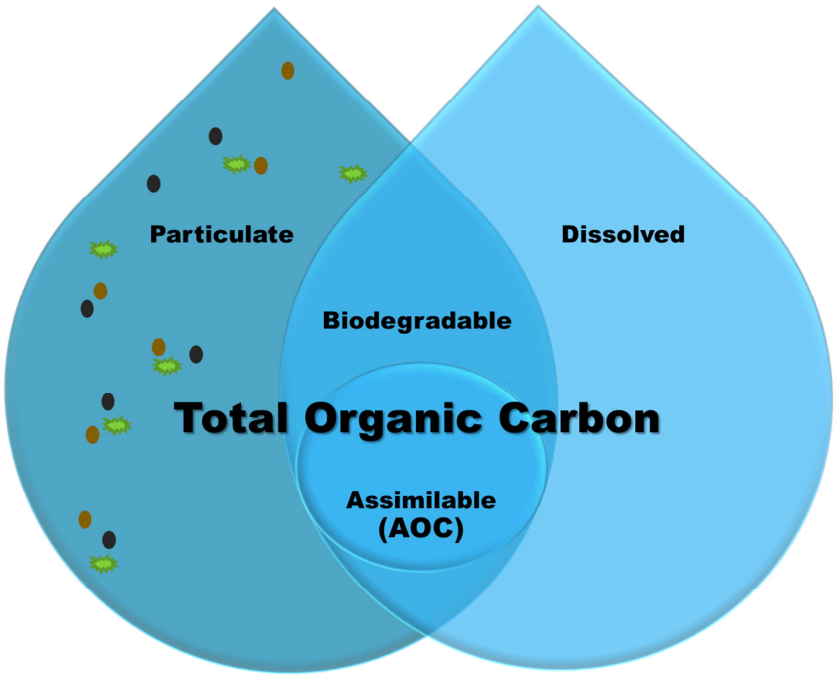

Figure 2 Relationship between organic carbon fractions in water. Particulate (colloids, algae, solids etc.) and dissolved fractions are collectively referred to as total organic carbon (TOC) and include subfractions which are operationally defined by the treatment as dissolved or biodegradable. Of the dissolved fraction, the assimilable organic (AOC) test measures the easily biodegradable fraction.

Given that biological growth responsible for fouling requires bacteria and nutrients in combination, and disinfection has not been successful for removing all of the bacteria in the RO feed, it would be prudent to evaluate the biodegradability of the organic carbon. Often however,

only the total organic carbon (TOC) is measured with some guidelines for pretreated seawater proposed to minimize fouling. TOC only reflects DOC concentration when other particulates (e.g. algae) are not present. TOC levels <0.5 mg/L may be sufficient to avoid biofouling with evidence that seawater above 2 mg/L may result in biofouling (Voutchkov 2010; Edzwald & Haarhoff 2011). TOC typically ranges from 2 to 5 mg/L (Edzwald & Haarhoff 2011), although levels can be much greater. In the recent Water Research Foundation report by Schneider et al. (2011), TOC ranged from <1 to >10 mg/L at desalination intakes from U.S. and international facilities. Intake TOC has also been influenced by algal blooms and aquatic humic matter found in rivers. Algal organic matter (AOM) mentioned previously is highly biodegradable, although it is often not measured using surrogates and individual chemical analyses to quantify are tedious. Fluorescence emission and excitation matrices (FEEM) are promising for qualifying changes at the seawater intake, though quantification would require additional development.

UV absorbance at 254 nm (UV_{254}) is often used as a surrogate for DOC. Specific UV absorbance (SUVA) has been extensively used in drinking water treatment to evaluate the characteristic of organic carbon in source waters for inclusion into monitoring and chemical pretreatment models. SUVA is the UV absorbance per unit concentration of DOC. Edzwald & Haarhoff (2011) adapt conventional drinking water guidelines to seawater in the following manner: (1) SUVA >4 L/mg-m indicates that NOM is mainly aquatic humic matter, (2) SUVA of 2–4 L/mg-m indicates that NOM is a mixture of AOM and aquatic humic matter, and (3) SUVA <2 L/mg-m indicates the NOM is composed primarily from AOM.

Liquid chromatography – organic carbon detection (LC–OCD) is an option for determining NOM having lower SUVA (Amy et al. 2011). These analyses provide information for NOM present at various MW often characterized from high to low molecular weight: biopolymers, humics, building blocks, low MW acids, and neutrals. Separation is based on size-

exclusion chromatography (SEC) followed by multidetection with organic carbon, UV_{254}, and organic bound nitrogen. LC–OCD was originally used for evaluating organic matter transformation in freshwater treatment, but has been modified for the high ionic strength of seawater.

Using a bulk parameter for quantification of biodegradable organic carbon that is readily available for microbial consumption, or assimilation have been investigated for providing information that traditional analytical chemistry approaches lack. The assimilable organic carbon (AOC) test has been applied extensively in drinking water and reclaimed waste water matrices. Until recently, the available procedures were only developed for fresh water applications. The AOC test is a microbial assay (bioassay) that traditionally uses two strains of bacteria, P17 and *Spirillum* NOX. Bacterial growth is monitored in a pasteurized water sample until maximum growth occurs (N_{max}). The AOC bioassay is considered to be an indicator for the biological growth potential of a water sample (LeChevallier et al. 1993); similar application for SWRO treatment provides a quantifiable, comparative and predictive tool for biofouling potential. However, highly saline conditions are not conducive to growth and previous AOC attempts using these traditional strains have had to drastically alter the sample (Ong et al. 2002). A saltwater AOC test using a naturally occurring, bioluminescent marine organism, *Vibrio harveyi*, was developed and previously evaluated in the field on environmental samples from seawater intake points and treatment points in full-scale SWRO desalination facilities (Schneider et al. 2011; Weinrich et al. 2011). Unlike traditional spread plating techniques in bioassays, bioluminescence is used for measuring bacterial growth using a photon counting luminometer. Bioluminescence is the amount of light produced and is the key measurement for this bioassay. Standard curves produced linear relationships between maximum bioluminescence and acetate carbon equivalents. There are numerous advantages to this bioassay, including minimal consumables and a short turnaround time. In addition to available substrate (AOC, N_{max}) determination, it is possible to fit

observed data to the Monod kinetic model and thereby determine the bacterial rate of utilization in solution (μ_{max}). When determined throughout the treatment process, a higher μ_{max} indicates greater biodegradability, or lability, of that water sample. Alternatively, depressed lability suggests a lowered potential for biofouling, though the extent of this relationship is currently being confirmed through further testing. For example, a consistent decreasing pattern throughout the treatment system would suggest that the AOC reaching the RO feed would be less labile for microbial uptake.

1.5.2 Microbiology of Biological Fouling

Qualifying the microbial populations that are responsible for growth and proliferation on RO membranes is also an important step to understand biofouling in SWRO. Bacterial isolates from a biologically fouled SWRO membrane at a full-scale facility in Carlsbad, California were determined by 16S rRNA to be well-known biofilm-forming bacteria (Zhang et al. 2011). Isolates matched the genera *Shewanella*, *Alteromonas*, *Vibrio*, and *Cellulophaga*. 16s rRNA terminal restriction fragment length polymorphism (T-RFLP) was used to determine that the bacteria responsible for biofouling in the SWRO were found in the seawater intake. Samples were analyzed at four points during treatment including the intake, phytoplankton epibionts, cartridge filter, and SWRO membrane. A comparison between these locations indicated that microbiology of the cartridge filter was not the same as that of the biofouled SWRO. The research indicates an important aspect about bacteria colonizing the cartridge filter, which is not actively incubating bacteria responsible for SWRO biofouling. T-RFLP analysis was also conducted on bacterial communities from five separate international SWRO membranes with biofouling. Those results indicated that, while overall profiles were not identical, there was consistent occurrence of dominant bacteria. The researchers state that determining dominant biofilm bacteria is difficult because >99% of the natural microbial community is not culturable on nutrient-rich artificial

medium. This has important implications. *Pseudomonas* and other similar easily cultivable model organisms are typically used for membrane fouling research. However, *Pseudomonas* was not dominant either in seawater intakes or RO biofilms. Bacteria in marine environments are α-proteobacteria from the culture-independent clone library, whereas isolation on nutrient-rich medium favors γ-proteobacteria (e.g., *Vibrio*). Regardless, bacteria most often observed on SWRO membranes from international locations are often similar and therefore their survival is expanded from oligotrophic to chemolithotrophic conditions. Finally, the study reports that seasonal change has marked impacts on microbial communities in seawater and it was observed that this was more impactful than geographic location (Zhang et al. 2011).

Conventional pretreatment (coagulation by ferric chloride ($FeCl_3$), sedimentation, and two-stage sand filtration) showed average turbidity removal of 93% in a pilot system operating for 1.7 years in which average turbidity was 3.6 ± 2.9 NTU, but went as high as 20 NTU during the rainy season because of runoff from the coastal area near the plant (Bae et al. 2011). Compared to the raw seawater, bacterial diversity in the conventional system increased while diversity decreased in a parallel MF setup. Carefully managed treatment could use the diversity as an advantage for removing BOM and minimizing bacterial breakthrough. Numerous studies identify α- and γ-proteobacteria to be responsible for biofilm formation in seawater based on the 16S rRNA from both culture-dependent and –independent methods (Lee et al. 2009; Bae et al. 2011; Zhang et al. 2011). Qualitative results from a SWRO pilot system employing MF indicated removal of putative biofilm-forming bacteria, decreasing relative abundance from 98 to 10%. However, the conventional system was also shown to reduce γ-proteobacteria *Alteromonas*, *Cowellia*, and *Glaciecola* from 79.8 to 50%. This qualitative analysis could be improved by quantitative measurements of the abundance of biofilm forming bacteria through quantitative polymerase chain reaction (qPCR) or other culture-independent tools. While these approaches to better understand SWRO biofouling are important, practical applications and routine use have not

been established. The use of a surrogate measurement for determining the growth potential of raw seawater and RO feed would be more practical for developing approaches for mitigating SWRO biofouling.

1.5.3 Modeling RO Membrane Fouling

Models are important for designing RO desalination processes and are present in two major areas in the literature: (1) mechanistic or membrane transport model and (2) lumped parameter model (Sobana & Panda 2011). Estimating flux in a membrane that has not yet been fouled can be expressed as $J_w = \Delta P – \pi/(\mu \times R_m)$ where J_w is the pure water flux estimated from resistance-in-series model, ΔP is the applied pressure, π is the osmotic pressure, μ is the permeate viscosity, and R_m is the membrane resistance (Antony et al. 2011). Research has focused on biological fouling and modeling bacterial growth in non-seawater matrices, such as drinking water and wastewater treatment. There are limited modeling applications for biofouling on seawater RO membranes; although recent advancements using high pressure membranes such as NF or RO in other matrices is available. Some of this information will be useful for developing models, though specific testing in a saline matrix needs to be completed. Computational fluid dynamics (CFD) is based on determining fluid flow through the Navier–Stokes equation. Using CFD in membrane systems is well documented in the literature. For the optimization of feed spacer geometry, CFD has been applied for decreasing pressure losses in the past 10 years (Panglisch et al. 2011). Picioreanu et al. (2009) report that the common issue with the previous models is that they do not relate flow and mass transfer to biofilm growth. To account for this, they have developed a model for describing biofilm development in feed channels of spiral-wound NF and RO membranes that includes description of the liquid flow and the mass transport of a soluble substrate. The additional benefit of their model is that it includes changes in the geometry of the feed spacer that occurs from biofilm growth. The resulting flow channeling from

biofilm clogging is accounted for by an expanded computational domain of five by three squares, which is an expansion of other three-dimensional (3-d) CFD which have previously only focused on one square element formed by four crossing filaments. The research determined that biofilm growth affects pressure drops on the feed spacer filaments to a greater extent than growth on the membrane only, which is determined from a more uniform drop in pressure over the feed channel length. The study reinforced previous experimental observations about the residence time distribution of solutes and the permitting of dead zones caused by biofouling. These effects, in turn, cause local accumulation of high salinity water which leads to a lower permeate flux.

CFD and biofilm modeling are useful in a 3-d approach for more detailed investigation of feed spacers, and advantages of CFD include a minimization of time, cost, and risk from associated experiments that can be avoided using CFD to predict flow and mass transfer (Panglisch et al. 2011). However, there are a few drawbacks that have been reported elsewhere (Radu et al. 2010). Validation through experimental data for membranes is still necessary. Also, cost of producing full-scale models is prohibitive, so CFD membrane studies have focused on a small section of the spiral-wound membrane module in 2-d. 3-d was modeled without permeation and therefore concentration polarization (CP) could not be investigated. In addition, more advanced 3-d models would require additional time and resources that are not convenient or cost-effective. A study using brackish water was completed in which biofilm formation was modeled and combined with CFD to investigate local effects (irregular biofilm distribution) and macro-effects on loss of performance as a result of biofilm-enhanced CP, increased hydraulic resistance to trans-membrane flow and feed channel pressure drop in membranes having feed spacers (Radu et al. 2010). Radu et al. (2010) had performed the modeling using brackish water and indicated that CP enhanced by biofilm formation was the major contributor to permeate flux decline.

Radu et al. (2010) compiled an overview of multiple causes for the deterioration of membrane process performance that occur because of biofouling. These have been defined experimentally and include transmembrane flow studied by McDonogh et al. (1994), biofilm-enhanced CP (Herzberg & Elimelech 2007; Chong et al. 2008), and increased feed channel pressure drop (Vrouwenvelder et al. 2009). CP is the layer of concentrated solutes that remains near the membrane surface as the solvent (water) passes through. Therefore a layer formed by CP has a secondary effect of increasing the osmotic pressure at the membrane surface. Measuring osmotic pressure is a challenge in RO systems and is therefore investigated through CP modeling studies (Subramani et al. 2006; Lyster & Cohen 2007). Research presented by Chong et al. (2008) is the only effort that has explicitly included the presence of biofilm in the model. The Monod kinetic approach is used in mass balance equations in the model, and reflects substrate consumption by the biofilm. Substrate consumption leads to biological growth in the model, and other accommodations for biomass attachment, transport, and detachment are also considerations in the model (Radu et al. 2010). Parameters used for the model are sourced from available activated sludge modelling inputs. A recent report experimented with Monod kinetics and the bacterial growth rate of *Vibrio harveyi* for modeling flow rates, AOC concentration, and substrate utilization rates (μ_{max}). The model was calibrated to match existing operational data at a full-scale desalination facility that experiences high BOM and RO membrane biofouling (Schneider et al. 2011). Operational data included pressure drops along RO pressure vessels. The development of this model showed that increased pressures in the pressure vessels can be almost entirely explained by bacterial growth (biofouling) and thus points to the importance of AOC control through pretreatment. This new approach considers the following phenomena: (1) Biofilm growth on the surface of the membrane is nonuniform and is induced by AOC concentrations. (2) Biofilm growth in the spacers of the spiral-wound membrane that induces longitudinal pressure reduction from a restriction in the effective cross-sectional flow area. (3) Pressure losses along the elements

inside the pressure vessel caused by friction. (4) Dynamic conditions including changes in operational characteristics of the membrane filtration cycle such as influent water quality and crossflow velocities. This model would use daily measurements of AOC and μ_{max} along with forecast flow rates to each train in a real time application. Based on these results, alternative operational strategies, such as pretreatment optimization, flow rate distribution, and the use of biocides, can be identified for balancing flow rates among trains and reducing cleaning times. The model addresses short-term pressure losses caused by reversible fouling, assuming that the pressure drops are from biological growth; however, colloidal fouling would be revealed through increases in pressure drop. This phenomenon may not be an issue at all facilities, but where it is significant, colloidal fouling can be accounted for by including a term in the hydraulic radius calculation.

1.5.4 Biological Fouling Prevention

Strategies for biofouling prevention typically include continuous or intermittent biocide application or nutrient limitation or chemical and physical cleaning programs in SWRO pretreatment, or even membrane surface modification (Yang et al. 2009; Mansouri et al. 2010). Conventional desalination pretreatment often includes prechlorination, coagulation/flocculation, clarification, and filtration. Filtration can be achieved using granular media such as sand or dual media filtration (DMF). Low pressure membrane treatment is increasingly used in the industry. However, ultrafiltration and nanofiltration membranes exhibit a low degree of removal of fouling substances (Hilal et al. 2004). In the interest of sustainability, membrane filters have limited usage and must be cleaned or replaced. Given the challenges with various types of fouling, the robustness of membrane filters for pretreatment is debatable (Resosudarmo et al. 2013; NRC 2008). Alternatively, proper operation of sand filtration for RO pretreatment has shown that beach wells, i.e., natural sand filters, have lower biofouling potential than in the raw water

(Ebrahim et al. 2001; Saeed et al. 2004; Veza et al. 2008). Intake considerations are also a crucial aspect of water quality in the treatment plant but this topic is outside the scope of this review.

1.5.4.1 RO Membrane Amendment

Biofouling management at the membrane level is another strategy for controlling O&M cost and maintaining membrane performance. Researchers are developing membrane components that are inherently resistant to fouling. Biofouling control includes various strategies that have been divided into two main categories, 'anti-adhesion' and 'anti-microbial' (Mansouri et al. 2010). Research using the model organism *Pseudomonas aeruginosa* has identified predictors of cell adhesion with zeta potential, surface roughness, and hydrophobic character. However, as noted previously, this organism has not been identified as a key member in RO membrane biofilm studies (Zhang et al. 2011). Anti-adhesion reduces initial macromolecular adsorption and antimicrobial approaches attack, disperse, or suppress activity of organisms that have already attached to the membrane. While advances are made in membrane technology and researchers continue to investigate methods for reducing fouling at the membrane site, investigations have been mostly evaluated in freshwater.

Recent research has identified the importance of mitigating fouling by early detection. Cai & Benjamin (2011) investigated antibody-based sensors in their study. These biosensors were attached to cellulose acetate UF membranes using a temperature-responsive polymer film. In combination with a modified film layer, the membrane was capable of detecting bacteria and reducing fouling. In addition, its thermally responsive layer can be exploited to control fouling specifically of the sensor surfaces.

Feed channel spacers (Figure 1) have also been targeted. Studies have shown that biological fouling can be related to feed spacers in spiral-wound membrane elements (Cornelissen et al. 2007). Modification of the element using copper-charged polypropylene feed spacers was shown

to maintain 75% of the initial flux compared to 30% maintained by an unmodified membrane feed spacer in drinking water experiments (Hausman et al. 2010). Although experiments with both modified and unmodified feed spacers exhibited instantaneous flux declines, the unmodified units fouled rapidly over time. Other work has focused on using silver nanoparticles for inhibiting or reducing biological growth on the feed spacers (Yang et al. 2009). Specifically, Yang et al. (2009) tested a surface modified RO membrane and membrane spacer coated with silver nanoparticles in sand-filtered seawater. The coated membrane was able to better maintain permeate flux than the unmodified membrane; however, initial permeate flux was lower (0.8 m^3 m^{-2} day^{-1}) than that of the unmodified membrane (1.3 m^3 m^{-2} day^{-1}). Extended operation of the membrane indicated that foulant accumulation may reduce the bactericidal effects of the silver ions. This limitation was mitigated by additional testing of silver-coated feed spacers, which showed improvement of the initial permeate flux and were able to minimize flux loss over the duration of the experiment.

Recent studies have also prepared membranes with micrometer-sized heated aluminum oxide particles. This approach is referred to as microgranular adsorptive filtration (μGAF) and has been shown to enhance NOM removal (Cai & Benjamin 2011). The μGAF coating adsorbed the organic matter, and the membrane permeability was nearly fully recovered when the particles were washed off, which suggests that fouling did not occur in the membrane material. Other applications include silver nanoparticles, but that remains a controversial technique because of the possibility for detachment of silver nanoparticles or disposal of components coated with these substances. Their fate in the environment is still not fully understood.

A comprehensive review by Matin et al. (2011) detailed the challenges of membrane biofouling specifically in SWRO. Previous approaches including biocide application have limited success as a control strategy for biofouling and recent advancements in membrane surface

modification offer promise. Surface modification would inhibit biofilm formation in the critical stages of bacterial adhesion, microcolony formation and maturation (Matin et al. 2011). Until this approach can be widely adopted and applied in full scale facilities with a degree of confidence for long term operational reduction of biofouling occurrence, biofouling remains as a challenge in SWRO. In addition to advancing membrane materials for fouling reduction, removing and reducing foulants in the RO feed would also be a formidable control strategy.

1.5.4.2 Pretreatment and Nutrient Limitation

Nutrient limitation is a practical approach for reducing the quantity of life-sustaining elements, carbon, nitrogen, and phosphorus, in order to minimize unwanted microbial assimilation and growth. Although this is a fairly simple concept, the ubiquitous nature of nutrients that are naturally occurring and found in treatment chemicals poses a challenge. Current strategies include acid cleaning, intermittent biocide application and nutrient removal for biofouling control (Mansouri et al. 2010). The area of nutrient limitation warrants further investigation for optimizing SWRO treatment and minimizing biofouling, but has not been fully investigated in part because of the lack of tools for monitoring or measuring biofouling potential.

Effective pretreatment is critical in the efficient operation of SWRO membranes (Kumar et al. 2006). There is evidence that biologically active sand filtration prior to polyamide composite RO filters significantly enhanced the membrane performance (Griebe & Flemming 1998), presumably by removing BOM. A study of biodegradable organic carbon in an RO facility that experienced extreme biofouling was conducted by Schneider et al. (2005). Very high levels of AOC and biodegradable dissolved organic carbon were created by chlorination of river feed water. Furthermore, the application of chlorine on the sludge blanket inhibited any microbiologically-facilitated AOC reduction. The drinking water industry often practices preoxidation as part of pretreatment, which creates biologically available organic carbon, i.e.,

AOC. For example, ozone reacts with NOM to form aldehydes and low MW organic acids (Glaze et al. 1989; Miltner et al. 1992; Schechter & Singer 1995; Siddiqui et al. 1997), which can then be removed by biological filtration to increase biological stability and decrease disinfection byproduct formation. It is unfortunate that there is no biofiltration research to this extent in desalination, yet there is significant interest in mitigating irreversible biofouling of RO membranes and has been referenced by numerous authors (Flemming et al. 1997; Griebe & Flemming 1998; Schneider et al. 2005; Fujiwara & Matsuyama 2008; Voutchkov 2010). Anecdotal results and some limited research have shown that application of disinfectants increases biofouling potential in seawater, presumably resulting from the reaction between the oxidant and NOM, which produces more easily biodegradable compounds as described above in freshwater. Therefore, background information suggests that approaches to mitigating membrane biofouling would be effective if BOM is controlled in the RO feed. By measuring BOM using the seawater AOC test, the following research seeks to support the hypothesis that BOM provides available nutrients that support biological growth on the membranes. This growth leads to membrane fouling that reduces SWRO operational efficiency.

1.6 Hypothesis and Objectives

Based on the literature review, the SWRO industry would be prudent to affect collective seawater pretreatment for reducing fouling occurrence. In particular, biological fouling is not well managed in part because of a lack of predictive measurements. A need exists to establish quantitative metrics for biofouling potential in seawater RO feed through bench- and full-scale investigations. Techniques have not been specific or widely applied in seawater to measure the biodegradable fraction of organic carbon that contributes to biofouling. Given the fact that biofouling remains to be a challenge and SWRO continues to grow as a reliable drinking water source, the research approach presented in this dissertation was designed to investigate the conditions during desalination pretreatment that are conducive to bacterial growth on RO membranes. The approach was driven by the following hypothesis:

Biodegradable organic matter, specifically easily assimilable organic carbon (AOC) contributes to biological fouling of RO membranes used for seawater desalination.

The following objectives were designed to evaluate the hypothesis:

- Investigate the relationship between biofouling potential, chemical dosing, operational data and AOC in full scale seawater reverse osmosis (SWRO) desalination plants.
- Determine the influence of AOC on biological fouling in bench- and pilot-scale RO membrane testing.
- Evaluate AOC formation and other organic carbon changes in seawater treated with three commonly used oxidants: chlorine, chlorine dioxide, and ozone.
- Assess pretreatment chemicals, including antiscaling, membrane cleaning and dechlorinating agents for AOC formation and other organic carbon changes following chlorination.

The scope of work was developed to investigate biofouling potential and occurrence using the seawater AOC test. AOC is considered to be the nutrient fraction that provides the energy and carbon needed for bacterial growth by quantifying the growth potential on a reference biodegradable carbon source, acetate. There are numerous AOC applications, but this project uses a test specifically for saline conditions by using a naturally occurring, bioluminescent marine organism, *Vibrio harveyi*. The approach is depicted in Figure 3 for investigating the hypothesis that AOC is an important factor in biofouling which ultimately leads to operational changes in SWRO including loss of permeate flux and increased differential pressure on the membranes. Correlations between AOC and operational changes (membrane differential pressure, specific flux) were investigated in full scale facilities that experienced biological fouling problems and in bench- and pilot-scale configurations. Pretreatment chemicals were evaluated for their potential to increase the biodegradability of seawater and included oxidizing, antiscaling, cleaning and dechlorinating agents. Evidence was collected to support the hypothesis that AOC contributes to biofouling and the seawater AOC test is a useful tool for understanding the impact of pretreatment on biological fouling at bench-, pilot-, and full-scale desalination plants. A better understanding of water quality and RO pretreatment impacts on biofouling potential is revealed through the project findings, along with recommendations for identifying sources of AOC during pretreatment and minimizing biofouling potential.

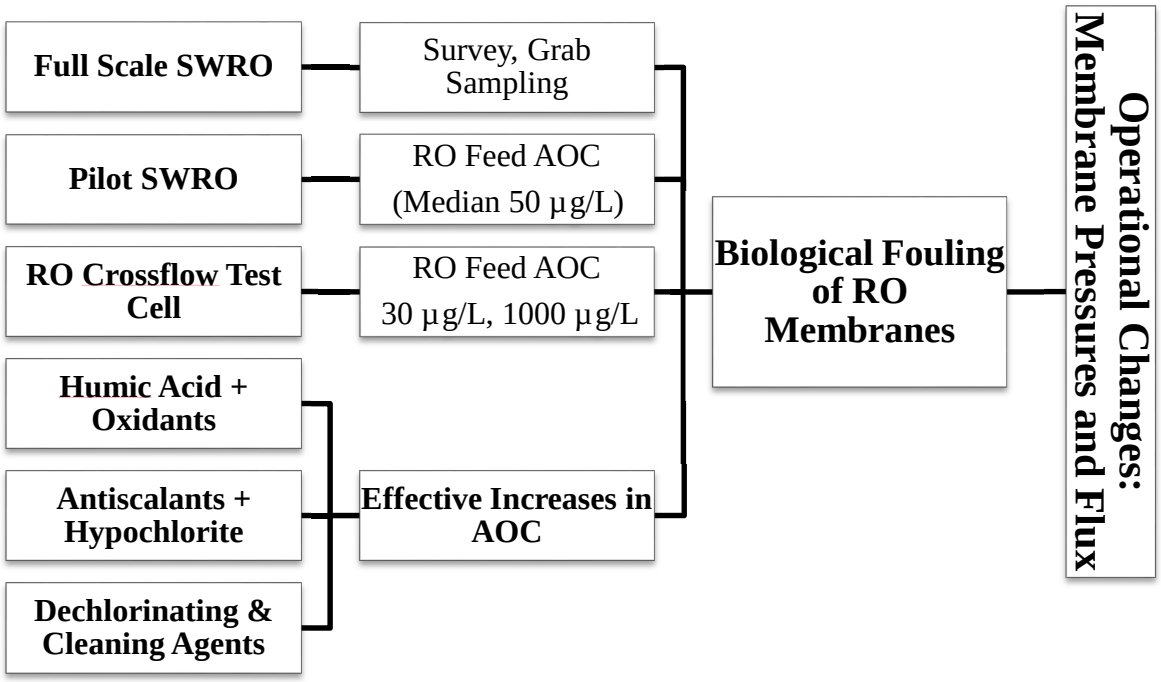

Figure 3 Hierarchy of the investigations in this project to identify whether assimilable organic carbon (AOC) results in biological fouling that impact SWRO membrane operations.

CHAPTER 2: OPERATIONAL IMPACTS FROM BIOLOGICAL FOULING ON SEAWATER REVERSE OSMOSIS MEMBRANES

Abstract

Biological fouling occurs on RO membranes when bacteria and nutrients are present in conditions that are conducive to growth and proliferation of the bacteria. Biofouling management is typically limited to biocide application (i.e., disinfectants) in seawater RO plants to control microbial growth. However, biological growth and subsequent fouling has not been well-managed. Pretreatment has not been focused on nutrient limitation. This project used a biological assay, the assimilable organic carbon (AOC) test to evaluate pretreatment effects on the nutrient supply. The AOC test provided a useful surrogate measurement for the biodegradability or biofouling potential of RO feed water. Biofouling observed in controlled conditions at the bench- and pilot-scale resulted in statistically significant correlations between AOC and the operational effects caused by biofouling. Membrane fouling rates are observed through operational changes over time such as increased differential pressure between the membrane feed and concentrate locations and decreased permeate flux through the membrane. In full scale plants there were strong correlations when AOC was used as a predictor variable for the increased differential pressure (4 – 8 psi from September – December, 2012) and the decreased specific flux (0.00004 gpm/ ($ft^2 \cdot$ psi) or 1.40 liters per hour/ ($m^2 \cdot$ bar)). Increased differential pressure was associated with RO membrane biological fouling when the median AOC was 50 µg/L during pilot testing. Conditions were also evaluated at the bench-scale using a flat sheet RO membrane. In a comparison test using 30 and 1000 µg/L AOC, fouling was detected on more portions of the membrane when AOC was higher. Biofilm and bacterial deposits were apparent from scanning electron microscope imaging and biomass measurements using ATP.

2.1 Introduction

Biofouling is neither well understood nor consistently prevented and continues to be a challenging problem in seawater reverse osmosis (SWRO) membrane separation processes (Griebe & Flemming 1998; Vrouwenvelder et al. 2000; Vrouwenvelder & Van Der Kooij 2001; Pang et al. 2005; Kumar et al. 2006). The growth of microorganisms into a biofilm on the membrane surface leads to costly increases in SWRO treatment. Decreasing permeate flux, increasing pressure drops in the RO modules, increasing salt passage, and irreversible damage to the RO membrane are all issues associated with biofouling. Pilot- and full-scale SWRO were investigated to identify fouling and correlate assimilable organic carbon (AOC), water quality, and other organic carbon results. Pretreatment records were used to corroborate the water quality conditions and chemical usage. The objectives were to 1) identify relationships among biofouling potential, chemical dosing, operational data, and AOC in full-scale SWRO treatment plants, and 2) evaluate AOC as a predictor of biofouling potential by monitoring operational changes (i.e., permeate flux, differential pressure) using a flat sheet membrane test cell and a 500 gallon per day (gpd) pilot-scale SWRO.

2.2 Sampling Approach and Experimental Overview

Water quality variation and organic carbon removal were examined throughout three full-scale SWRO desalination plants. The plants all treat seawater from surface intakes, but have geographic variability and different pretreatment configurations. Grab samples were collected from various points within the pretreatment process. The grab samples provided information on source water quality fluctuations, and the effectiveness of treatment for removing organic carbon and AOC as related to biofouling potential. Organic carbon removal was determined through typical measurements such as total organic carbon (TOC) and UV absorbance at 254 nm (UV_{254}) as well as more specific determination of biodegradability using the seawater bioluminescent

AOC test. Operational data were supplied by treatment plant personnel to supplement the grab sampling efforts and evaluate the plant's performance. Cleaning procedures, treatment changes, flow rates, membrane flux, and differential pressure data were used to correlate the significance of AOC as an indicator of biological fouling potential in the following treatment plants: Tampa Bay Seawater Desalination Plant (TBSDP), West Basin Municipal Water District (WBMWD) Ocean-Water Desalination Demonstration Facility, and the Al Zawrah SWRO facility.

Using a single membrane provided testing conditions that were easily monitored and controlled and therefore a focused investigation of the RO feed water quality, specifically AOC, was effective for evaluating biological fouling and the resulting impact on differential pressure and specific flux. Two approaches examined these operational conditions; the first used a 500 gallon per day (gpd) RO pilot that housed one-29 ft^2 membrane, and the second was a bench-scale test unit that housed one-0.0452 ft^2 membrane coupon that could be changed for testing RO feed water with variable AOC.

2.3 Full Scale Desalination Plants

2.3.1 Tampa Bay Seawater Desalination Plant (TBSDP)

TBSDP is located on Tampa Bay in Gibsonton, FL. The plant is co-located with the Tampa Electric Company (TECO) coal-fired power plant and receives feed water from the plant's cooling loop; if the cooling water exceeds the temperature limits of the membranes, then bay water can be mixed in. A process flow schematic of the plant is shown in Figure 4. The combined bay water and cooling water (i.e., raw water) was treated with chlorine dioxide (0.5 – 1.1 mg/L) and further treated with sodium hypochlorite, sulfuric acid, and ferric chloride in the coagulation step. The water is flocculated prior to the sand filters: upflow, deep bed granular media filters with continuous backwash. From these filters, the water is sent to two parallel banks of diatomaceous earth (DE) filters. Any residual sediment from the DE filtrate is then removed in

cartridge filters prior to the SWRO desalination membranes. Cartridge filters (Fulflo Durabond and Honeycomb Filters, Parker Hannifin Corporation, Oxnard, CA) are replaced once a year. Sodium bisulfite (SBS) is added at this step to control the oxidation-reduction potential (ORP) of the water and prevent oxidative damage to the membranes. Samples were collected from pretreatment locations at TBSDP on September 20 and October 24, 2012 and January 3, 2013 for the purpose of evaluating treatment effectiveness for AOC removal and comparing biofouling potential (i.e., AOC content) of the RO membrane feed. The project team initially proposed to collect samples quarterly from TBSDP; however, because of the ongoing operational directives, the plant was online from August through December and had adjusted pretreatment in preparation for shutting down the plant in January. The plant was offline from January 7 through 24, 2013.

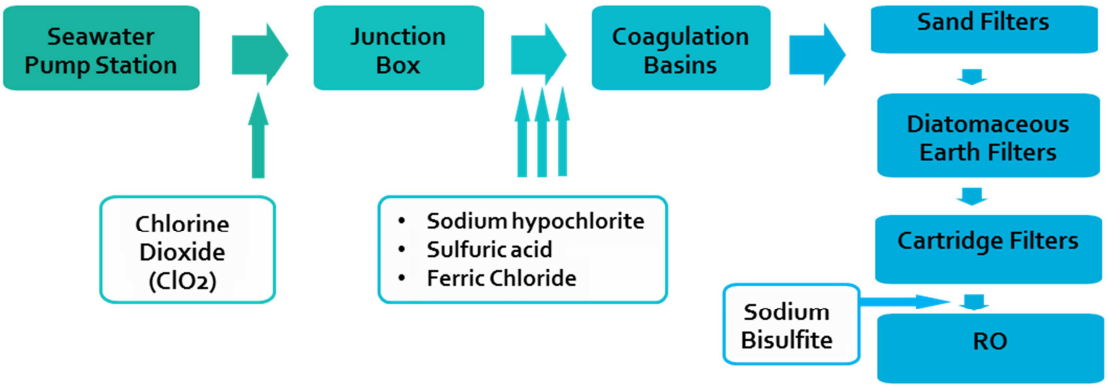

Figure 4 Tampa Bay Seawater Desalination Plant (TBSDP) Process Flow Diagram.

2.3.2 West Basin Municipal Water District (WBMWD) Ocean-Water Desalination Demonstration Facility

WBMWD is co-located with a natural gas power plant, and the seawater intake is located at Redondo Beach, CA, 0.5 mile into the Pacific Ocean and 30 feet below the surface. The plant was chosen because of its relatively low organic content (TOC ~1 mg/L), reported challenges with biological fouling and Pacific Ocean location. The desalination process consists of a 2 mm intake screen, 100 µm Arkal disk filters, followed by ultrafiltration (UF) and RO. UF membranes

were ZeeWeed 1000 (GE, USA). Hypochlorite and citric acid were used for UF maintenance cleaning. There were two parallel RO pressure vessels, and each vessel contained seven membrane elements. RO membranes were from the QuantumFlux™ line by NanoH2O (California, USA). NanoH2O membranes used in the first pass RO had a surface area of 400 ft^2 for a total surface area of 5600 ft^2.

2.3.3 Al Zawrah Desalination Plant in Ajman, United Arab Emirates

Al Zawrah is located in the Emirate of Ajman (United Arab Emirates) and the seawater intake uses surface water from the Arabian Gulf. Water quality in the gulf is poor, often with elevated temperatures and red tide occurrences; total dissolved solids (TDS) may be as high as 48,000 ppm, and there are numerous large-scale desalination plants (both thermal and RO) that discharge brine and waste in the area. Shock chlorination and post-treatment with SBS was historically conducted every 3 to 4 weeks. The desalination process consists of coagulation with ferric chloride, dual media filtration (DMF), cartridge filtration, and RO. Coagulant doses were 2.6 mg/L in May, 1.7 mg/L in July, and 2.5 mg/L in November. The media used in the DMF included a top layer of pumice (1.2 – 1.5 mm), which was 800 mm deep and a bottom layer of silica sand (0.4 – 0.6 mm), which was 600 mm deep, at a filtration rate of 8 to 10 m/h. Cartridge filters were replaced approximately every 90 to 100 days. Adjustment of pH was done using sulfuric acid at the feed to the cartridge filters to achieve a level between 6.9 and 7.0.

2.4 Focused Investigation of Biological Fouling on RO membranes

2.4.1 Pilot Unit Configuration with TBSDP Feed

Water quality and operational data were collected from a 500 gallon per day (gpd) pilot unit deployed at TBSDP. A new thin film composite RO membrane was installed into the system and operated under constant permeate flux for the purpose of further evaluating AOC as a tool for monitoring fouling. The pilot unit (Figure 5; Tomar TV-500SW, Tomar Water Systems, Inc., San Marcos, CA) contains a multimedia (sand) prefilter, chemical injection system, and a UV

sterilizer integrated on a stainless steel skid frame powered by a single-point AC power connection. SBS was used in the chemical injection system. The unit was operated at 13% recovery; permeate flow rate was set at 0.317 gpm (457 gpd). By maintaining constant product water settings (e.g., flux), operational changes were monitored daily. Feed water from TBSDP was pumped from the rapid mix basins prior to the sand filters. A sump pump lifted water from the treatment basin over the basin wall and down through piping into a 32 gallon reservoir in the pilot unit shed. An automatic feed of SBS was dosed into the reservoir to quench the residual. A lift pump moved the water from the reservoir to the sand filter, followed by a cartridge filter prior to the RO membrane vessel. Pressure gauges were installed before and after the cartridge filter and after the RO feed pump to the RO vessel and brine flow. A digital readout monitored temperature and conductivity of RO permeate. A new RO membrane was installed at the beginning of the test, a DOW FILMTEC™ seawater element SW30-2540. This unit can withstand 800 psi applied pressure at a 700 gpd flow rate with average 99.4% salt rejection. The element is 40 inches long and 2.4 inches wide. The active area of the membrane is 29 ft^2 and made of polyamide film wrapped in fiberglass.

Seawater was pretreated at the plant with approximately 0.5 to 1.1 mg/L as Cl_2 of chlorine dioxide. Chlorine dioxide residual ranged from 0.01 to 0.39 mg/L. After the junction box, seawater was dosed with sulfuric acid (~20 – 22 mg/L), hypochlorite (4 – 6 mg/L), and ferric chloride (~4 – 5 mg/L). Daily water quality data were collected from TBSDP, including temperature and conductivity at the intake; turbidity, pH, alkalinity, and chlorine dioxide residual at the junction box; chlorine residual in the rapid mix basin; and SDI_{15} of the RO feed (Table 1). Grab samples were collected at the pilot unit and analyzed for TOC, assimilable organic carbon (AOC), UV_{254}, and phosphate. Phosphate was 0.3 mg/L and nitrate was 0.09 mg/L.

Figure 5 Mobile RO skid deployed at the Tampa Bay Seawater Desalination Plant (TBSDP; source: the author).

Table 1 Seawater pretreatment records from TBSDP.

	Day	Intake Temp (°C)	pH	Alkalinity (mg/L)	Chlorine dioxide (mg/L)	Cl_2 (mg/L)	SDI_{15} Cart. Filter
3/26/2013	1	27.1	7.90	127	0.161	0.84	3.76
3/27/2013	2	22.8	8.03	123	0.010	0.77	3.62
3/28/2013	3	16.7	7.96	127	0.173	0.87	3.73
3/28/2013	3.5	25.9					
3/29/2013	4	21.4	7.96	127	0.010	1.09	3.77
3/29/2013	4.5	23.9					
3/30/2013	5	23.9	7.82	123	0.199	0.74	3.74
3/30/2013	5.5	27.0					
3/31/2013	6	26.5	7.91	114	0.010	0.94	3.52
4/1/2013	7	26.0	7.82	124	0.392	1.10	3.66
4/1/2013	7.5	28.6					
4/2/2013	8	27.1	7.76	127	0.010	1.22	3.39
4/2/2013	8.5	30.4					
4/3/2013	9	29.3	7.89	124	0.010	0.69	3.43
4/3/2013	9.5	28.7					
4/6/2013	12	28.5	8.00	119	0.039	0.65	3.39

2.4.2 Membrane Test Cell

The experimental setup included a cross flow test cell, pump, motor, pressure gauges, valves for flow and pressure control, and flow meters. The CF042 membrane cell (Sterlitech, Kent, WA) holds a flat sheet RO membrane with an active area of 42 cm^2. The permeate carrier was a 20 µm sintered 316L stainless steel plate. Dow Filmtec SW30HR membranes were used for the experiments and purchased pre-cut. The SW30HR is a smooth, hydrophilic commercial flat sheet thin film, composite RO membrane. A high-pressure positive displacement, diaphragm pump with a maximum flow rate of 1.8 gpm (6.8 Lpm) was used. Pressure was manually adjusted to remain constant over the experiment. Feed to the cell was pumped from a 5 gallon stainless steel conical feed tank onto the test cell at a flow rate of 5.5 Lpm. There was no recirculation of the concentrate or permeate to preserve the representative organic loading directly from the RO feed at TBSDP. Prior to testing, TBSDP second pass RO permeate was used to compress the membrane at the operating pressure for 1 hour before testing. Permeate was also used to flush the system at the end of the experiment. Temperature, feed pressure, flow, pH, and conductivity were measured at 20 minute intervals. After the initial compression period, the unit was operated for each test for 2 days. Specific flux was calculated from the driving pressure and normalized for temperature and the initial flux of the SW30 membrane. Operational parameters between the two membrane tests were nearly the same, as seen in Table 2.

Experiments to monitor the biological fouling effect on permeate flux decline were conducted onsite at TBSDP with a bench-scale membrane test cell using the pretreated RO feed because it was the most representative water source for conducting fouling tests. Pretreated seawater from TBSDP was diverted from the sampling station prior to the high-pressure RO pump to the test cell's feed tank. The RO feed water had undergone complete pretreatment conditions at TBSDP, and SBS was added to remove remaining chlorine residual after the cartridge filtration step. Inherent water quality and organic solute concentration were maintained by configuring the feed

in once-through mode to most effectively capture the water quality of the RO feed to TBSDP. The effects from recirculation and bacterial consumption may have varied the concentration of solute (AOC). Operational data from TBSDP were collected for the RO feed and included turbidity, SDI, pH, and ORP at 4 hour intervals. At the end of the experiments, the membrane was retrieved from the test cell and prepared for imaging using scanning electron microscopy (SEM).

Table 2 Membrane test cell feed water quality and operating parameters.

	AOC baseline	**AOC 1,000 µg/L**
AOC (µg/L)	30	997
TOC (mg/L)	4.3	5.4
SUVA (L/mg-m)	1.4	1.3
UV_{254} (cm^{-1})	0.06	0.07
Total Nitrogen (mg/L as N)	0.4	0.8
Phosphate (mg/L)	0.16	0.13
Operating pressure (psig)	820	820
Temperature (°C)	28.2	28.0
pH	6.88	6.89
Feed Conductivity (mS/cm)	40	40
SDI (15 min)	3.2	2.9
Feed Turbidity (NTU)	0.12	0.09
Permeate Conductivity (mS/cm)	0.3	0.3
Salt Rejection	99.2%	99.2%
Membrane Flux J_0 (lmh)	20	20
Flux decline	3%	24%

2.5 Materials and Methods

2.5.1 Assimilable Organic Carbon (AOC)

AOC was measured using the luminescence assay described by Weinrich, Schneider, and LeChevallier, 2011 (Appendix A). All experimental and environmental samples (50 mL) were prepared in AOC-free glassware and pasteurized in a water bath for 30 min once the temperature of the proxy reached 70°C. Samples were then cooled in an ice bath. After pasteurization the cooled samples were inoculated with *Vibrio harveyi* at approximately 10^3 colony forming units (cfu) per mL. *V. harveyi* is a naturally occurring marine organism and therefore is an appropriate test organism for seawater. In addition, the inherent bioluminescent characteristic of *V. harveyi* facilitates the use of an automated photon-counting luminometer for monitoring bacterial growth in a water sample. Samples were gently swirled and duplicate 300-µL aliquots were transferred into the microplate immediately after inoculation. A laminar flow hood (SterilGARD II; The Baker Co., Sanford, ME) was used to maintain sterility during sample handling, inoculation, and transfer to the microplate. The microplate was covered with adhesive film to minimize evaporation, and measurements were taken immediately and at hourly intervals (generally 2 to 5 hours) until peak luminescence (or maximum growth, N_{max}) during the stationary phase was reached.

2.5.2 Total Organic Carbon (TOC)

TOC was measured using a platinum-catalyst combustion TOC analyzer (TOC-VCSH, Shimadzu Scientific Instruments, Inc., USA) with an autosampler according to Standard Method 5310 B. Samples were acidified using sulfuric acid to pH greater than 2 prior to analysis. Results shown are the average of triplicate injections.

2.5.3 Ultraviolet Absorbance at 254 nm (UV_{254}) and SUVA

UV_{254} was measured using a UV-Vis spectrophotometer (DR 5000, Hach, Co., USA) set at a single wavelength of 254 nm; water samples were filtered through Whatman GF/F glass fiber filters with a nominal 0.7-µm pore size and measured using a 1-cm quartz cuvette. The filtrate was also used for measuring dissolved organic carbon (DOC). Specific UV absorbance (SUVA) was calculated by dividing UV_{254} (meters) by DOC in mg/L; units are L/mg-m.

2.5.4 Adenosine Triphosphate (ATP) on the Membrane Surface

ATP analysis was conducted on the RO membrane surface from the pilot unit to evaluate microbial activity. ATP occurs in all living organisms and is a useful assay because it measures metabolically active biomass irrespective of whether such biomass is culturable. Small sections of about 1 square centimeter (cm^2) were portioned for triplicate ATP analysis. The sections were placed in 1.5 mL microcentrifuge tubes containing 100 µL of phosphate buffer and incubated in a 30 °C water bath. At the same time a tube containing 300 µL of BacTiter-Glo™ reagent is placed in the water bath, and both tubes are incubated for 3 minutes. Then the reagent is transferred to the tube for 1.5 minutes in the water bath and mixed every 30 seconds. The tube containing the membrane portion and the reagent are then removed, and 200 µL is transferred to a clean tube. Luminescence is measured 30 seconds later on a GloMax™ 20/20 luminometer. Triplicates for each sample were established. Luminescence is measured and then converted to ATP concentration using a calibration curve constructed using rATP (Promega Cat# E6011). Final results are reported on an ATP per area basis by dividing the concentration of the 200 µL sample by the area of the RO portion; units are reported as ng ATP/m^2 RO membrane.

2.5.5 Scanning Electron Microscopy (SEM)

Membrane surfaces were imaged using FEI XL30 environmental scanning electron microscope (ESEM; FEI Hillsboro, OR, USA) operating under high vacuum between 10 and 20

kV to observe the extent of biological fouling deposited on the RO membrane surface removed from the membrane testing cell and pilot unit. Membrane sections were processed to stabilize biofilm and other fouling deposits prior to being mounted on aluminum SEM stubs and sputter-coated with a thin layer of gold and palladium. The procedure was modified from the US Environmental Protection Agency for SEM imaging of biomass on granular activated carbon used in filters for drinking water treatment. Other modifications include drying in a desiccator and sputter coating with platinum and palladium instead of gold and palladium.

Sections from the RO membranes were cut using a sterile razor blade, gently rinsed with deionized water for 30 seconds to remove extra debris, and then fixed with 2.5% gluteraldehyde with 4% paraformaldehyde in 0.1M cacodylate buffer adjusted to pH 7.3. Samples were fixed overnight and washed with cacodylate buffer twice, for 15 minutes each. They were then washed again in deionized water for an additional 15 minutes. After washing the samples were postfixed for an additional hour in 1% osmium tetroxide in deionized water, and then washed three times for 15 minutes each. After osmium fixation the samples were dried using a dilution series of ethanol (25, 50, 75, 95 and 100% x2) for 30 minutes each. RO membrane portions were air dried in a chemical fume hood for 1 hour on filter paper then transferred to a desiccation jar overnight. Prior to imaging, the membrane was mounted on aluminum SEM stubs and sputter coated with platinum and palladium for 30 seconds. Multiple sets were examined to ensure continuity of imaging for the samples.

2.5.6 Nutrients

Samples were collected from the RO feed and analyzed immediately onsite at TBSDP for nitrogen and phosphorus with a portable spectrophotometer (DR2400, Hach, USA). Phosphate was measured as orthophosphate through the ascorbic acid method (Standard Method 4500-P-E; Hach 8048) at 880 nm; results are reported as mg/L PO_4^{3-}. Ammonia was measured as ammonia-

nitrogen using the salicylate method (Hach 8155) at 655 nm; results are reported as mg/L NH_3–N. Nitrate was measured as nitrate-nitrogen using the cadmium reduction method (Hach 8171) at 400 nm; a standard curve was prepared according to the seawater calibration as outlined in the method, and the results are reported as NO_3^-N. Nitrite was measured as nitrite-nitrogen using the diazotization method (Hach 8507) at 507 nm; results are reported as NO_2^-N. Additional samples were shipped overnight on ice to Delran, NJ where they were processed and analyzed for AOC, UV_{254}, TOC and SUVA.

2.6 Results and Discussion

2.6.1 Tampa Bay Seawater Desalination Plant Pretreatment and Organic Carbon Removal

TOC removal throughout pretreatment between coagulation and cartridge filtration was 3% in September and 6% in October, which is consistent with the limited TOC removal at TBSDP reported previously (Schneider et al. 2011). This does not include organic removal before coagulation as the intake was not included as a result of sampling issues. AOC was generally below detection (<10 µg/L) after DE filtration. Although not directly investigated in this study, bioactivity in the DE may have been sufficient to reduce AOC after that treatment step. AOC was less than 10 µg/L following DE treatment, but after the cartridge filter AOC increased to 97±19 µg/L in September and 23±1 µg/L in October (Table 3). Chemical addition after the cartridge filter is limited only to SBS to remove the residual oxidant from sodium hypochlorite added prior to coagulation (Figure 4). The staff reported that SBS was typically dosed between 5 and 22 mg/L but the records from August through December 2012 indicated that the range was 3 to 123 mg/L (specifically in Train 4) for controlling oxidation-reduction potential (ORP). There were no other chemicals added at this treatment step; antiscalant was not used at TBSDP.

Table 3 TBSDP organic carbon data.

	Treatment step	UV_{254} (cm^{-1})	TOC (mg/L)	AOC (µg/L)
September	Coagulation	0.135	6.20	20
	Sand filter	0.133	6.38	60
	DE filter East	0.127	6.29	1
	DE filter West	0.128	6.12	8
	Cartridge filter	0.132	6.00	97
October	ClO_2	0.173	5.85	29
	Coagulation	0.131	5.49	2
	Sand filter	0.103	5.29	1
	DE filter East	0.106	5.13	1
	DE filter West	0.103	5.07	2
	Cartridge filter	0.110	5.17	23

2.6.2 TBSDP Data Modeling

TBSDP went online in August after new RO membranes were installed in Trains 1 and 7, which provided a unique opportunity for the research team to conduct an in-depth analysis on membrane changes caused by fouling. By capturing this time period immediately after restarting, the operational impacts from fouling on new membranes were investigated from August until December 2012, when the plant was online and operating. There are seven first-pass RO trains at TBSDP. Each train is preceded by a lift pump, cartridge filter, and a high pressure feed pump. There are two stages in each vessel separated by a block. The first stage contains Elements 1 through 3; after a block, permeate from the five Lag Elements 4 through 8 is sent to the second-pass RO for further treatment. In the performance tracking software, data are entered for the two stages separately. The first three elements were selected for additional analysis because the incoming water from the cartridge filter would be the most representative RO feed for the purpose of investigating fouling effects. The flow rates, total flow, and differential pressure were used for further evaluation. The operating time was compared between the RO trains. Total flow

(in billion gallons) for each of the seven trains during the time period of interest is listed in Table 4. Because of maintenance and variable production needs, not all of the trains were continuously operated; those that were operated the longest were suitable for further data analysis and comparison. Trains 1, 4, and 6 were operating for 68, 65, and 80 days, respectively. These trains also received the greatest volume of seawater compared to the other trains. The following section describes the preliminary analyses for the type of membranes, flux, and differential pressure associated with these trains.

Table 4 TBSDP operating time, total flow, and average specific flux (normalized to 25 °C) from August – December 2012.

Train and membrane type	Total time in operation (days)	Total flow (billion gallons)	Average Sp. Flux (gpm/(ft^2 • psi))
1 SWC4-LD	68	11.5	0.000027
2 SW30HR	57	7.3	0.000021
3 SW30HR	22	1.1	0.000019
4 SW30HRLE	65	11.1	0.000033
5 SW30HR	32	2.4	0.000023
6 SW30HRLE	85	18.3	0.000028
7 SWC4-LD	60	8.5	0.000028

There were various membranes used during the time period of interest in 2012. Each train has 160 pressure vessels containing eight membranes. In August 2012, new Hydranautics SWC4-LD membranes were installed in Trains 1 and 7. The SWC4-LD membrane has 400 ft^2 of membrane area. Trains 2, 3, and 5 contained older SW30HR FilmTech membranes each having an area of 380 ft^2. Trains 4 and 6 had newer SW30HRLE-370/34i FilmTech membranes with an area of 370 ft^2 each. The area of the three lead elements in each train was calculated to determine specific permeate flux from each membrane type. Specific flux was calculated from the permeate flow

(gpm) from Elements 1 through 3 divided by the total area of the membranes used in that stage and the net driving pressure (psi) (Figure 6). For instance, in RO Train 1, flow from the three elements (400 ft^2each) in the 160 vessels crosses 192,000 ft^2 of RO membrane surface. Therefore, at a flow of 1,888 gpm and NDP of 260 psi, the specific flux is 0.000038 gpm/ (ft^2· psi).

$$Specific\ \ flux = Q_p \div NDP \div A$$

where :

Q_p *is the permeate flow* (*gpm*)

NDP is the net driving pressure (*psi*)

and

A is the membrane area (*sq. ft.*)

Figure 6 Specific Flux Calculation

Changes to specific flux and differential pressure were monitored to determine the impact of fouling in each RO train. Decreased specific flux is observed when water passage is reduced by a fouling layer, pore blockage or both. Alternatively, when additional force is needed to overcome osmotic pressure changes on membranes that had succumbed to fouling, the differential pressure increases. Membrane manufacturers typically set limits for differential pressure and when the limits are reached a cleaning procedure is triggered at the plant. During the time period evaluated, Train 4 underwent a cleaning on November 18, and Train 6 was cleaned on December 14, 2012. Trains 1, 4, and 6 produced the majority of the water (Table 4) during September and October; overall trends indicate that specific flux decreased and differential pressure increased. Specific flux decreased to a greater extent in October (Table 5). Most pronounced was a 53% decrease in specific flux in Train 4 prior to the cleaning on November 18, 2012.

The permeate flow from the first three RO units in Train 4 ranged from 1505 – 2025 gpm during the period investigated and averaged 1790 ± 131 gpm; NDP ranged from 235 - 386 psi and averaged 298 ± 42 psi. Operation of these new membranes following installation in 2012

achieved a maximum permeate flow of 2101 gpm (August 29, 13 days after installation) and a minimum NDP of 223 psi (first day of operation). Although these were achieved on different dates, the estimated maximum specific flux would be 0.000050 gpm/ ($ft^2 \cdot$ psi). The maximum specific flux measured during the period of investigation was 85% of the estimated maximum permeate flux. Conversely, the lowest permeate flux post-installation was 1505 gpm and the maximum NDP was 442 psi that results in an estimated permeate flux of 0.000018 gpm/ ($ft^2 \cdot$ psi). Given this estimation of the lowest permeate flow with the highest NDP the plant achieved 20% greater flux even at the minimum operating level during the period of investigation.

Table 5 TBSDP RO trains and delta specific flux. Plant operations started August 2012. (ND = no data, membranes were not in operation).

Train # and membrane type	**Delta sp. flux September**	**% decrease based on average**	**Delta sp flux October**	**% decrease based on average**	***% decrease during August - December***
1 SWC4-LD	0.000005	19	0.000010	37	***47***
2 SW30HR	0.000003	14	ND	ND	***39***
3 SW30HR	ND	ND	ND	ND	***ND***
4 SW30HRLE	0.000000	1	0.000012	36	***53***
5 SW30HR	ND	ND	0.000008	33	***36***
6 SW30HRLE	0.000005	18	0.000008	28	***49***
7 SWC4-LD	0.000007	25	0.000012	44	***45***
Average	**0.000004**	**16**	**0.000011**	**29**	**45**

2.6.3 TBSDP Operational Performance and Data Modeling Results

Grab sample collection coincided with the period of operation for RO membranes in Train 4. Other trains were periodically offline for maintenance and therefore did not provide a complete data set for comparison with the water quality samples. Train 4 was operating for 47 days prior to

the first cleaning on November 18, 2012. Figure 7 through 9 graphically depict the operational data beginning on September 22 for Train 4. Consistent trends were evident for decreasing specific flux (Figure 7) and increasing differential pressure (Figure 8); a strong correlation existed between the two data sets ($r^2 = 0.89$; Figure 9).

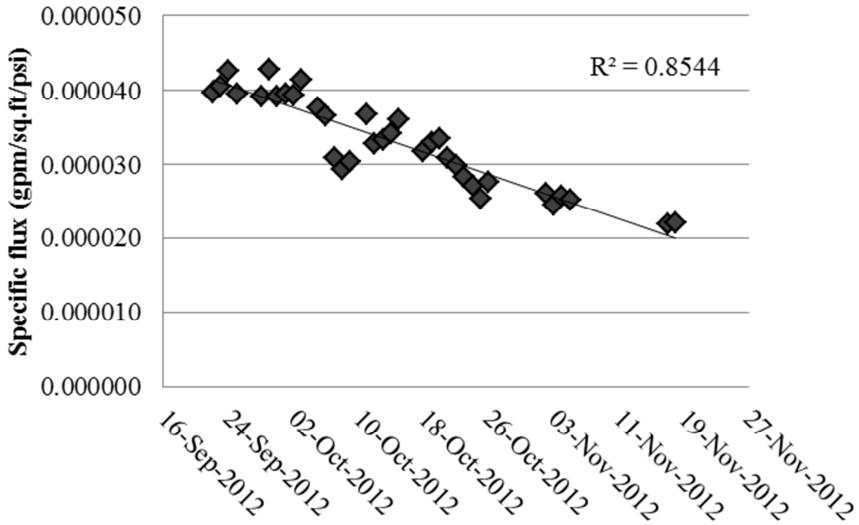

Figure 7 TBSDP: Specific flux of the first pass RO membranes in Train 4 from September to November 2012 (n=35). New membranes were installed in August, and the train was online beginning September 22.

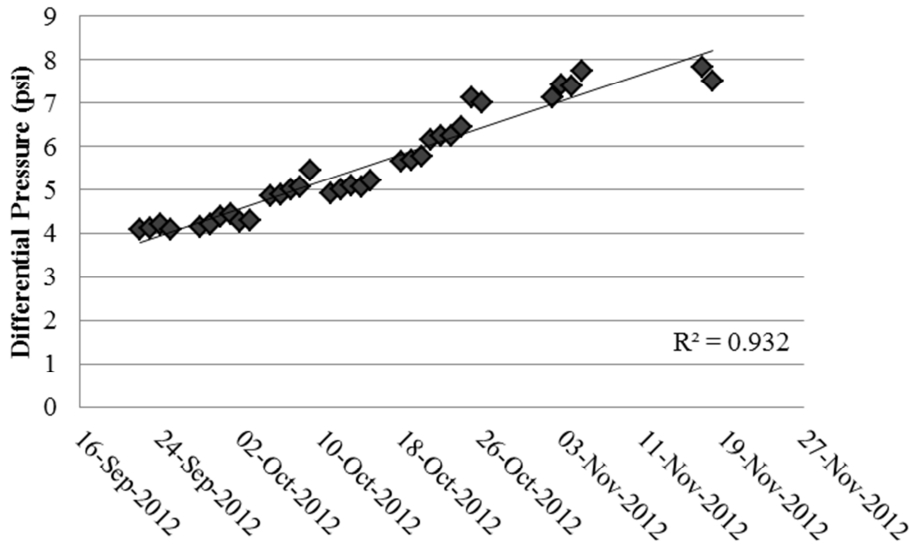

Figure 8 TBSDP: Differential pressure of the 1st pass RO membranes in Train 4 from September to November 2012 (n=35). New membranes were installed in August, and the train was online beginning September 22.

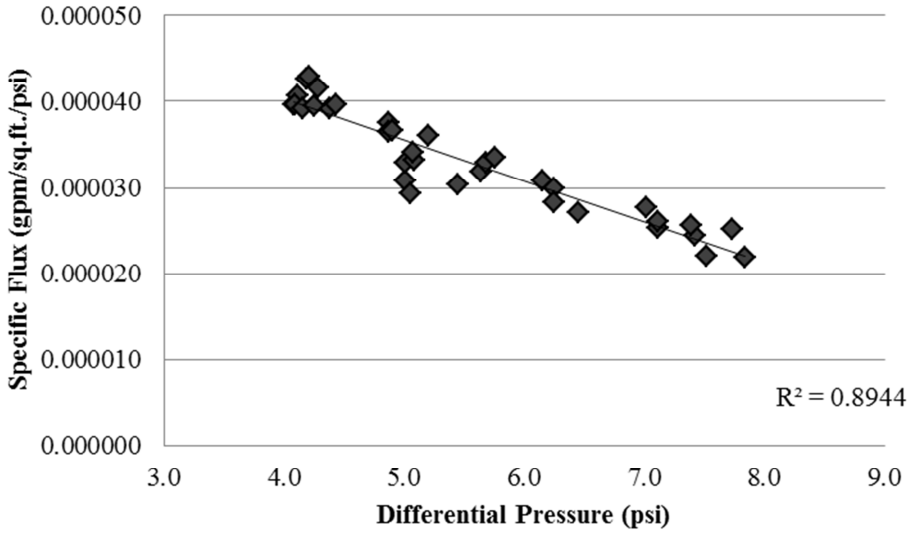

Figure 9 TBSDP: Correlation between specific flux and differential pressure in Train 4 (n=35).

Organic loading and cartridge filter monitoring data were examined to evaluate whether the operational changes to the RO membranes (specific flux and differential pressure) were a result of biological fouling. A small dataset (n = 16) for AOC, TOC, and UV_{254} suggested that organic content of the RO feed increased as specific flux decreased ($r = 0.933$, $n = 16$, $p < 0.01$). To confirm this, a larger dataset (n = 120) using monitoring data at the cartridge filter was investigated to ascertain treatment impacts and operational effectiveness on organic carbon removal and the impact on RO fouling. Monitoring and chemical dosing data after the cartridge filters were used for an evaluation of the plant condition at this treatment step. Cartridge filter monitoring data included differential pressure, turbidity and silt density index (SDI) compiled from hardcopy records at TBSDP for the period for August through December 2012. Differential pressure increased at two intervals, with peaks on October 15 and November 18, 2012 (average 6.9 psi; range 4 – 35; n = 120; Figure 10). During these same periods, SDI of the Train 4 cartridge filtrate averaged 3.9 (range 2.9 – 4.9; n = 119; Figure 11). Correlations were weak between differential pressure or specific flux and the predictor variable SDI (Table 6), which are not surprising; SDI is inadequate for addressing a range of fouling issues because the test is limited to only measuring particles and not the BOM that contributes to biofouling. Turbidity was generally low and stable below 0.5 NTU, in most instances less than 0.25 NTU (average 0.11; range 0.05 – 0.35; n = 119; Figure 12). Turbidity had an inverse relationship to differential pressure ($r = -0.45$, $p < 0.01$, $n = 34$), and in the absence of a positive relationship depicted, the results suggest that the increases in differential pressure were not solely caused by particulate or colloidal fouling. Interpretation of the data would suggest that the fouling was biological from AOC loading after startup in August, the effects of which were observed through November. It should be noted that the data exhibited autocorrelation based on parameters described in Durbin-Watson significance. Given that the increase of differential pressure and decline of specific flux is associated with

continued operation, the influence of time on the datasets appears to be a factor for certain outcomes of this full scale facility and limited operational periods of the data collection effort.

SBS was applied to the cartridge filtrate to remove the chlorine disinfectant residual and decrease ORP in the RO feed. The highest SBS doses from that quarter were applied in October and November (during the same periods in which differential pressure increased). From plant startup on August 14 until December 31, the average SBS dose was 8 mg/L and ranged from 3 to 123 mg/L. AOC concentrations in the RO feed were extrapolated from the SBS dose. SBS used at TBSDP was investigated in bench-scale testing (Chapter 3), and impurities in the solution increased AOC. In addition to bench-scale tests, SBS increased AOC at the RO feed during sample collection (Table 3). The reported concentrations represented more conservative estimates, in which average AOC was 150 µg/L (range 90 – 1830 µg/L; n = 123) versus another model that predicted average AOC to be 190 µg/L (range 70 – 3020 µg/L; n = 123). Using the conservative approach, calculated AOC results were similar to the grab sample results; cartridge filter AOC was 97 µg/L in September and the extrapolated AOC from SBS dosing was 98 µg/L. AOC in the RO feed for Train 4 during the period of investigation is depicted in Figure 13. AOC in the RO feed was evaluated as a variable for predicting fouling (observed from decreased specific flux and increased RO differential pressure; Table 6). Of the possible predictor variables for fouling including cartridge filter differential pressure, SDI, cartridge filtrate turbidity, and RO feed AOC, the strongest correlation was with AOC ($r = 0.563$, $p = 0.001$, $n = 34$; Table 6).

The relationships among TOC, UV_{254} and AOC were evaluated to determine whether these parameters were significantly correlated ($p < 0.05$). TOC and UV_{254} were correlated ($r = 0.61$, $p = 0.05$); however, AOC showed no significant relationship at TBSDP with UV_{254} ($r = 0.36$, $p = 0.28$) or TOC ($r = 0.43$, $p = 0.19$). Given the lack of specificity for TOC and UV_{254} in

measuring the biodegradability of organic carbon present, it is recommended that this utility track AOC for predicting pretreatment changes impacting biofouling potential.

Table 6 Correlation and significance of predictor variables at TBSDP cartridge filter (CF) and RO feed for differential pressure and specific flux from September – November 2012.

	Differential Pressure		Specific Flux	
	Pearson correlation	*p** (2-tailed)	Pearson correlation	*p** (2-tailed)
CF differential pressure (n=35)	0.187	0.282	-0.219	0.206
CF SDI (n=33)	-0.232	0.194	0.238	0.183
CF turbidity (n=34)	-0.450	0.008	0.397	0.020
AOC (n=34)	0.563	0.001	-0.495	0.003
Day (n=35)	0.965	0.000	-0.920	0.000

***Note: *p*-values are overestimated due to serial autocorrelation.**

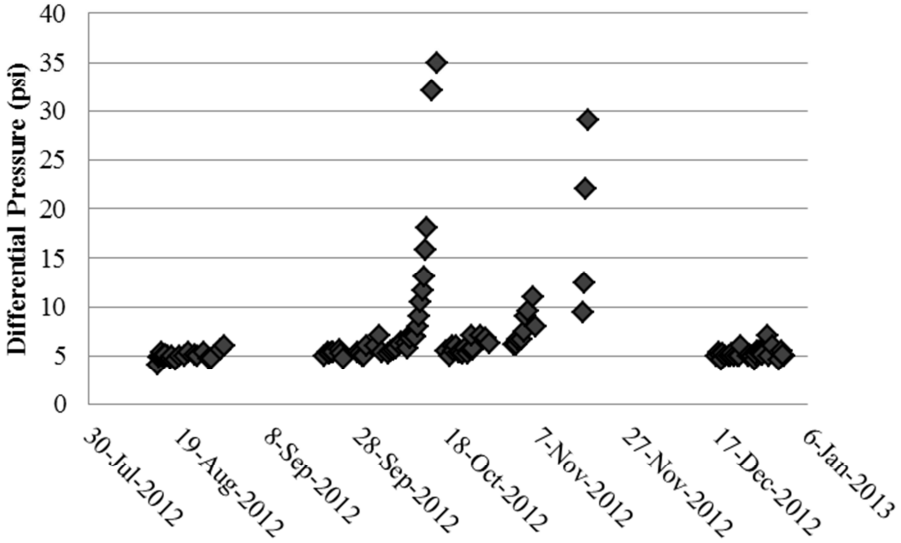

Figure 10 TBSDP Cartridge filters Train 4: Differential pressure during the analysis period in 2012. Peaks detected Oct. 15 and Nov. 18th. Average = 6.9 psi (range 4 – 34.9; n=120).

The SBS dose (n = 59, September – December) showed a positive relationship with differential pressure ($p < 0.01$) and a negative relationship with specific flux ($p < 0.01$). Increases

in differential pressure and decreases to specific flux occurred because of fouling on the membranes during the periods investigated. TBSDP has experienced biofouling in the past on account of water quality issues at the intake and the high concentration of organic carbon in the RO feed. Pretreatment generally removes less than 10% of TOC, and sampling events indicate that AOC was increased in the post-cartridge filter sampling point (i.e., RO feed). The only chemical addition at that point was SBS, and in conjunction with the bench-scale testing, operational records and statistical evidence, the addition of SBS increased AOC in the RO feed. These conditions were conducive to biological growth on the RO membranes, and, given the low potential for particulate fouling, chemical dosing and operational parameters suggest that the fouling was biological in nature.

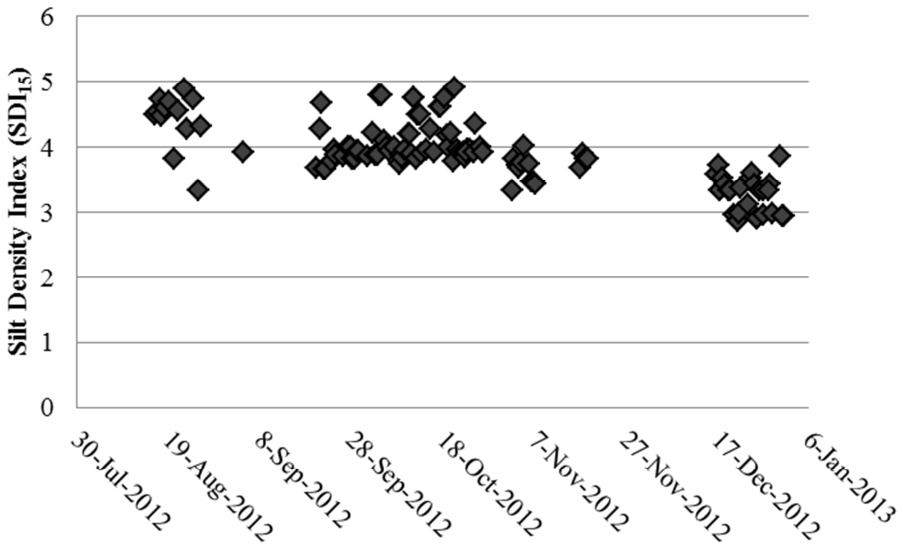

Figure 11 TBSDP Cartridge filters Train 4: Silt Density Index during the analysis period in 2012. Average = 3.9 (range 2.9 – 4.9; n=119).

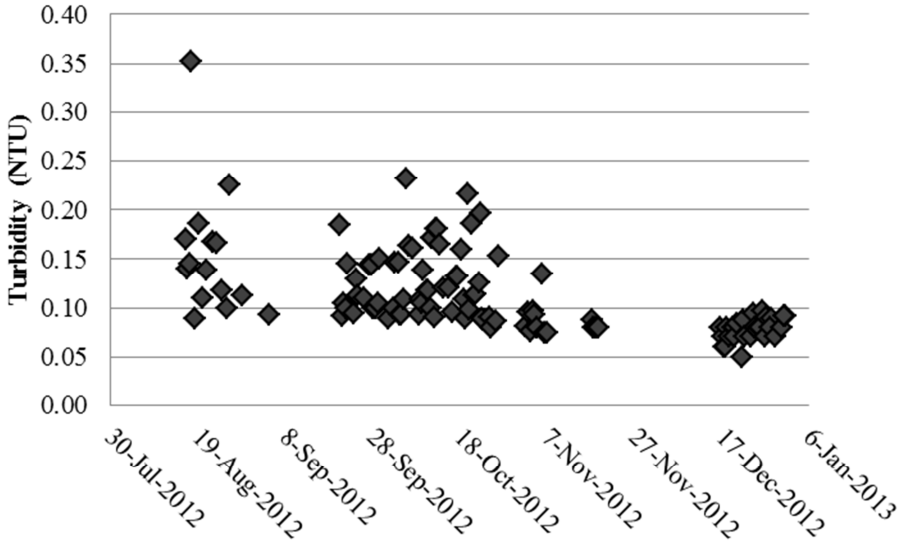

Figure 12 TBSDP Cartridge filters Train 4: Turbidity during the analysis period in 2012. Average 0.11 NTU (range 0.05 – 0.35; n=119).

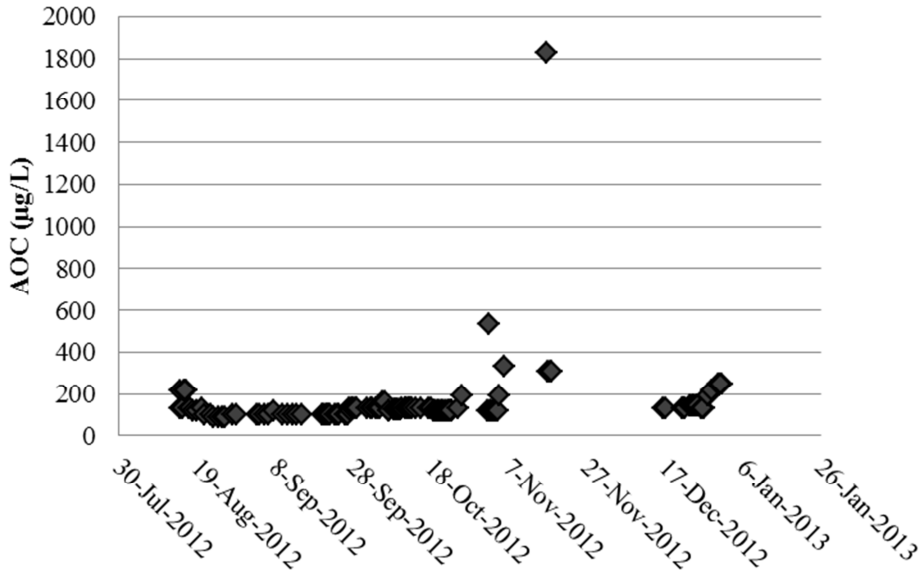

Figure 13 TBSDP Train 4 AOC in RO feed. Average AOC 150 µg/L (range 90 – 1830 µg/L; n = 123).

2.6.4 West Basin Municipal Water District Pretreatment and Organic Carbon Removal

Four sampling sets were collected from WBMWD for the purpose of evaluating the changes to organic carbon through the pretreatment process (Table 7). Samples were collected on June 5, July 31, November 29, and December 28, 2012. During that time the plant was producing about 0.05 MGD of desalinated water. The sampling locations included raw seawater (after intake screen and before Arkal filter pods), UF feed following Arkal screening and ferric chloride addition, UF filtrate, feed to the cartridge filter after chemical addition (when applied), and at the RO feed after the cartridge filters. A shipping issue during the November sampling resulted in a loss of the UF filtrate and RO feed samples.

Average TOC throughout the treatment train was 1.09 ± 0.07 mg/L in June, 0.9 ± 0.03 mg/L in July, and 0.7 ± 0.05 mg/L in December. In the fall and winter sampling events, TOC was lower than in the summer but increased during pretreatment. During June and July, TOC was only removed by 5% throughout pretreatment. Average AOC throughout treatment was also greatest in June, particularly before UF treatment. In June the water quality evidence from lower pH, higher ORP, higher AOC, TOC, and UV_{254} were all different from the other sampling events. Changes to organic carbon during pretreatment are graphically represented in Figure 18. In July, both AOC and UV_{254} were higher at the RO feed than in the intake, which was not reflected in the TOC dataset. Average AOC from July was 55 ± 30 µg/L and in June it was 79 ± 57 µg/L. In the June event, AOC was reduced between the intake and RO feed by 110 µg/L. In July, AOC at the intake was < 30 µg/L but increased to 90 µg/L in the RO feed during the time in which preformed chloramine was dosed at 5 mg/L (ORP 468 mV). No other chemical addition was responsible for both the increase in AOC and UV_{254} in the cartridge filter and RO feeds. AOC was incrementally higher at two pretreatment locations: after coagulation and after SBS dosing at the location before the cartridge filter. Chemical dosing at the plant accounted for the higher AOC levels upstream of

the RO feed. Increased AOC from the presence of cleaning agent residuals and the addition of SBS was not reflected in the TOC levels.

Table 7 WBMWD organic carbon and water quality data. UF = ultrafiltration step; SBS = sodium bisulfite. ORP = oxidation reduction potential.

	Treatment Step	TOC (mg/L)	AOC (µg/L)	UV_{254} (cm^{-1})	pH	ORP (mV)
June (18° C)	Raw seawater	1.08	131 ± 24	0.014	7.9	311
	UF Feed	1.16	145 ± 2	0.017	7.9	305
	UF Filtrate	1.01	33 ± 9	0.013	7.9	301
	Cartridge filter feed	1.15	67 ± 26	0.011	7.8	265
	RO feed	1.03	20 ± 5	0.010	7.8	270
July (17°C)	Raw seawater	0.91	27 ± 4	0.013	8.1	294
	UF Feed	0.92	20 ± 13	0.011	8.1	276
	UF Filtrate	0.88	62 ± 9	0.010	8.1	282
	Cartridge filter feed	0.91	79 ± 20	0.042	8.1	463
	RO feed	0.86	89 ± 20	0.040	8.1	468
November (16°C)	Raw seawater	0.88	8	0.009	8.1	270
	UF Feed	0.87	3	0.007	8.1	228
	Cartridge filter feed	0.92	14	0.007	8.0	210
December (15°C)	Raw seawater	0.68	18 ± 2	0.010	8.0	144
	UF Feed	0.62	30 ± 15	0.017	7.9	168
	UF no SBS	0.64	12 ± 2	0.006	7.7	173
	UF SBS	0.63	63 ± 9	0.007	6.5	123
	Cartridge filter feed	0.75	15 ± 4	0.010	7.2	173
	RO feed	0.73	15 ± 0	0.010	7.2	164

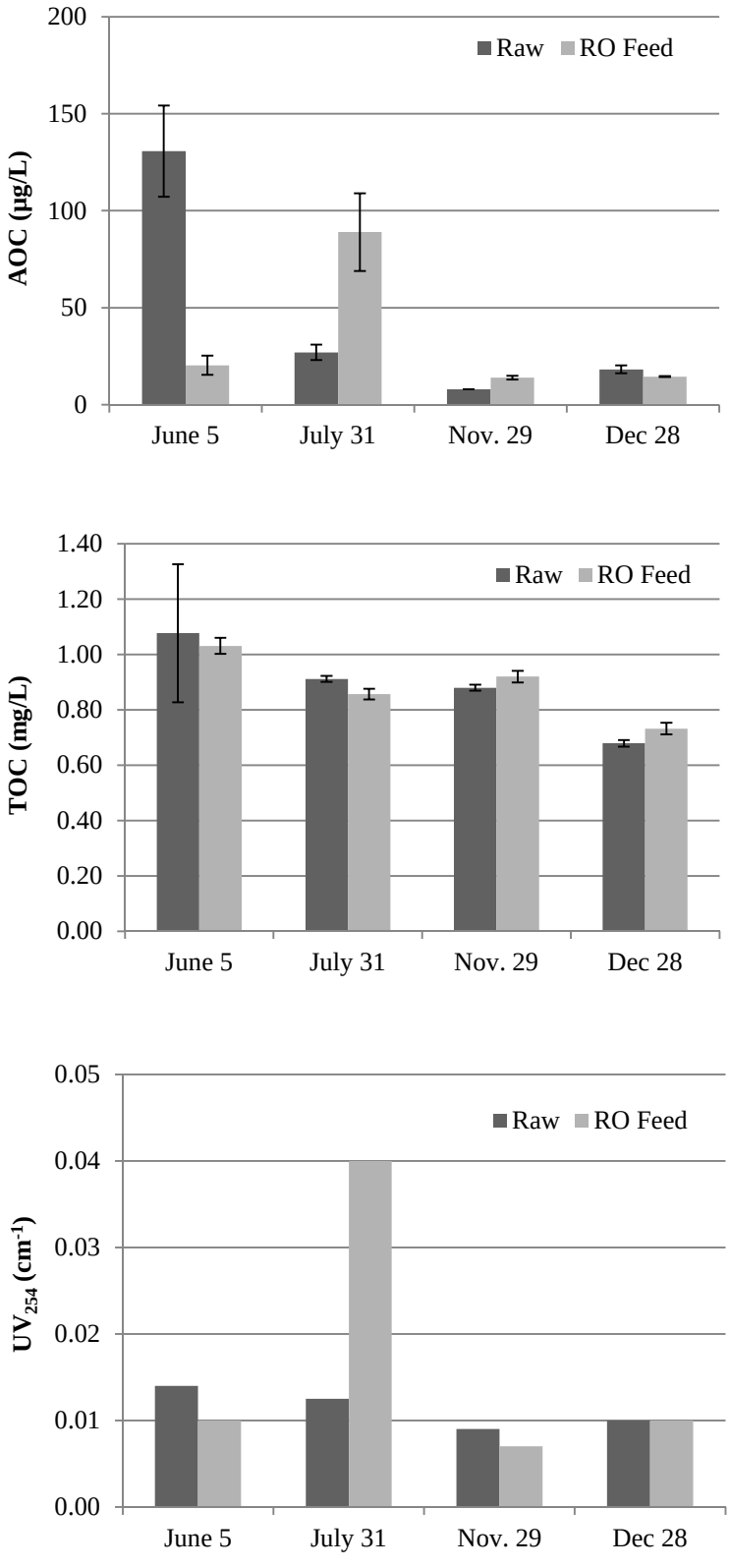

Figure 14 WBMWD: Organic carbon in the raw seawater and the RO feed.

The relationships among TOC, UV_{254} and AOC were evaluated to determine whether these parameters were significantly correlated ($p < 0.05$). TOC did not have a significant relationship with UV_{254} ($r = - 0.05$, $p = 0.75$) or AOC ($r = 0.01$, $p = 0.97$); however, AOC and UV_{254} are very strongly correlated at WBMWD ($r = 0.995$, $p < 0.001$). Through additional testing using long term correlations, it may be possible to track biofouling potential using routine UV_{254} and AOC measurements.

2.6.5 WBMWD Data Modeling

Operational performance of the plant that coincided with the grab samples was tracked to identify changes that were indicative of biological fouling. To that end, RO operational monitoring data were collected for June through August and November through December 2012 and included flow (gpm), conductivity (mS), RO feed temperature (°C), differential pressure (difference between feed and concentrate pressure, psi), permeate flow from the front and tail, and conductivity from the front and tail permeate. Specific flux of the entire RO train was calculated from the permeate flow (sum of front and tail flows in gpd) divided by the net driving pressure (psi) and total area of the membranes (5600 ft^2). Net driving pressure was calculated according to the equations provided by the consulting contractor for WBMWD (Figure 15). Daily averages were calculated from the 15-minute increments and outliers embedded in the data set were removed from the averages (loss of system correspondence or briefly offline). Observations of the data indicated major changes between July and November with regard to differential pressures and specific flux. From June through August, normal trends were apparent, but the November through December data were noticeably different (Figure 16 and Figure 17). WBMWD confirmed that the changes were from ongoing testing of new membranes and hybrid configurations, which consisted of 21 separate runs using two models of membranes alone in the vessels and combined as hybrids.

P_{net} = NDP = Net Driving Pressure (psi)

$$P_{net} = P_{feed} - \Delta\pi - \frac{\Delta P}{n+1} - P_{Permeate}$$

where:

$\Delta\pi$ = Average Osmotic Pressure Differential (psi)

$= 0.006 \times$ Average Feed/Brine Conductivity

n = Number of stages in Array

$$\text{Average Feed/Brine Conductivity} = \text{Conductivity of Feed} \times \left[\frac{\ln\left(\frac{1}{1-Y}\right)}{Y}\right]$$

where:

$$Y = \text{Recovery} = \frac{\text{Permeate Flow}}{\text{Concentrate Flow + Permeate Flow}}$$

ΔP = Feed Pressure - Concentrate Pressure (psi)

$P_{Permeate}$ = Permeate pressure (psi)

Figure 15 Calculations for net driving pressure (NDP) of the RO membranes.

The organic carbon results from the water quality sampling were incorporated into a 2 week period before and after the sampling date. Extending the values in this way followed the assumption that water quality changes would be minimal in the absence of major treatment changes or incoming water quality fluctuations otherwise not detected during the four periods in June, July, November, and December. The data were extended based on similar differential pressure and specific flux near the sampling dates. Water quality data were input for June 1 through 16, July 27 through August 9, November 17 through 25, and December 11 through 29. Because of a shipping issue during the November sampling event the RO feed was not available, and therefore the water quality data from the cartridge filter feed were used. The data were analyzed using statistical software (SPSS19; IBM Corp.).

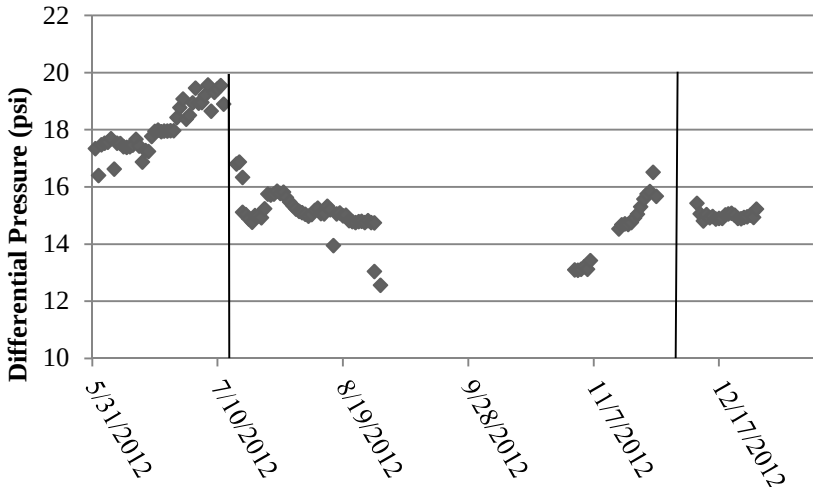

Figure 16 WBMWD: Differential pressure of the first pass RO from June to December 2012 (n=163). Data are reported for the months in which grab samples were collected (June, July, November, December). A clean in place (vertical line) was conducted on the RO membranes on July 12 and December 6, 2012. Membrane configurations were changed during the duration of testing.

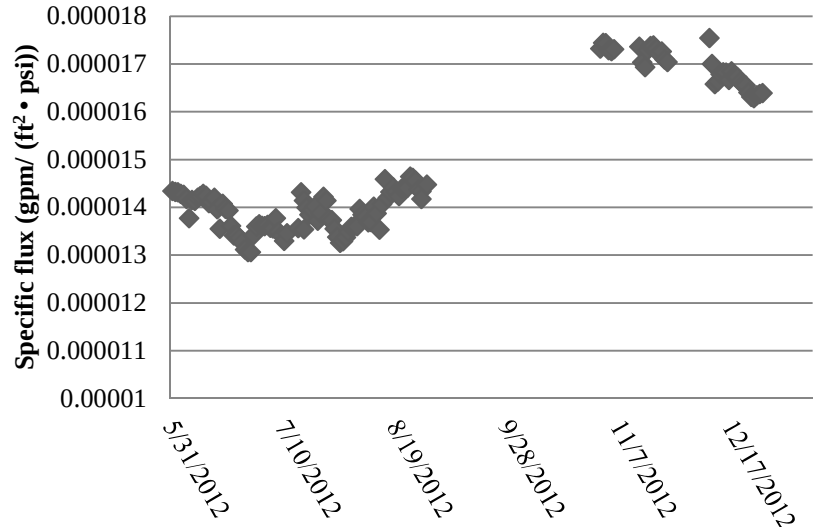

Figure 17 WBMWD: Specific flux of the first pass RO from June – December 2012 (n=163). Data are reported for the months in which grab samples were collected (June, July, November, and December). Membrane configurations were changed during the duration of testing.

2.6.6 WBMWD Operational Performance and Data Modeling Results

During the year in which this study was conducted, both chemical pretreatment and membrane types were varied at WBMWD. Membranes were changed between October 30 and November 15, 2012 and again between November 15 and December 31, 2012; other changes included adjustments to recoveries, flux, and feed flow. Because of the inherent variability, there was limited opportunity to evaluate meaningful relationships between the water quality of the seawater and long term operational impacts. Although the approach for correlating differential pressure or other operational changes to organic carbon in the RO feed was limited, there was evidence that pretreatment chemicals and oxidation increased the biodegradable organic carbon in seawater. The addition of chloramines and SBS were indicative of increases in AOC but less often for changes to TOC and UV_{254} measurements (Table 7). Clean in place was performed on the RO membranes after increases in differential pressure were observed and reported by the plant's operations staff to be related to biofouling. Clean in place was performed on July 12 and December 6, 2012. Raw seawater results in June indicated more organic carbon compared to other sampling events (Table 7).

Bivariate correlations for organic carbon are reported in Table 8. In the full dataset, differential pressure decreased over time as a result of cleaning and new membrane installations ($r = -0.778$, $p < 0.01$, $n = 58$) which was also reflected in a strong correlation with increasing specific flux ($r = 0.884$, $p < 0.01$, $n = 58$). TOC had a very strong positive relationship with differential pressure and a strong negative relationship with specific flux. AOC and UV_{254} in the RO feed did not have any remarkable relationship to differential pressure. Specific flux and AOC in the RO feed had the strongest negative correlation compared to TOC and UV_{254} results. The team anticipated that differential pressure would be related to AOC assuming that operating conditions and membrane types were the same in a modeled dataset; but this was not the case

during the time in which the data were collected. The membranes were changed in a set of 21 tests in November and December, which was part of another project being conducted at the plant. Although differential pressure could be higher with higher average feed/concentrate flow (for constant water temperature), the normalized specific flux should not vary unless the membranes were fouled. As seen in Figure 17, a flux decline occurred in the November and December dataset. The decline in specific flux during the monitoring period correlated to each of the organic parameters that were measured, and AOC had the strongest and most significant relationship.

Table 8 Correlation and significance of predictor variables from the WBMWD RO feed for differential pressure and specific flux from June – December 2012 (n=58).

	Differential Pressure		**Specific Flux**	
	Pearson correlation	***p** (2-tailed)**	**Pearson correlation**	***p** (2-tailed)**
AOC	-0.134	0.317	-0.705	< 0.01
TOC	0.817	< 0.01	-0.513	< 0.01
UV_{254}	-0.176	0.185	-0.683	< 0.01
Day	-0.778	< 0.01	0.884	< 0.01

*Note: *p*-values are overestimated due to serial autocorrelation.

2.6.7 Al Zawrah Pretreatment and Organic Carbon Removal

Samples were collected within the treatment train from Al Zawrah on May 29, July 29, and November 4, 2012. Samples for water quality analysis included raw seawater from the intake without chemical addition, DMF feed and filtrate and filtrate from the cartridge filters. In the May event, TOC ranged from 3 to 14 mg/L through the treatment steps and AOC was 75 to 197 µg/L (Table 9). In the July sampling event TOC averaged 1.1 ± 0.1 mg/L, and AOC averaged 9 ± 5 µg/L. Discussions with the plant manager indicated that during the May event an algal bloom in the area affected the intake pH of the seawater, which was typically 8.1 had dropped to 7.5. Changes to organic carbon during pretreatment are graphically represented in Figure 18. AOC and TOC concentrations were lower in July than in the May event presumably because there were

no impacts from red tide at the intake. TOC and UV_{254} measured in the November sampling were minimally impacted during pretreatment, but the AOC increased in the filtrate from the DMF. DMF filtrate removed between 21 and 43% of the AOC in the DMF feed in the previous sampling events. Organic carbon removal by DMF may occur through adsorption or biodegradation mechanisms (Naidu et al. 2013). Biologically active filters are dynamic in the sense that maturation of the filter affects organic removal potential; depending on the filter age, filtration rate, presence of disinfectant or other factors, biodegradation in the filter could be reduced and organic carbon breakthrough or microbial detachment may occur.

Table 9 Al Zawrah organic carbon and water quality data. DMF = dual media filtration; CF = cartridge filtration.

	Treatment Step	TOC (mg/L)	AOC (µg/L)	UV_{254} (cm^{-1})	pH
May (32 °C)	Raw seawater	2.9	197	0.017	7.5
	DMF Feed	13.7	143	0.033	7.5
	DMF Filtrate	3.8	113	0.012	7.5
	CF filtrate	5.6	75	0.012	6.9
July (35 °C)	Raw seawater	1.21	2	0.020	7.7
	DMF Feed	1.17	14	0.052	7.7
	DMF Filtrate	0.96	8	0.012	7.7
	CF filtrate	1.04	12	0.011	7.0
Nov. (30 °C)	Raw seawater	1.26	4	0.013	7.7
	DMF Feed	1.24	2	0.012	7.7
	DMF Filtrate	1.22	147	0.010	7.7
	CF filtrate	1.24	181	0.012	7.0

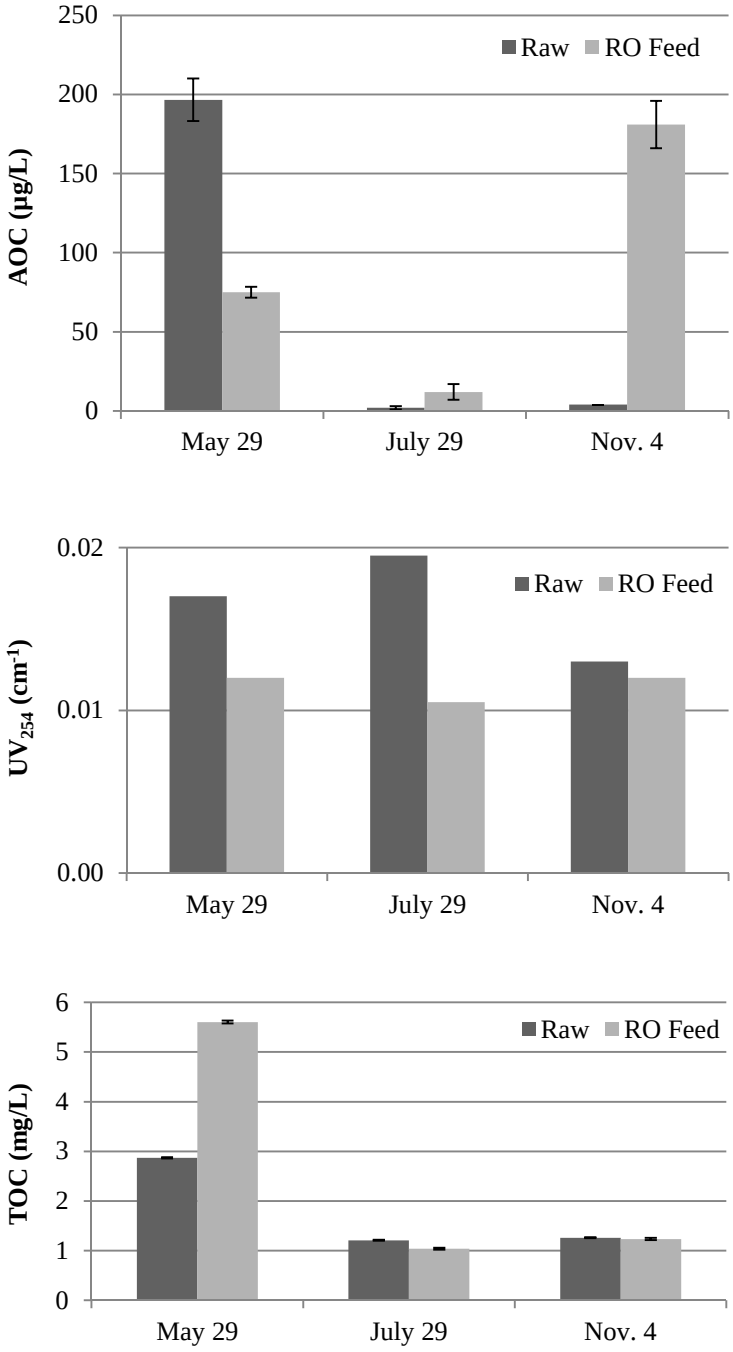

Figure 18 Al Zawrah organic carbon in the raw seawater and the RO feed.

2.6.8 Al Zawrah Data Modeling Approach

Al Zawrah plant performance was evaluated using DMF and cartridge filter operational data. Manual log sheets were copied and submitted to the project team for analysis of the plant's

condition. Records were submitted for the DMF (pressure, flow, temperature, online differential pressure transmitter, online filtrate turbidity, free chlorine in filter outlet), cartridge filter (online differential pressure transmitter, SDI, ORP), and pH of the RO feed. Operational data were collected in 4-hour increments for May, July, and October through November. During the collection times in 2012 the plant was not using normalization software for its record keeping. The absence of RO operating information limited the evaluation of water quality impacts on the RO system; however, the condition of the plant was evaluated with respect to differential pressure of the media and cartridge filters in conjunction with the organic carbon results from the same collection periods. Changes in differential pressure at the cartridge filter would provide evidence that biological growth may have occurred on the filters.

2.6.9 Al Zawrah Operational Performance and Data Modeling Results

Organic measurements were extrapolated between May 28 and 30, July 28 and 30, and November 1 and 6. Differential pressure in the cartridge filter increased in July and November near the sampling events (Figure 19). ORP of the cartridge filtrate was greatest in November (Figure 20). The data showed strong positive correlation between differential pressure of the cartridge filters and AOC in the RO feed ($r = 0.984$, $p = < 0.01$, $n = 48$). UV_{254} had strong positive relationships to the cartridge filter data (ORP and differential pressure; Table 10) but the measurements in the dataset were 0.011 and 0.012 cm^{-1} (average = 0.01 cm^{-1} ± 5%), which indicates no meaningful impact of UV_{254} on fouling. The pressure differential for the DMF had strong relationships to the organic carbon data, but the meaning of that is not as clear because the function of the filters is not impacted only by organic carbon content of the water, but more so by flow rates, backwash frequency, source water quality, and turbidity. Of the plants investigated, only the Al Zawrah facility had the potential for biological removal of AOC by a media filter (Tampa's sand filters contain chlorine residual), but biological activity and subsequent removal of

AOC was not consistent. TOC removal was not consistent either; maximum removal was 14%, but the other sampling events showed less. Poor organic removal and inconsistent operations are widespread challenges in desalination. The positive and strong relationships determined when AOC was investigated as a predictor variable for biological growth confirms the presence of biodegradable organic carbon and its impact on operations. Furthermore, AOC was not significantly correlated to TOC ($r = 0.38$, $p = 0.22$) or UV_{254} ($r = -0.11$, $p = 0.74$). No relationship was apparent for TOC and UV_{254} ($r = 0.29$, $p = 0.37$). Given the lack of relationships among these parameters, additional monitoring using AOC and operational changes to identify increases in biofouling potential are recommended. Although RO data were not available, relationships between AOC and biological growth that lead to changes in differential pressure and other operational data exist. If AOC is monitored and pretreatment optimized for removal of organic carbon, biological fouling on both cartridge filters and ultimately on RO membranes would be reduced.

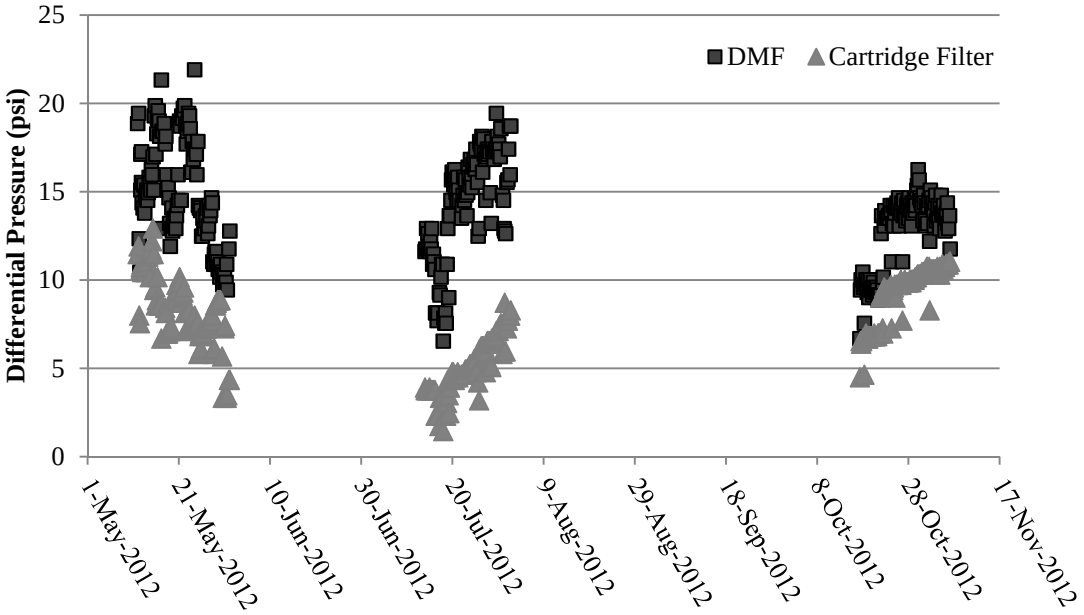

Figure 19 Al Zawrah differential pressures during the collection periods for the dual media filter (DMF) and the cartridge filters.

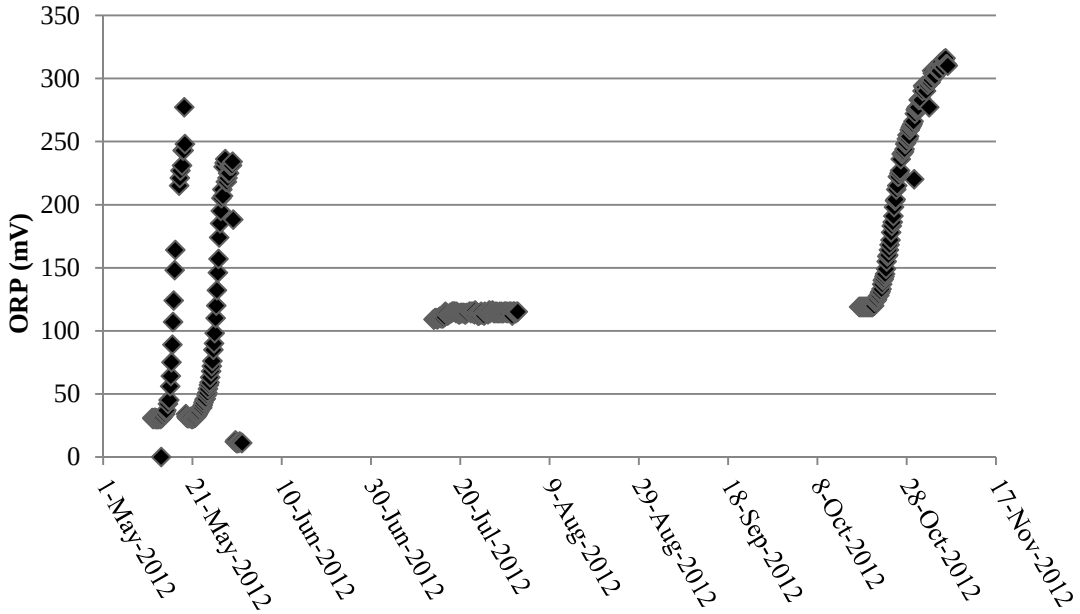

Figure 20 Al Zawrah oxidation reduction potential (ORP) of the RO feed during the collection periods.

Table 10 Correlation and significance of predictor variables from the Al Zawrah RO feed from May – November. ORP = oxidation reduction potential.

	Dual Media Filter Differential Pressure		Cartridge Filter Differential Pressure		Cartridge Filter ORP	
	Pearson correlation	***p** (2-tailed)**	**Pearson correlation**	***p** (2-tailed)**	**Pearson correlation**	***p** (2-tailed)**
AOC	-0.521	< 0.01	0.980	< 0.01	0.984	< 0.01
TOC	-0.670	< 0.01	-0.099	0.505	-0.034	0.816
UV_{254}	-0.852	< 0.01	0.901	< 0.01	0.930	< 0.01

***Note: *p*-values are overestimated due to serial autocorrelation.**

2.6.10 Pilot Unit Results and RO Membrane Inspection

The system was set at 13% recovery; under this constant setting for permeate flow the changes to driving pressure were monitored and further evaluated. Feed pressure ranged from 660 to 720 psig during operation, and pressure of the concentrate (or brine) ranged from 590 to 620

psig. Initial pressure conditions were 660 psig at the feed line and 610 psig at the brine outlet. Differential pressure was monitored from March 26 through April 3, 2013 and increased from 50 to 90 psig during the 9 day operating period (Figure 21, Table 11). Even though the permeate flow rate was set at 0.317 gpm (457 gpd), specific flux decreased during operation. Permeate flow was normalized for temperature and pressure at each of the data points and then divided by the net driving pressure to determine specific flux. Specific flux decreased from 0.32 to 0.25 gpm, a 22% decrease (Figure 21). Salt rejection remained consistent and ranged from 99.6 to 99.8% (data not shown).

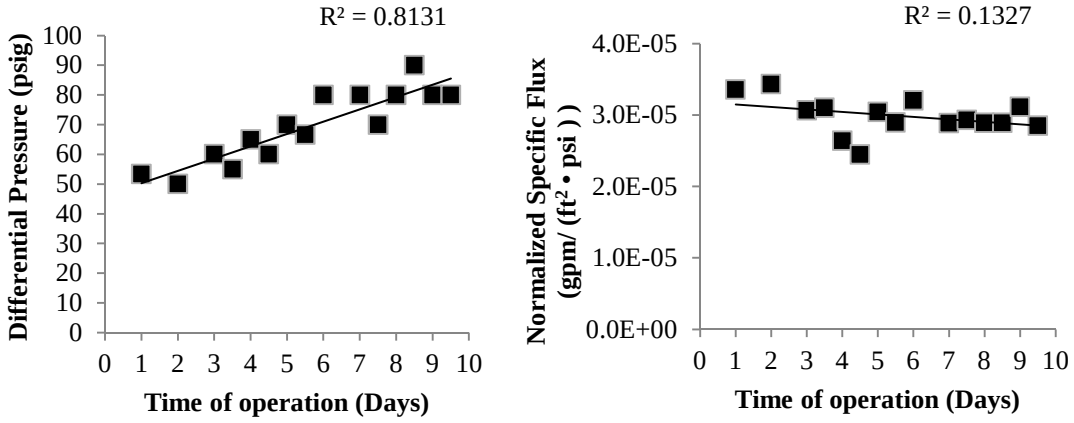

Figure 21 Pilot unit RO differential pressure and specific flux during operation.

Organic carbon was present in the RO feed throughout the duration of the experiment (Table 11). TOC ranged from 3.6 to 4.3 mg/L, and UV_{254} ranged from 0.09 to 0.12 cm^{-1}. SUVA ranged between 2 and 3 L/mg-m which suggests that the organic matter may be a mixture of algae-derived organic carbon with less humic matter present; the water had already been coagulated, so the low ratio of humic matter was consistent. AOC fluctuated during the first 5 days of operation between 22 and 161 µg/L and decreased throughout the duration of the testing, following a trend exhibited by TOC data. Average AOC was 60 µg/L, and the median was 50 µg/L AOC.

Increases in differential pressure detected between the feed and concentrate suggest that fouling material deposited on the membrane inhibited the flow through the RO membrane. The nature of the fouling that caused the increase was further investigated during the membrane autopsy described later in this section. AOC present in the feed provided a source of nutrients for bacterial growth and proliferation on the membrane. Biological fouling was evident on the membrane surface; it inhibited flow and led to the observed increase in differential pressure. To further evaluate the impact of the different organic carbon measurements, the data were modeled. Statistical significance of the constituents is discussed in the following section.

Table 11 Pilot unit operational and organic carbon data.

Day	Differential Pressure (psi)	Specific flux (gpm/(ft^2• psi))	AOC (µg/L)	AOC μ_{max} (hr^{-1})	TOC (mg/L)	UV_{254} (cm^{-1})	SUVA (L/mg-m)
1	53	0.000034	63	0.01	4.29	0.09	2.07
2	50	0.000034	161	0.02	4.09	0.09	2.11
3	60	0.000031	60	0.02	4.01	0.10	2.37
3.5	55	0.000031	68	0.02	3.75	0.08	2.19
4	65	0.000026	57	0.02	3.73	0.09	2.34
4.5	60	0.000025	113	0.01	3.46	0.09	2.66
5	70	0.000030	22	0.03	3.71	0.10	2.72
5.5	67	0.000029	71	0.01	3.79	0.09	2.29
6	80	0.000032	48	0.01	3.67	0.09	2.45
7	80	0.000029	36	0.01	3.50	0.09	2.54
7.5	70	0.000029	43	0.01	3.77	0.12	3.26
8	80	0.000029	45	0.02	3.80	0.10	2.55
8.5	90	0.000029	20	0.01	3.65	ND	ND
9	80	0.000031	50	0.01	3.62	0.09	2.54
9.5	80	0.000029	50	0.01	3.50	0.09	2.63

Regression analyses and bivariate correlations were investigated for differential pressure and normalized specific flux using SPSS analytical software (SPSS19; IBM Corp). These dependent variables were selected for evaluation of the organic carbon constituents of the RO feed that were correlated to biological fouling. Although recovery was held constant throughout operation, a 22% decline in normalized specific flux occurred (Figure 21). Predictor variables were AOC, TOC, SUVA, and UV_{254}, listed by significance in Table 12. The dependent variables (differential pressure and normalized specific flux) were also analyzed for correlation and significance to the day of operation.

The correlation between differential pressure and operating day was 0.90 ($p < 0.01$), which is consistent with the trends observed. In other words, differential pressure showed a positive increase over the duration of the testing. For normalized specific flux, the correlation indicated that a decrease occurred during operation (r = - 0.41), which was also determined by the calculations, which showed a 22% decrease. Bivariate correlations indicated that AOC was more significant ($p < 0.01$) than TOC ($p < 0.05$) for predicting differential pressure changes. Correlations between differential pressure with AOC and TOC were negative; AOC and TOC decreased over the duration of the test (Table 11). Plots of the predictor variables showing linear regression trends and coefficients of correlation (R^2) are presented in Figure 22. Conclusions drawn from this dataset would suggest that AOC measured in the RO membrane feed has a statistically significant impact on changes to differential pressure of the RO. Similar to the previous results reported in Section 2.6.3 for TBSDP water quality monitoring, AOC showed no significant relationship with UV_{254} (r = - 0.36, $p = 0.20$) or TOC (r = 0.32, $p = 0.24$). Although TOC and UV_{254} were correlated at TBSDP during the previous monitoring, there was no relationship between these parameters in the pilot testing reported here (r = - 0.06, $p = 0.84$). Given that TOC and AOC both had a significant relationship with differential pressure, a regression model was determined for these parameters. By incorporating TOC and AOC into a

model, both AOC and TOC were significant predictor variables for differential pressure (p = 0.001, F(2,12)=12.83, adjusted R^2 = 0.628). UV_{254} was not a significant predictor in the regression model. Given the consistent evidence for AOC as a significant predictor of operational impacts from biological fouling, it is important that utilities incorporate this evaluation into their monitoring plan. In some cases TOC, in addition to AOC, would be useful for understanding organic impacts on fouling.

Table 12 Pilot unit correlation and significance of predictor variables (n=15).

	Differential Pressure		**Normalized Specific Flux**	
	Pearson correlation	***p* (2-tailed)**	**Pearson correlation**	***p* (2-tailed)**
AOC	-0.71	< 0.01	0.19	0.488
TOC	-0.63	0.012	0.73	< 0.01
SUVA	0.52	0.059	- 0.51	0.065
UV_{254}	0.26	0.380	- 0.19	0.514
Op. Day	0.90	< 0.01	- 0.41	0.133

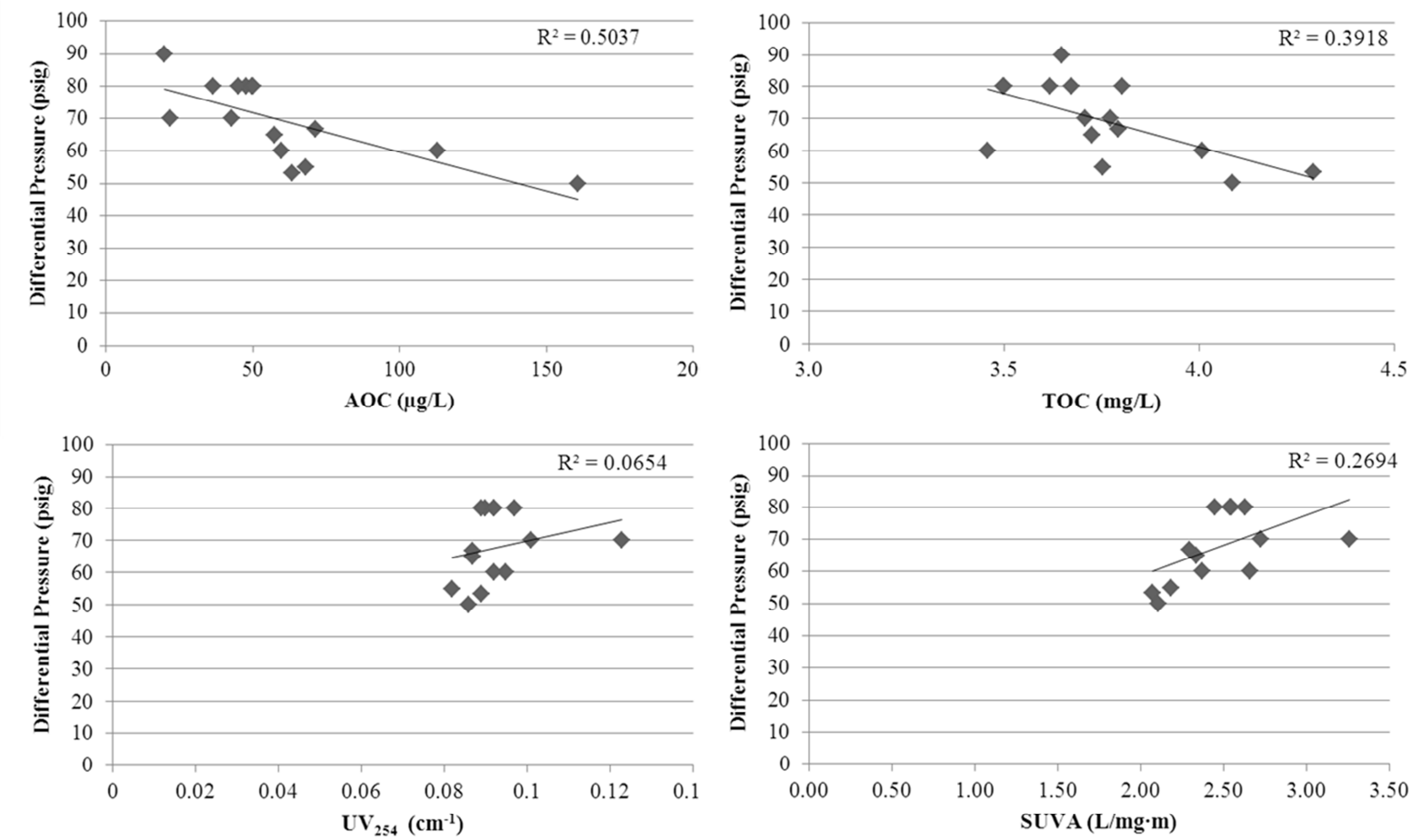

Figure 22 Pilot unit differential pressure and organic carbon data regression plots.

The membrane was removed on April 6, 2013 and sent to Delran, NJ for an autopsy. Photos were taken of the membrane prior to dissection (Figure 23). A circular saw was used to remove the end caps and split the fiberglass housing. The crossflow direction was noted to track the feed, middle, and brine regions of the element. It was carefully unrolled, and membrane swatches were removed from the three regions using a sterilized razor and portioned for ATP analyses and SEM.

Visual inspection indicated brownish deposits on the membrane and the feed spacer. The deposited material was slimy in texture and did not appear to be hard scale buildup. The deposition appeared to be organic or biological. The product collector did not show any discoloration or buildup. When the feed spacer was separated from the membrane the pattern was evident in the deposited material (Figure 23).

Figure 23 Pilot RO membrane after operation. The spiral wound membrane element opened during autopsy had evidence of biological fouling (source: the author).

ATP analysis of the membrane surface was conducted for three replicates from each location at the feed, middle, and brine areas on the membrane. ATP ranged from 1900 to 6200 ng

ATP/m^2 on the RO membrane surfaces. The lowest ATP was measured from the feed sections (Table 13).

Table 13 Pilot unit RO membrane ATP results.

Location	Replicate	Area (cm^2)	Area (m^2)	Luminescence	ng ATP/m^2 RO
Feed	1	1.40	0.000140	720161	1.9E+03
	2	1.40	0.000140	763553	2.1E+03
	3	1.08	0.000108	864099	3.1E+03
	Mean			782604	2.4E+03
	SD			*73835*	*6.4E+02*
Middle	1	1.56	0.000156	1848179	5.3E+03
	2	0.80	0.000080	962957	4.8E+03
	3	0.60	0.000060	941638	6.2E+03
	Mean			1250924	5.4E+03
	SD			*517347*	7.3E+02
Brine	1	0.36	0.000036	493725	4.8E+03
	2	0.91	0.000091	881294	3.8E+03
	3	0.84	0.000084	799109	3.7E+03
	Mean			724709	4.1E+03
	SD			*204215*	6.5E+02

There was a slimy fouling layer on the membrane and spacer observed during the visual inspection. Chemical fixation was conducted on the membranes to prepare the sections for imaging using SEM. By fixing and dehydrating the sample, evidence of biological fouling and bacterial deposition was preserved on the membrane. Fouling was examined on the membrane and feed spacers in SEM images. Bacteria approximately 1 µm in length were evident on both the feed spacer and the membrane (Figure 24 and Figure). The biofilms did not cover the entire imaged areas but were evident in patchworks in all samples. Images from the membrane spacer

the brine side and on the RO membrane had fouling layers and diatom fragments as well (Figure 26). The fouling layers had an accumulation of bacterial growth byproducts surrounding the bacteria, known as extracellular polymeric substances (EPS). Bacteria (as well as other cellular organisms) and EPS form the biofilm on the surface of the membrane. Based on the inspection and imaging of the membrane and ATP analysis, the results suggest that biological growth occurred on the membrane. The relatively short operation of the pilot system still provided sufficient biological growth substrate for proliferation as well as an observed decline in permeate flow and increase in differential pressure. By the fifth day of operation, sufficient fouling had occurred to maximize differential pressure to a constant 80 psi for the duration of the testing.

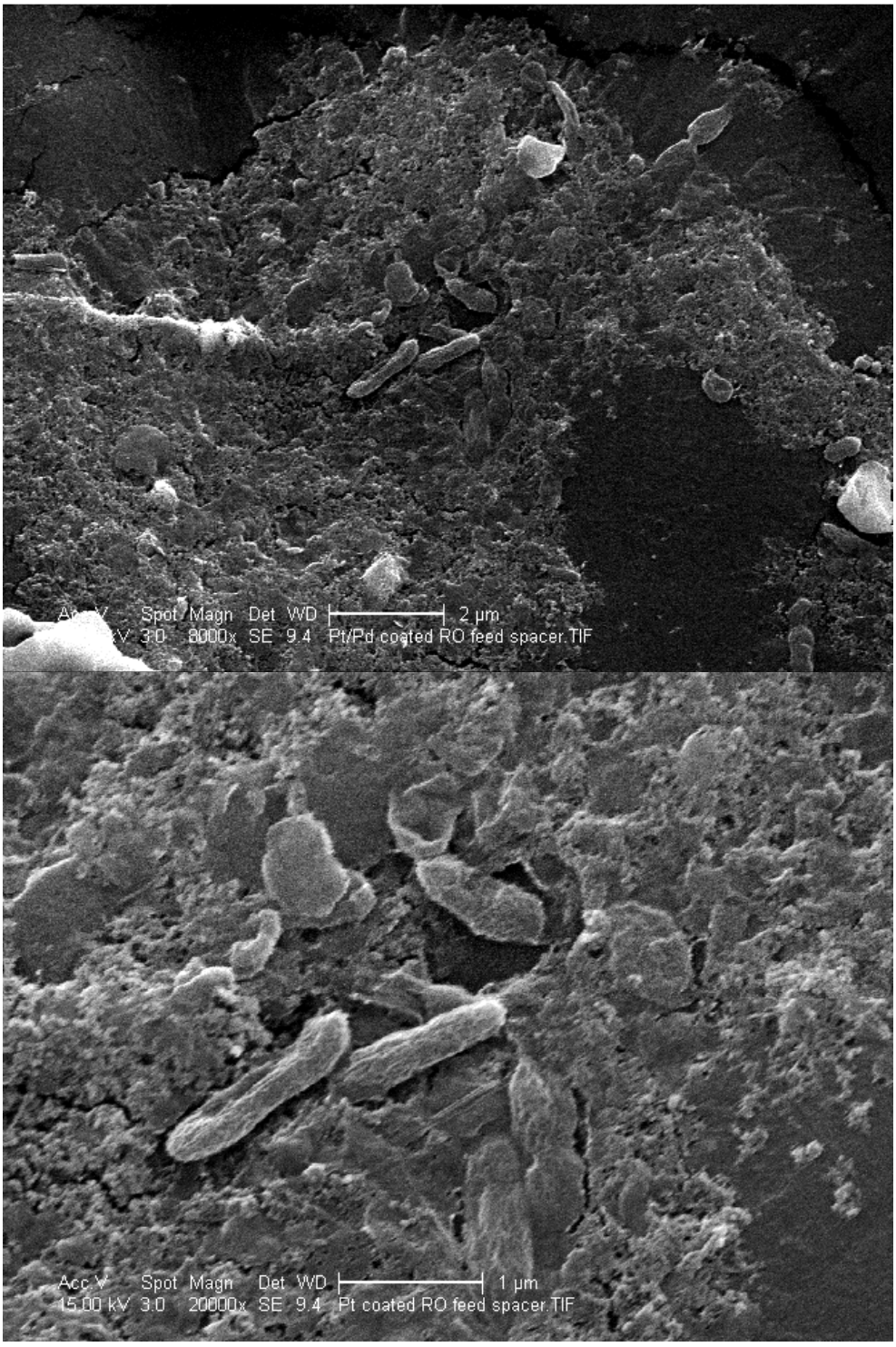

Figure 24 SEM images of pilot RO membrane feed spacer at 8000 and 20000 times magnification. Bacterial rods approximately 1 µm were detected within a biofilm matrix (source: the author).

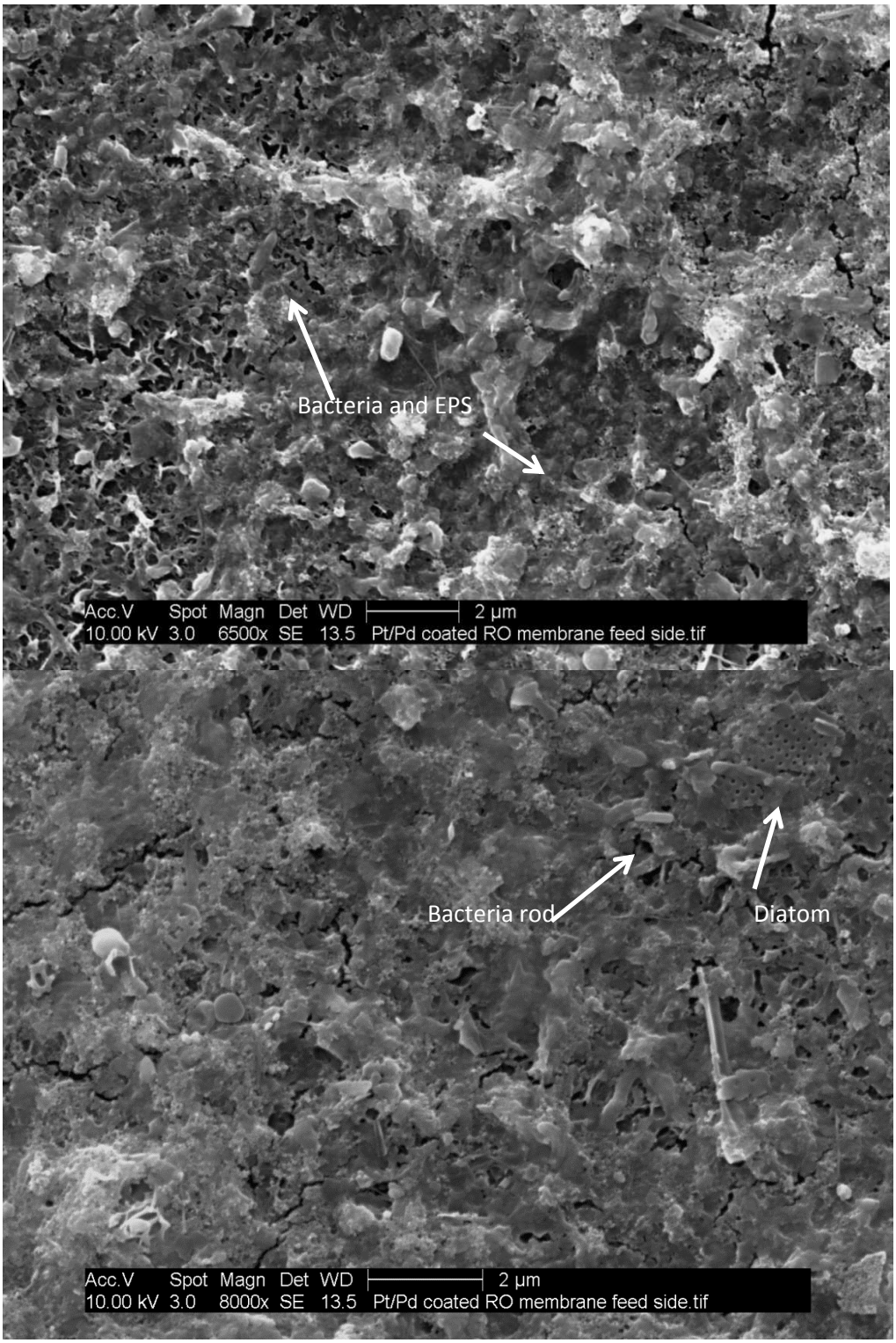

Figure 25 SEM images of pilot RO membrane from two different locations on the feed side. Biofilm contains bacteria, EPS and diatoms (source: the author).

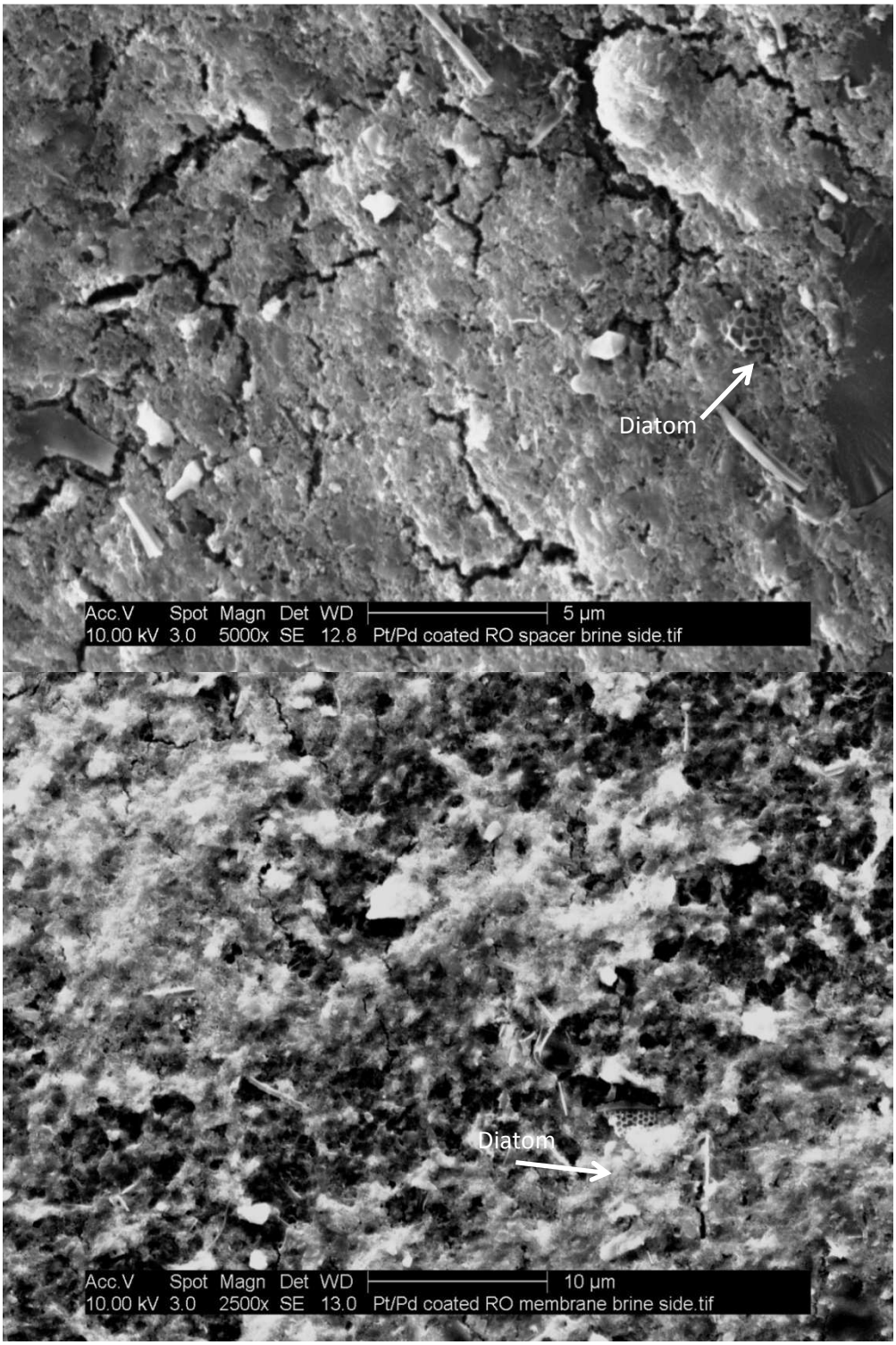

Figure 26 SEM images of pilot RO membrane feed spacer (top image) and brine side RO membrane (bottom) with fouling layer and diatoms (source: the author).

2.6.11 Membrane Test Cell Results and RO Membrane Inspection

Experiments were conducted using a once-through mode without recirculation to most closely mimic RO feed conditions and determine whether elevated AOC would be indicative of increased fouling potential. To achieve this objective, changes to permeate flux were compared in two experiments under similar operational conditions and constant pressure. RO feed water from TBSDP was used for the first baseline test. In a second test, acetate was injected to amend the RO feed with 1000 µg/L acetate carbon as an additional AOC nutrient source. Comparisons of permeate flux and autopsied membrane sections were evaluated to determine the extent of fouling from two different AOC feeds.

The permeate flux (J) from the baseline test was compared to the test from the elevated AOC experiment (Figure 27). Flux was calculated by dividing permeate flow (Lpm) by the membrane surface area (0.0042 m^2). The initial flux (J_0) of the membrane was 20 $L/m^2/h$; average normalized flux was 97 ± 5% during the baseline experiment and 76 ± 7% during the experiment in which seawater contained 1000 µg/L AOC (as acetate-carbon). With comparable nutrient levels and operational conditions in the two experiments, AOC was the targeted variable to evaluate its impact on flux. Biofilm growth and deposition occurred during these experiments and resulted in 24% flux decline in the AOC amended test compared to just 3% decline in the baseline test. SEM images confirmed that the membrane from the AOC amended test having greater flux decline showed evidence of bacterial, algal, and biofilm deposits throughout the membrane sections.

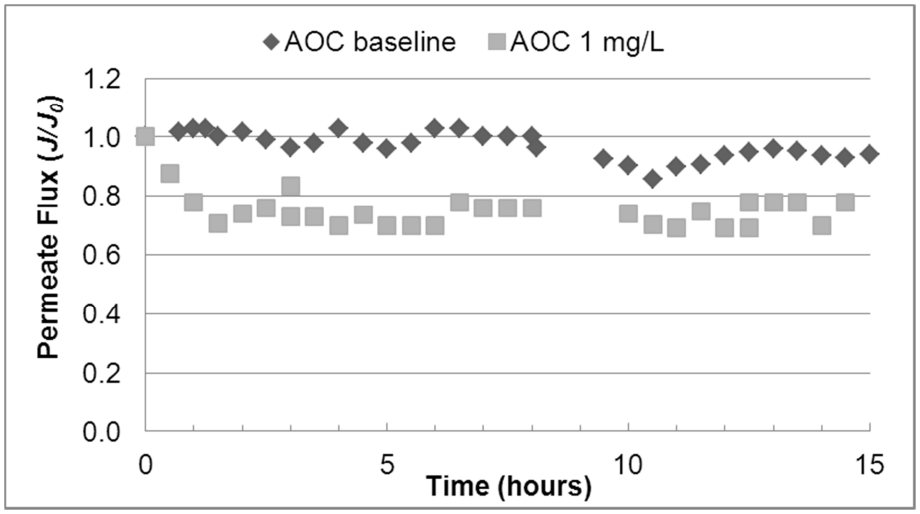

Figure 27 Normalized permeate flux from the membrane test cell using TBSDP RO feed. Pretreated TBSDP RO feed contained 30 µg/L AOC (baseline). Separate test used RO feed that was amended with 1,000 µg/L acetate.

Visual inspection of the membranes revealed the compression marking from the permeate carrier plate in the center of the element (Figure 28). Sparse brownish particulate was visible across the active areas of the membrane. In the membrane from the test with the acetate-amended feed (Figure 28, right) membrane wrinkling that occurred and appeared to follow the flow direction of the feed across the membrane (horizontally from right to left).

Figure 28 RO membrane from the membrane test cell (left: baseline feed test; right: acetate amended feed; source: the author).

Images of the membrane were taken of the feed, middle, and brine sides according to the orientation in the test cell. SEM was useful for evaluating the morphology of the membrane

surface after operation. Compared to the virgin membrane cut from a section beyond the active area in the test cell (Figure 29), the images of membrane from the baseline tests (Figure 30 – Figure 32) were similar, and nearly no occurrence of fouling material was detected on the feed and middle sections. On the sections taken from the brine side of the membrane (Figure 32), there were areas of compression on the membrane and singular 2 µm rods that were either bacteria or inorganic deposit.

In the SEM images taken of the membrane with acetate amendment, there was evidence of organic or biological fouling. The feed side had numerous areas of biofilm and bacterial rods within a biofilm and inorganic deposits (Figure 33). Images from the middle of the membrane mostly depicted slight coverage of fouling material; the membrane structure was still visible underneath (Figure 34), and some locations had more extensive deposits and areas of fouling and singular organisms (not shown). Images from the brine side of the membrane had less fouling, but there was some inorganic scaling and even a singular diatom with biofilm deposited near the upper left of the structure (Figure 35). Overall, the membrane from the AOC amended feed had more areas of fouling material covering the membrane compared to the membrane with the unamended baseline RO feed.

TOC concentrations differed by 1.1 mg/L in the two experiments on account of the amendment of acetate-carbon (1000 µg/L was delivered through injection of a concentrated feed). The baseline RO feed had 30 µg/L AOC versus 997 µg/L AOC in the amended feed. SUVA was near 1.4 L/mg-m, which is lower than the reported values in the previous sections because of pretreatment coagulation that removed humic material. Phosphate and nitrogen were present in sufficient supply and varied slightly between the two experiments. Phosphate was 0.16 and 0.13 mg/L in the baseline and amended AOC tests, respectively. Nitrogen was reported as the sum of nitrite, nitrate, and ammonia. In both tests, nitrite was 0.001 mg/L NO_2^-N, and nitrate was 0.3

mg/L NO_3^-N. Ammonia was 0.07 mg/L NH_3^-N in the baseline feed and 0.4 mg/L in the amended feed. The limiting nutrient in the baseline test was carbon, as determined by the molar carbon:nitrogen:phosphate (C:N:P) nutrient ratio of 69:5:1. In the AOC amended feed, nutrients were present in sufficient supply and had a C:N:P ratio of 107:11:1.

Nutrient balancing has been investigated as a way to control membrane fouling caused by biological growth and the production of EPS, which is generated when bacteria are present in a nutrient-limited environment specifically with reference to phosphate. The bacteria excrete a nutrient reserve to protect continued proliferation and adhesion to the surface. In conditions where the nutrients are balanced, bacteria are able to proliferate freely and do not produce EPS in the same amounts. The lower carbon ratio in the baseline test in conjunction with evidence from the SEM images of minimal bacterial attachment suggest that biofilm development did not occur to the same extent as in the amended feed, and therefore the difference in carbon (i.e., AOC) between the baseline and amended feed was critical to changes in substrate loading available for bacterial growth on the membrane.

When the test cell was operated under constant pressure, the membrane permeate flux decreased when the RO feed contained 1000 µg/L of AOC and a nutrient ratio of 107:11:1 C:N:P. In that experiment, SEM imaging showed a higher distribution and occurrence of fouling and bacterial growth compared to the membrane without acetate amendment. Elevated AOC affected operation by reducing flux as a result of deposition and proliferation of bacteria into a biofilm as seen on feed and middle sections of the membrane. SWRO flux decrease typically is affected by poor water quality and deposits on the membrane or in the membrane pores (fouling). Compared to a water source fully pretreated both with a minimum and maximum AOC content under similar operating conditions, the permeate flux decreased by more than 20% as a result of fouling of the membrane. There are numerous opportunities in which AOC could increase in RO feed water.

AOC increases occur from oxidation of organic matter, increased chemical dosing, and water quality fluctuations such as algal blooms. In full-scale applications, RO permeate flux decline would be exacerbated during those water quality conditions in which AOC is elevated. Additional testing would be needed to identify the minimum AOC level and appropriate nutrient ratio for the control of biofilm growth and bacterial proliferation. From these results, a ratio of 72:6:1 and AOC 30 µg/L were effective for reducing bacterial adhesion and biofilm proliferation. Determining the critical level of AOC in which bacterial proliferation is minimized under normal operating conditions would be an appropriate step for RO treatment plants. Alternative treatment or maintenance strategies could be addressed to avoid flux decline and other operational issues that occur as a result of biological growth.

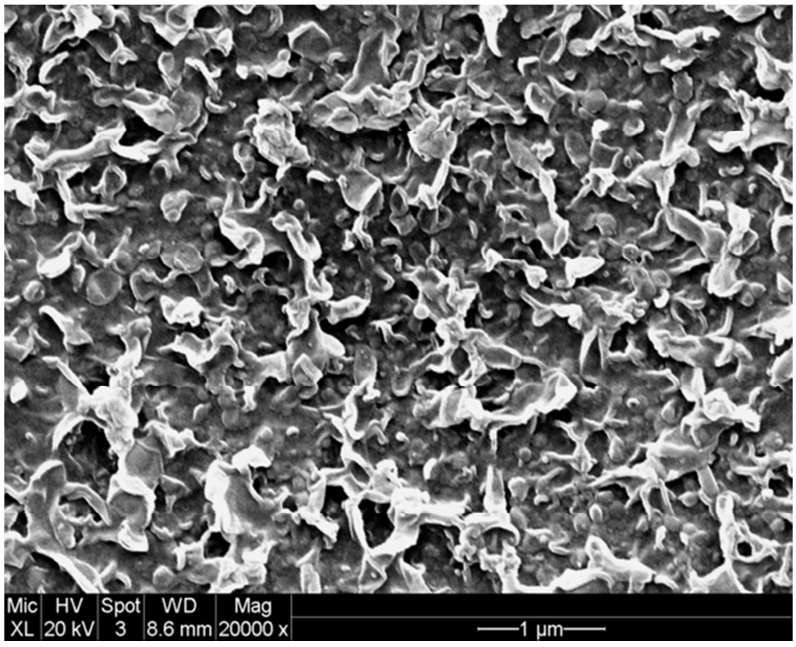

Figure 29 SEM image of virgin membrane at 20000X magnification (source: the author).

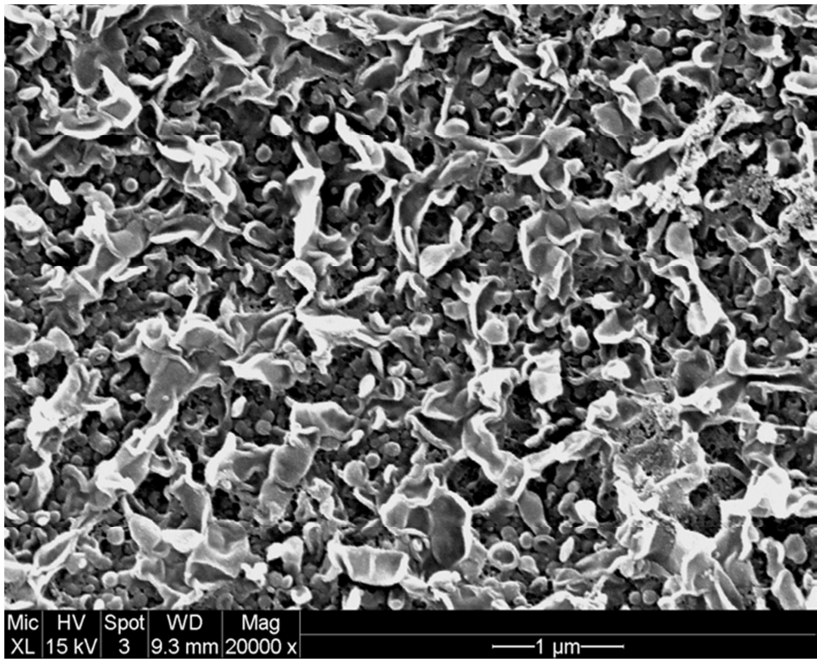

Figure 30 SEM image of Baseline test at 20000X magnification: Feed section (source: the author).

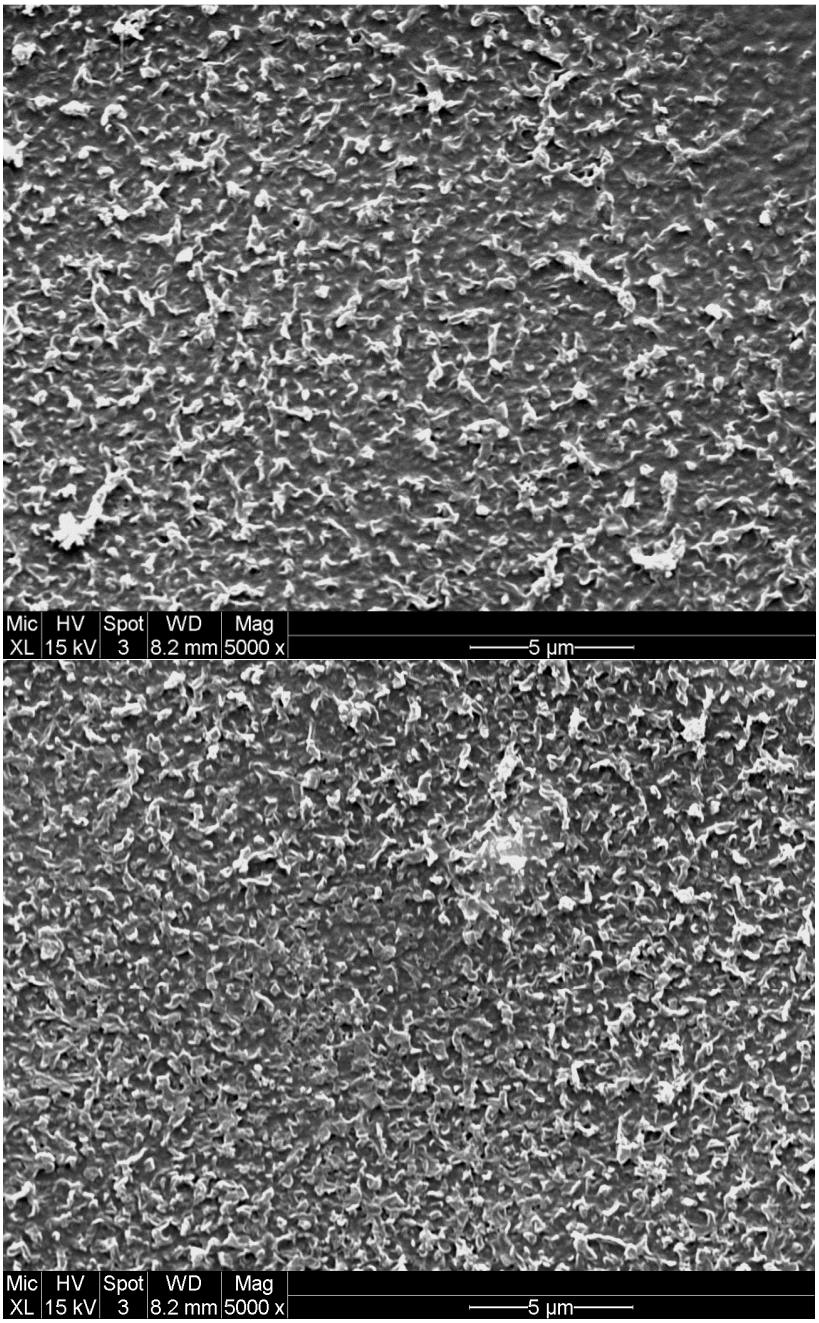

Figure 31 SEM images from Baseline test at 5000X magnification: Middle section of the RO membrane that is mostly intact without major occurrence of deposited fouling material (source: the author).

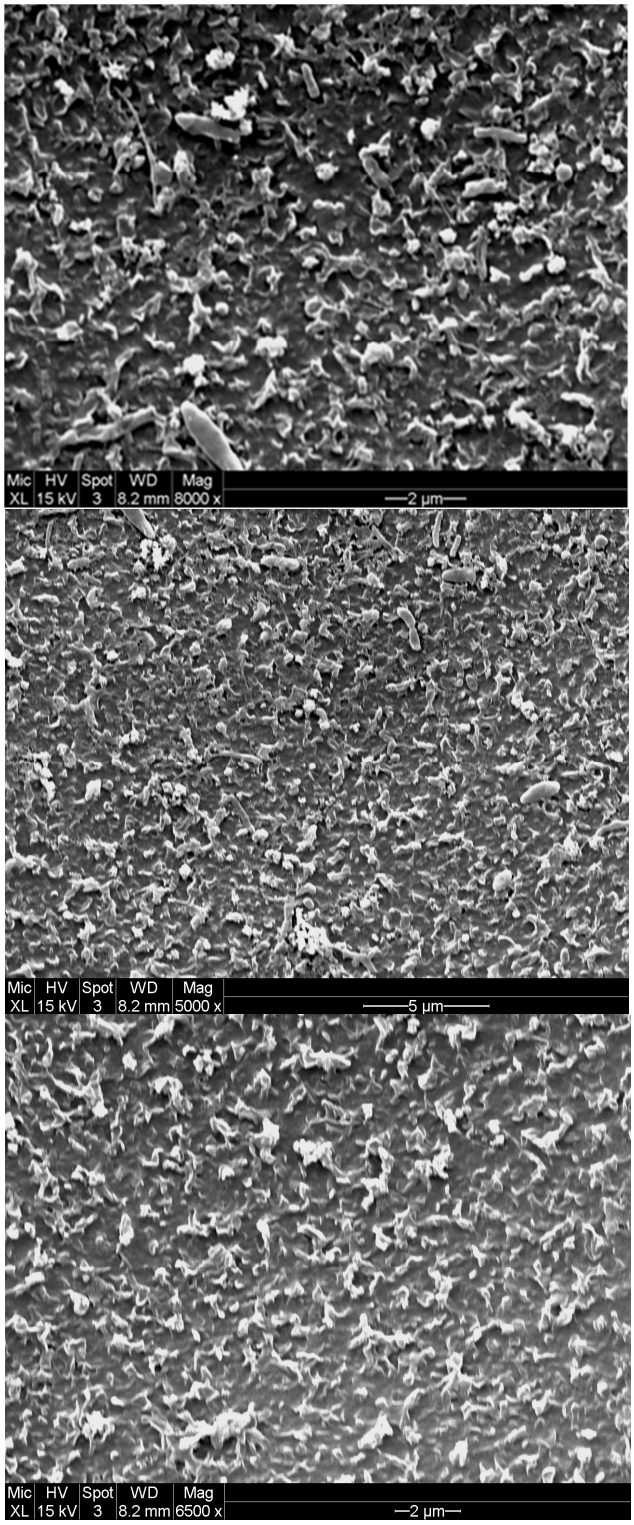

Figure 32 SEM images from Baseline test: Brine sections of RO membrane are visible (source: the author).

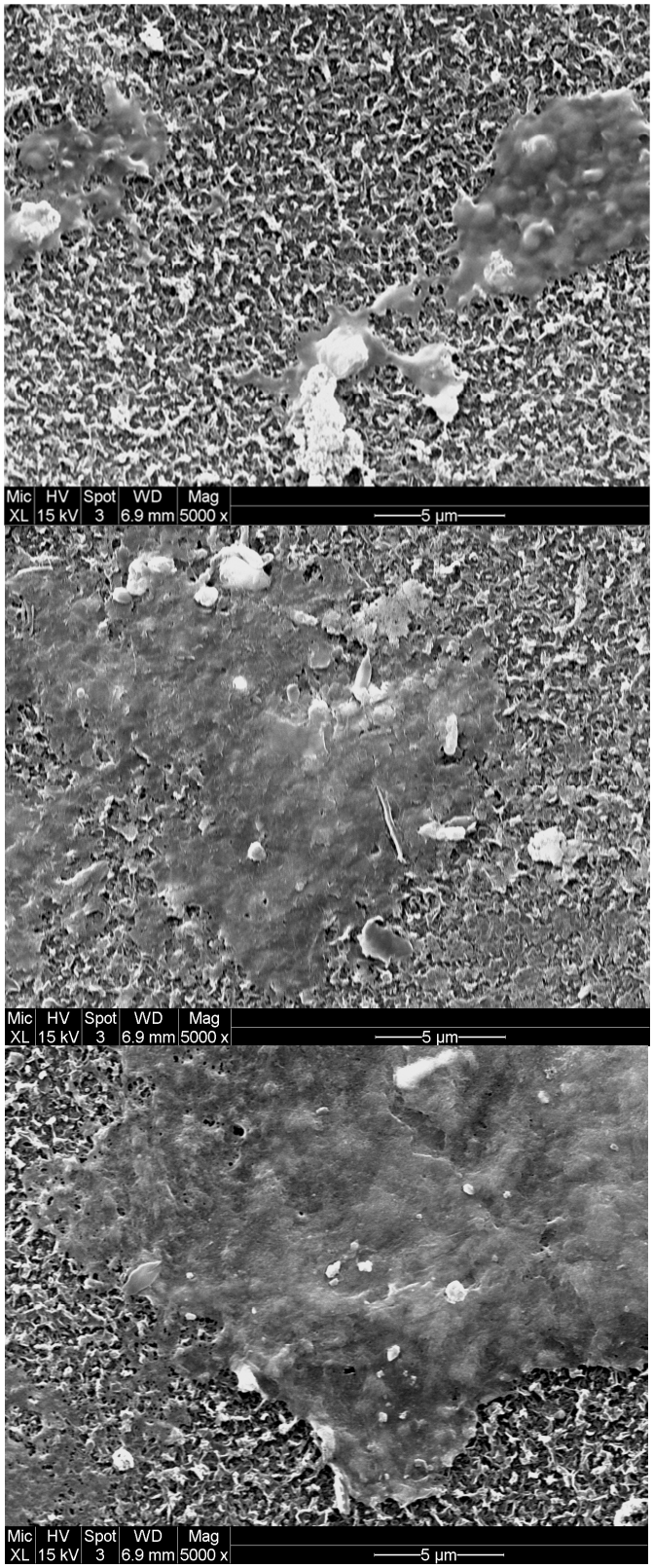

Figure 33 SEM images from AOC amended test at 5000X magnification: Feed sections of the RO membrane are largely covered with biofilm (source: the author).

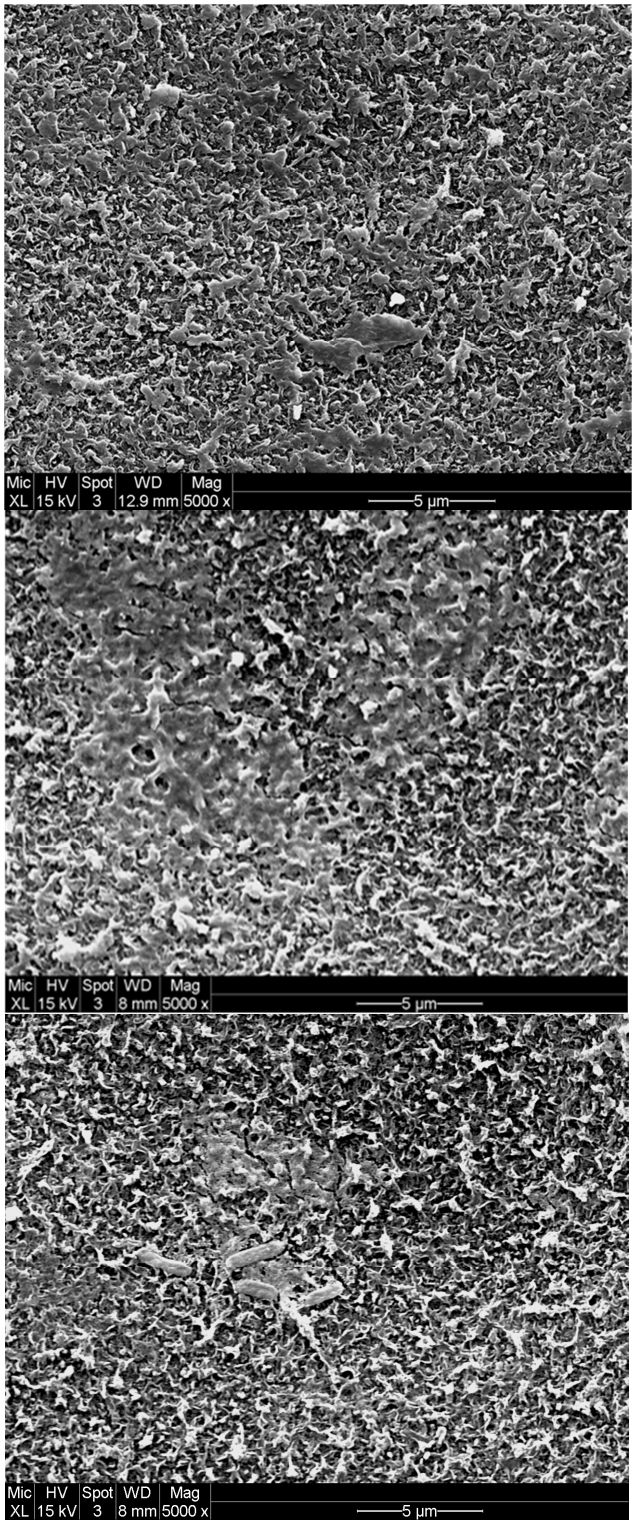

Figure 34 SEM images from AOC amended test at 5000X magnification: Middle sections of the RO membrane are intermittently covered with biofilm. Bacterial rods are present (source: the author).

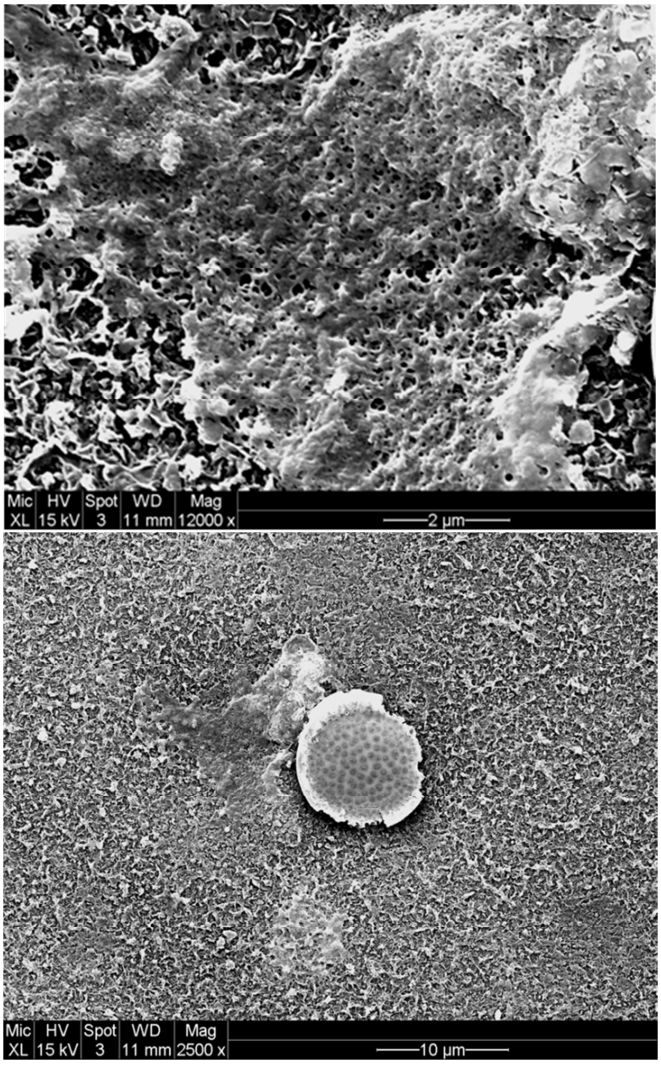

Figure 35 SEM images from AOC amended test at 12000X and 2500X magnification: Brine sections of the RO membrane are intermittently covered with fouling; diatom and surrounding fouling (source: the author).

CHAPTER 3: BIODEGRADABLE NUTRIENT BYPRODUCTS OF PRETREATMENT PRACTICES IN SEAWATER RO DESALINATION

Abstract

Application of seawater reverse osmosis membrane (SWRO) antiscaling, cleaning, and dechlorinating agents in most solutions and recommended doses increased AOC, and therefore the biodegradability of the seawater. AOC was also a byproduct of reaction between naturally occurring organic carbon or antiscalants and commonly used disinfectants, such as chlorine, chlorine dioxide and ozone. AOC was increased by 70% in seawater with 1 mg/L humic acid and a chlorine dose of 0.5 mg/L Cl_2. Increases in biodegradability and AOC were often not mirrored by TOC (TOC varied less than 3%). These and other results indicate that TOC is not an informative tool for the plant operators to predict biofouling potential, which is problematic because it is often the only organic carbon parameter used in SWRO water quality monitoring. Polyphosphonates and polymer-based antiscalants increased AOC less than 30 µg/L; however, phosphate-based antiscalants increased AOC levels nearly 100 µg/L. Depending on the active chemical or inherent impurities, antiscalants may increase biofouling potential of the RO feed despite the targeted application for controlling inorganic fouling. Better operational practices such as removing the chlorine residual prior to dosing the antiscalant would alleviate the adverse effect of AOC byproduct production. TOC removal efficiency is typically very poor and the pretreatment impacts on AOC levels should be controlled in SWRO plants that experience biological fouling problems on the RO membranes. Besides creating more effective organic carbon removal, minor pretreatment configurations and monitoring programs in the plants are recommended to help control AOC levels in the RO feed.

3.1 Introduction

In seawater reverse osmosis (SWRO) desalination plants, reactions between treatment chemicals and dissolved organic matter (DOM) have not been investigated for the purpose of

evaluating the biodegradability of the treatment chemicals or the formation of byproducts. Measuring easily assimilable organic carbon (AOC) will provide insight and quantifiable results about the biodegradability of seawater at different stages of pretreatment. The production of AOC would provide the nutrients for growth and proliferation of bacteria on the RO membranes thereby leading to biofouling, associated flux decline, and other operational challenges.

Seawater DOM originates from various sources including terrestrial runoff, byproducts from micro- or macroorganisms, and anthropogenic sources such as wastewater, industrial, or agricultural discharges. A major component of terrestrially-derived DOM is humic material. Humic matter has been reported to be an association of relatively small molecules bound together by intermolecular hydrophobic reactions (Conte and Piccolo, 1999) or high molecular weight macromolecules with aromatic structures and greater UV absorbance (on account of the molecular size) than other natural organic matter (NOM) and DOM fractions (Reckhow, 1990). In general, researchers agree that the humic structure is affected by pH, ionic strength, concentration, and divalent cations. A significant amount of research has focused on the oxidation of humic matter in surface water, but there is very little information about its behavior and reactivity in water having high ionic strength like seawater. A recent study by Schneider et al. (2013) reports that in tests using humic acid fortified seawater, removal of DOM is affected by ionic strength and divalent cations which create calcium or magnesium complexes and steric stabilization. These mechanisms can inhibit the effectiveness of coagulation during seawater pretreatment.

Because coagulation is relied upon for the removal of organic carbon, the chemistry of seawater has important implications for the presence of humic matter in desalination, and ultimately the ability of a given desalination pretreatment process to remove humic matter. Humic matter is not readily biodegradable; however, if it persists after the coagulation step during

pretreatment, then potential oxidation processes downstream could liberate AOC from the complex structures.

Although humic structures are generally considered refractory (i.e., not easily biodegraded or assimilated by microorganisms), photooxidation and biochemical transformations can liberate important nutrient reserves. Understanding the degree of transformation in seawater from refractory organic carbon into biodegradable organic carbon, including AOC, is of importance in seawater applications. Extensive literature has been published investigating the reactions of DOM with ozone, chlorine, or chloramine disinfectants typically used in drinking water treatment. Oxidation from ozonation or other advanced oxidation processes (AOP) transforms a complex organic structure into more biodegradable fractions and AOC used by bacteria for growth. Oxidation of specific components found in humic matter such as aromatic rings and carbon-carbon double bonds decreases the UV_{254} and can increase the proportion of biodegradable fractions, such as AOC or other disinfection byproducts in fresh water (Hammes et al., 2006; Glaze and Weinberg, 1993). Such byproducts are often more biodegradable and would be amenable to removal through biological filtration. Filtration through biologically active media produces water that is more biologically stable and can effectively reduce disinfection byproduct formation potential. This project was conducted to quantify the impact of AOC as an important parameter for understanding the biological stability of treated water and biofouling potential of seawater RO membrane processes.

Polyphosphates, polyphosphonates, polyacrylates, and polycarboxylates are the most frequent types of antiscalants manufactured and used during SWRO pretreatment to inhibit inorganic fouling (i.e., scaling) that occurs when the concentration exceeds solubility in the brine and the salts precipitate. Although antiscalant application is effective for preventative maintenance of salt precipitation onto the RO membrane, unwanted side effects such as biofouling have been

reported. Various reports in freshwater and seawater have indicated that these chemicals provide nutrients and promote conditions that lead to proliferation of bacteria and formation of biofilms. Recent studies using *Vibrio fischeri* have shown that bacterial deposition and biofilm formation increased in solutions containing between 20 and 100 mg/L polyphosphonate- and polyacrylate-based antiscalants (Sweity et al., 2013).

Predicting biofouling potential as a side effect of chemical dosing is further complicated by the proprietary nature of the chemical industry. Manufacturers provide dosing guidelines and often list the percent of the active component in the product, but the specific ingredients are trade secrets and rarely listed. Researching the chemical makeup was nearly impossible; manufacturer websites, distributors, and material safety data sheets (MSDS) lacked clarification. Available information does indicate that carbon and phosphate are often inherent components of antiscalant solutions, which are also essential nutrient supplies for the growth and proliferation of bacteria. Although antiscalants are complex molecules and not easily assimilated, they may contain impurities including phosphoric acid and phosphorous acid that may be present between 0.5 and 2.0%. Even if phosphate is specifically measured, an increased biofouling potential in the RO feed water from these impurities would be better evaluated by measuring the biodegradable nature of the substance through the AOC test.

Often the pretreatment strategy in SWRO plants is to manage ORP as a last step during pretreatment and immediately before the RO feed. Operators aim to control biological growth using chlorine throughout the treatment process and control inorganic fouling by dosing antiscalants. In this scenario, the chlorine residual is often not removed until after the antiscalant is added, providing the opportunity for the treatment chemicals to react.

The objectives were to 1) evaluate organic carbon changes and AOC formation from three commonly used oxidants: chlorine, chlorine dioxide, and ozone; 2) evaluate organic carbon changes, AOC formation from pretreatment chemicals and from reaction with chlorine.

3.2 Sampling Approach and Experimental Overview

Chlorine, chlorine dioxide and ozone were used in a series of bench scale oxidation tests for the purpose of evaluating the biodegradability of DOM after reactions with disinfectants commonly used in water treatment. The experiments are herein referred to as oxidation instead of disinfection because the testing was not conducted to evaluate biocidal effects but rather to observe changes to a model organic structure and the naturally occurring organic matter in seawater.

Pretreatment chemicals commonly used in SWRO for membrane cleaning and protection were analyzed for their biodegradability and potential to increase AOC in seawater matrices. Antiscalants, citric acid (cleaning agent), and SBS (for ORP control) were tested alone and in combination. Typical strategies in SWRO pretreatment were targeted to evaluate the production of BOM and AOC formation when sequential addition of antiscalants, oxidants, or SBS occurs. Antiscalants applied in SWRO processes were investigated to understand the biodegradable nature of these chemicals, the inherent chemical impurities and the byproducts, namely AOC that is formed from reaction with chlorine.

3.3 Materials and Methods

3.3.1 Glassware

Reaction vessels were graduated, 250-mL borosilicate bottles (KIMAX; Kimble Chase, Vineland, NJ) rendered carbon-free as previously described (Weinrich et al. 2009). Briefly, the

bottles are washed, rinsed and baked at 550°C for six hours. The bottle closures were acid washed in 10% hydrochloric acid overnight, rinsed with laboratory grade water, dried, and autoclaved.

3.3.2 Model Seawater Matrix

Model seawater matrices (used for humic acid testing) were prepared from Milli-Q water and American Chemical Society (A.C.S.) grade chemicals. Laboratory grade water was generated from a system using RO-purified, finished drinking water passed through ion exchange and activated carbon filtration and ultimately passed through a Milli-Q Academic System (Millipore Corporation, Billerica, MA). Prior to use, model waters were allowed to equilibrate at room temperature for at least 24 hours.

Milli-Q water (3 L) was amended with the following: 66 g sodium chloride (EMD Chemicals, Gibbstown, NJ), 1.65 g KCl, 0.024 g $NaHPO_4$, 0.006 g KNO_3, and 0.48 g $NaCO_3$. The solution is mixed, adjusted for pH, and autoclaved. Upon cooling, 3 mL each of 0.1 M calcium chloride and 1.0 M magnesium sulfate are added. This solution was used as the model seawater matrix into which humic acid was added.

3.3.3 Humic Acid Oxidation with Chlorine, Chlorine Dioxide

Three concentrations of humic acid from 1 to 5 mg/L were chosen to span the typical range found in seawater samples collected during field sampling (Chapter 2). A stock of humic acid was prepared in Milli-Q water at a concentration of 2.7 g/L of carbon (g/L as C) and was dissolved by sonication overnight. Humic acid was used as the model DOM source in a laboratory generated seawater matrix at pH 7.2.

Chlorine and chlorine dioxide tests were separately prepared at doses of 0.5 mg/L Cl_2 and reacted for 4 hours in laboratory generated seawater solutions containing humic acid. Sodium hypochlorite solution, 5%, Chemical Abstract Service (CAS) #7681-52-9 (J.T. Baker, Avantor,

Center Valley, PA) was used to prepare a working solution of 100 mg/L Cl_2 for dosing the test solutions. Chlorine dioxide was purchased as a 3000 mg/L stock solution (0.3% chlorine dioxide; CDG Environmental, Bethlehem, PA) and used to prepare a 100 mg/L working solution. Stock and working solutions of chlorine dioxide were measured at absorbance at 445 nm using a spectrophotometer (DR 5000; Hach, Co., USA). The stock solution was stored in between experiments at 4°C. At the end of the reaction, sodium thiosulfate was used to quench the oxidant residual.

3.3.4 Seawater Oxidation with Chlorine, Chlorine Dioxide

A series of bench-scale chlorination tests were conducted to evaluate changes to organic carbon naturally occurring in seawater with particular focus on AOC formation from geographically diverse locations. Bulk seawater samples were collected and shipped to Delran, NJ. Upon arrival the water was stored at 4 °C. Seawater from the intake at West Basin Municipal Water District (WBMWD) RO demonstration facility in Redondo Beach, CA was collected on May 14, 2012 and shipped in a 10 gallon carboy. Staff from WBMWD reported the following water quality: pH 8.1, ORP 352 mV, TDS 32.2 ppt (g/L), conductivity 50.3 mS. Weekly variability (June 13 – July 5, 2012) was detected in control solutions retrieved from the container stored at 4°C. AOC ranged from 88 to 224 µg/L, TOC from 0.6 to 1.2 mg/L, and UV_{254} from 0.009 to 0.011cm^{-1}. Controls were analyzed with each experimental set to accommodate these differences.

Seawater from the Arabian Sea (35°C collection temperature, pH 7.7) from the Al Zawrah RO treatment plant in the Emirate of Ajman was collected on July 29, 2012 and pasteurized at 70°C for 30 minutes prior to shipment to inactivate any indigenous bacteria. The pasteurized samples were cooled and shipped in 0.5 L bottles.

Seawater from intake of the intake of Tampa Bay Seawater Desalination Plant (TBSDP) at TECO was collected in a 5 gallon carboy and shipped to Delran, NJ for testing. Prior to testing, water was filtered through a 0.7 µm size glass fiber filter (GF/F).

Amber glass reactors were rendered chlorine-demand-free by soaking in a 40 mg/L chlorine bath overnight. Sodium hypochlorite solution, 5%, CAS #7681-52-9 (J.T. Baker, Avantor, Center Valley, PA) was diluted in Milli-Q water to prepare a working solution of 430 mg/L Cl_2 for dosing test solutions. Chlorine dioxide was purchased as a 3000 mg/L stock solution (CDG Environmental, Bethlehem, PA) and used to prepare a 330 mg/L working solution for dosing. The raw seawater (250 mL volume) was treated with chlorine and chlorine dioxide for 4 hours at ambient temperature (22°C). At the end of the reaction time, sodium thiosulfate was used to quench the oxidant residual. Chlorine and chlorine dioxide tests covered a range of oxidant doses from 0.5 to 15 mg/L as Cl_2. Chlorine dioxide was tested at doses from 0.5 to 4 mg/L as Cl_2 in WBMWD seawater, and 1 to 10 mg/L in water from Tampa Bay and Arabian Sea. Chlorine demand was measured at the end of the reaction time to quantify the amount of disinfectant that remained after reactions with various microbial and chemical components in the water.

3.3.5 Oxidation with Ozone

An ozone stock solution was prepared from Zero Grade oxygen (> 99.8 %; Airgas, Inc.; Malvern, PA) using an ozone generator (Pacific Ozone Technology, Benicia, CA) according to the batch method as outlined in Standard Methods 2350D (APHA, 2005) in Milli-Q water chilled in an ice bath. Ozone concentrations in the stock were determined after dilution and preparation for measurement on the spectrophotometer at 600 nm using Indigo Method 8311 (DR 5000, Hach, Co., USA).

Humic acid was prepared at concentrations ranging from 0.3 to 5 mg/L and tested at variable ozone:TOC dose ratios to identify maximum formation of AOC. Humic acid stock preparation is

described in Section 3.3.3. Raw seawater collected from Tampa Bay and the Arabian Sea was tested at doses of 1:2 and 1:1 ozone:TOC.

3.3.6 Antiscalant and Pretreatment Chemicals

Antiscalants and other chemicals (Table 14) were tested in a laboratory generated seawater matrix (Section 3.3.2) and in seawater (Section 3.3.4) from the Arabian Sea, Redondo Beach, CA, and Tampa Bay, FL. The matrix enabled the project team to evaluate the results for the inherent organic carbon content from the antiscalant without any influence or contributing background organic levels found in environmental seawater. The seawater matrix was prepared with necessary nutrients including nitrogen, phosphorus, and sulfate, but without bromide to minimize formation of hypobromous acid. By preparing the matrix in the laboratory, the project team was able to evaluate reaction and degradation of the antiscalants in the presence of free chlorine residual.

Batch experiments targeted low and high range dosing scenarios for each antiscalant. Chemical manufacturers were contacted to discover the most widely used antiscalants in SWRO and for guidance on treatment conditions and dosing. Antiscalants were prepared at two concentrations in the laboratory generated seawater matrix and dosed with 10 mg/L Cl2 from a 5% sodium hypochlorite solution (J.T. Baker, Avantor Performance Chemicals, Inc., Center Valley, PA). Sodium hypochlorite was employed as the oxidant for testing because of its widespread use in the SWRO industry. The concentrations of the chlorine stock and its dosing solutions were measured by ferrous ammonium sulfate titration with N,N-diethyl-p-phenylenediamine (DPD) indicator in accordance with Standard Method 4500-Cl F (APHA, 2005). After the chlorine dosing solution was added to the individual antiscalant solutions and mixed in volumetric flasks, the solution was transferred headspace-free into 250 mL chlorine-demand-free amber bottles and placed in the dark at 25°C where the reaction took place for 18

hours. At the end of the reaction time, chlorine residual measurements indicated that the initial high dosage of chlorine was not depleted and the samples were, therefore, appropriately quenched of the free chlorine residual before analysis. A control was also subjected to the same chlorine dosing, reaction, and storage conditions. An aliquot of the initial antiscalant solution was reserved for the same suite of analyses, and results are reported relative to the control. The control had the following amounts: 20 µg/L AOC, 0.04 mg/L TOC, UV_{254} 0.003 cm^{-1}, and phosphate 5.5 mg/L PO_4^{3-}.

Table 14 Common SWRO pretreatment chemicals (phosphate, phosphonate, polymer/polycarboxylate, and dechlorinating agent). *Antiscalant MSDS/info sheet available.

Type	Name	CAS #	Manufacturer and Description	Dose (mg/L)
Phosphate	Hypersperse™ MDC 704*	7722-88-5	Contains 1-5% (w/w) of sodium pyrophosphate (a.k.a diphosphoric acid, sodium salt). GE Betz, Inc. (Trevose, PA).	2 – 10
	Sodium hexametaphosphate (SHMP); molecular formula $(NaPO_3)_6$	68916-31-1	A. Pfaltz & Bauer (Waterbury, CT)	Variable
		10124-56-8	B.Tech grade, Alfa Aesar (Ward Hill, MA).	
		68916-31-1	C.Glassy, approx $(NaPO_3)_n$; Spectrum Chemical Mfg. Group (Gardena, CA).	
		68916-31-1	D. Macron Fine Chemical, Avantor Performance Materials, Inc. (Center Valley, PA).	
Polyphosphonate (carbon – phosphorus bond)	A-102 Plus*	Composition proprietary.	American Water Chemicals (Plant City, FL). TOC 26 mg/g.	1 – 10
	1-hydroxyethylidene-1,1-diphosphonic acid (HEDP)	2809-21-4	Min 95%. StremChemicals (Newbury, MA).	1 – 5
	Hypersperse™ MDC 150*	22042-96-2	Contains diethylenetriamine pentamethylene phosphonic acid, sodium salt (DTPMPA-Na). GE Betz (Trevose, PA). TOC 40 mg/g.	3 – 6
	Vitec® 3000	Composition proprietary.	Avista Technologies, Inc. (San Marcos, CA). Contains a bacteriostat to inhibit bacterial growth during storage.	2 – 5
Polymer / polycarboxylate	Acumer-DOW™ 1035*	Composition proprietary.	Polyacrylic acid, sodium salt (34.0 – 36.0%). Average molecular weight (MW) = 2000. (Rohm and Haas/The Dow Chemical Company).	1 – 10
	Acumer-DOW™ 2000*	Composition proprietary.	Sulfonate, carboxylate; Acrylic polymer(s) (42.0 – 44.0 %). <500 ppm residual monomers. Average MW=4500. (Rohm and Haas/The Dow Chemical Company).	1 – 11
	Acumer-DOW™ 2100*	Composition proprietary.	Sulfonate, carboxylate. Acrylic polymer(s) (36.0 – 38.0 %). Average MW=11,000. (Rohm and Haas/The Dow Chemical Company).	1 – 7
	AWC A-104*	Not available.	American Water Chemicals (Plant City, FL). Information provided only for similar product on MSDS.	1 – 10
	Citric Acid	77-92-9	Anhydrous. EMD (Gibbstown, NJ).	1 – 5
	Flocon + N	Not available.	20% active ingredient. A neutralized aqueous solution of organic acids. BWA™ Water Additives (Tucker, GA).	10% w/w
	SpectraGuard™ Super Concentrate (SC) 11X	Not available.	Professional Water Technologies. Phosphate and phosphate-derivative free, macro-molecule “dendrimer” antiscalant.	2 – 6
Other	Sodium bisulfite	120002-56-4	A.C.S. Grade; Fisher Sci (Fair Lawn, NJ). Dechlorinating agent/ORP control.	1 – 5

3.3.7 Water Quality Analyses

Samples were analyzed for UV_{254}, TOC, and AOC (Methods described in Section 2.5). Free and total chlorine were measured using DPD reagents (Hach Co., USA) according to Standard Method 4500-Cl G (APHA, 2005). Phosphate was measured as orthophosphate using the ascorbic acid method (Standard Method 4500-P-E; Hach 8048) at 880 nm; results are reported as mg/L PO_4^{3-}.

3.4 Results

3.4.1 Humic Acid Oxidation with Chlorine, Chlorine dioxide

AOC concentrations in the humic acid control averaged 110 µg/L ± 19% before dosing with the oxidant (Table 15). The addition of more humic acid did not significantly increase the amount of AOC, but increasing concentrations were reflected in the UV_{254} and TOC measurements. In this case, a source of refractory carbon such as humic acid would be easily detected using non-specific organic analyses, including UV_{254} and TOC. AOC was not expected to vary in the control solutions because humic acid is mostly refractory and not readily biodegradable.

Oxidation with chlorine (Cl_2) and chlorine dioxide (ClO_2) produced 155 and 103 µg/L AOC, respectively, at the lowest concentration of humic acid. Only in the chlorinated solution was AOC significantly increased (70%) compared to the control after reaction. There were no significant changes to UV_{254}, TOC, or AOC from the solutions with higher concentrations of humic acid using the same doses of chlorine or chlorine dioxide. Chlorine dioxide has a lower redox potential than hypochlorous acid (the active species during chlorination); therefore, the oxidation and chlorine-substitution reactions may be further limited in high ionic strength seawater.

The structure of organic molecules, such as humic acid, is affected by high ionic strength; therefore, the increased concentrations of humic acid (5 v. 1 mg/L) may not necessarily be more amenable to oxidation with only 0.5 mg/L of chlorine or chlorine dioxide (Table 16). Post-oxidation with chlorine and chlorine dioxide effected nearly no change in UV_{254} absorbance (± 2%) or TOC (-4%). Świetlik et al. (2004) reported that chlorine dioxide is capable of producing biodegradable byproducts including aldehydes and carboxylic acids from humic acid in freshwater at doses of 1.2 mg ClO_2 mg^{-1} DOC reacted for 24 hours; however, under the doses and conditions in the seawater experiments reported here, biodegradable byproducts measured as AOC were not affected.

In this report, the experimental conditions consisted of a reaction time of just 4 hours, which was more consistent with preoxidation in a desalination plant. For instance, an oxidant is often added at the intake to inactivate organisms from the raw seawater and the residual would be carried through the treatment until SBS is added before the RO membranes. Also, the dose ratio of chlorine dioxide to organic carbon ranged from 0.1 to 0.5 mg ClO_2 mg^{-1} DOC which was a fraction of the dose tested by the Świetlik team. In practice, seawater desalination plants are often restricted by the potential formation of chlorite from chlorine dioxide disinfection. The maximum contaminant level for chlorite is 1.0 mg/L with a goal of 0.8 mg/L. The results from these preliminary experiments indicate that at low doses of 0.5 mg/L of chlorine and chlorine dioxide, the higher redox potential of chlorine is capable of breaking down the carbon bonds contained in humic acid and rendering the structure into BOM and therefore AOC as a reaction byproduct.

Table 15 AOC formation in humic acid solutions with chlorine or chlorine dioxide (applied dose of oxidant was 0.5 mg/L).

Humic Acid (mg/L)	Oxidant (0.5 mg/L)	UV_{254} (cm^{-1})	% Diff Rel. to Control	TOC (mg/L)	% Diff Rel. to Control	AOC (µg/L)	% Diff Rel. to Control
1	Control	0.091		1.16		91	
1	Chlorine	0.093	2%	1.11	-4%	155	70%
1	Chlorine dioxide	0.089	-2%	1.04	-10%	103	13%
2	Control	0.182		2.48		109	
2	Chlorine	0.182	0%	2.39	-4%	121	11%
2	Chlorine dioxide	0.179	-2%	2.30	-7%	116	6%
5	Control	0.456		6.43		128	
5	Chlorine	0.456	0%	6.30	-2%	118	-8%
5	Chlorine dioxide	0.454	0%	6.48	1%	121	-5%

3.4.2 Seawater Oxidation with Chlorine, Chlorine dioxide

In many locations, SWRO plant operators regularly apply chlorine during pretreatment at doses as high as 5 mg/L to reduce biological growth but may intermittently shock chlorinate using higher concentrations of chlorine to remove biofilm on intake structures, inactivate organisms in the feed and overcome chlorine demand of the water. Operational evidence has suggested that this procedure can lead to biological fouling of the RO membranes downstream of the initial application. The team hypothesized that chlorine and chlorine dioxide treatment would produce BOM leading to reductions in UV_{254} and increases in AOC.

Organic constituents and byproduct precursors were expected to vary across the three seawaters tested on account of the geographical diversity of the sources and therefore would behave differently when dosed with an oxidant. The inherent variability between the types of water and constituents would explain the non-monotonic results in AOC formation or removal

(Table 16), but trends among the water types became apparent. In most treatments TOC levels generally did not show any remarkable differences compared to the control. In Tampa Bay, TOC changes post-treatment varied from -7 to 2%, and Arabian Sea chlorination decreased TOC by 14% on average from 1.4 mg/L in the control to 1.2 mg/L after chlorination. TOC changes were more variable for chlorine dioxide treatment in Arabian Sea water; TOC decreased in 1 to 4 mg/L as Cl_2, but in the 10 mg/L chlorine dioxide dose TOC increased by 29%.

There is evidence that particulate matter may be rendered easier to oxidize in the TOC instrument (using high temperature combustion) after preoxidation (i.e., chlorine dioxide) which would be evident as an increase in TOC compared to the non-oxidized seawater control. In the same 10 mg/L chlorine dioxide treatment of Arabian Sea water, UV_{254} also increased by 44%, compared to the control when the lower dose treatments decreased UV_{254} by 22%. UV_{254} decreased in Tampa Bay water in both the chlorine and chlorine dioxide treatments at 10 mg/L; there was a 30% reduction from the starting absorbance in the control at 0.18 cm^{-1}. TOC also showed slight reductions to 8% in the same treatments. A study previously published reported that increasing doses of chlorine corresponded to decreasing UV absorbance at wavelengths greater than 250 nm, in which the chlorine treatment ranged from 0.2 to 1 mg/L (Weinrich et al. 2011).

The observations contained in this report indicate that UV_{254} decreased at all chlorine doses (1 - 10 mg/L) in TECO raw water from TBSDP and at 1 and 4 mg/L doses in Arabian Sea raw water. UV_{254} for Arabian Sea raw water was 0.02 cm^{-1} and was reduced with both chlorine and chlorine dioxide doses of 4 mg/L. When dosed with 10 mg/L, UV_{254} increased by 44% from the chlorine dioxide treatment and 51% from chlorine. These reported inconsistencies with organic carbon were not observed in West Basin seawater where UV_{254} increased consistently for both oxidants. UV_{254} increased between 122 and 322% at 5 to 15 mg/L chlorine doses and from 9

to 136% in 0.5 to 4 mg/L chlorine dioxide treatments. Out of the three sources tested, West Basin seawater had the lowest organic carbon (UV_{254} and TOC) but had the highest AOC in the control.

Changes to aromaticity or carbon-carbon double bonds and other structures in humic acid would be exhibited as reductions in UV_{254}, but that change was not detected at the doses tested. Therefore the data suggest that the organic carbon present in the West Basin water was not dominated by humic acid because consistent UV_{254} increases were observed. From the testing conducted in humic acid solutions treated with chlorine or chlorine dioxide, UV decreased or stayed the same. SUVA at 254 nm has been recently applied to evaluating the humic nature of seawater. Edzwald & Haarhoff (2011) adapt conventional drinking water guidelines to seawater in the following manner: (1) SUVA greater than 4 indicates that NOM is mainly aquatic humic matter; (2) SUVA of 2 to 4 indicates that NOM is a mixture of AOM and aquatic humic matter; and (3) SUVA less than 2 indicate the NOM is composed primarily from AOM.

SUVA for West Basin was 0.9 L/mg-m which suggests that the seawater did not contain much aquatic humic matter. The increases in West Basin suggest that liberation of organic matter during oxidation may have occurred. A study by Hammes et al. (2007) confirmed that the cytoplasm released from phytoplankton during ozonation increased AOC in both laboratory generated water spiked with *Scenedesmus vacuolatus* and an environmental source from a lake. As an alternative to chemical treatment, physical disruption of algal cells would also liberate cytoplasm and increase AOC. During RO treatment, the shearing effect caused by physical treatment processes specifically the high-pressure pumps used to deliver water to the membranes, can break algal cells apart. Rupturing algal cells through either physical processes or chemical oxidation could potentially increase AOC, thereby increasing biofouling potential of the pretreated water.

Tampa Bay seawater had the most significant increases in AOC compared to the other water sources after chlorine and chlorine dioxide treatment. AOC increased as much as 114% with chlorine dioxide and 142% with chlorine treatment. Treatments with both chlorine and chlorine dioxide suggest that normal and shock chlorination doses would react to produce or liberate biodegradable organic carbon. AOC formation was confirmed with these treatments, although changes to TOC concentrations were not detected.

The variability of organic carbon present in these geographically diverse waters indicates that AOC formation occurs when water is treated with disinfectants to control biological fouling. TBSDP experienced operational problems with organic fouling and biofouling of its RO membranes; it also had the highest organic concentrations of the seawaters tested. The type of organic matter present at the intake may also be predictive of the extent of reaction and type of transformations. It appears that, out of the sources tested, Tampa Bay contains the most humic material, which was highly reactive with oxidants and formed AOC as biodegradable oxidation byproducts. SUVA of TBSDP was 3.18 L/mg-m indicating that it is in fact a mixture of humic and microbially-derived (autochthonous) organic matter. The presence of humic material in TBSDP raw water was consistent with a previous study that evaluated coagulant removal (Schneider et al. 2011). In that report, raw TBSDP water was characterized using liquid chromatography - organic carbon detection, and humic substances were 50 to 70% of the organic carbon; SUVA was 3.24 to 5.5 L/mg-m. AOC is consistently formed as a byproduct from oxidation of humic acid and the organic carbon present in TBSDP raw water. The formation of AOC as a byproduct would generate conditions amenable to bacterial proliferation and subsequent biological fouling of the RO membranes.

Table 16 AOC formation in seawater with chlorine or chlorine dioxide (applied dose of chlorine was 0.5 – 15 mg/L and chlorine dioxide was 0.5 – 10 mg/L. SUVA (L/mg-m): WBMWD = 0.9, Tampa Bay = 3.18, Arabian Sea = 1.45.

		Dose (mg/L Cl_2)	Dose (mg ClO_2 mg TOC)	UV_{254} (cm^{-1})	% Diff Rel. to Control	TOC (mg/L)	% Diff Rel. to Control	AOC (µg/L)	% Diff Rel. to Control
WBMWD	Chlorine	Control		0.009		1.00		110 ± 21	
		0.5		0.012	*33%*	0.94	*-6%*	56 ± 20	*-49%*
		2		0.015	*67%*	0.92	*-8%*	71 ± 6	*-35%*
		4		0.025	*178%*	0.95	*-5%*	29 ± 9	*-74%*
		10		0.031	211%	1.10	10%	2 ± 0	-98%
		15		0.038	256%	1.15	15%	92 ± 11	-17%
	Chlorine dioxide	Control		0.011		0.6		88 ± 19	
		0.5	0.8	0.012	*9%*	0.59	*-2%*	58 ± 11	*-34%*
		2	3.3	0.021	*91%*	0.65	*8%*	34 ± 8	*-61%*
		4	6.7	0.026	*136%*	0.65	*8%*	34 ± 9	*-61%*
Tampa Bay	Chlorine	0		0.176		5.54		36 ± 12	
		1		0.153	*-13%*	5.63	*2%*	78 ± 4	*117%*
		4		0.127	*-28%*	5.60	*1%*	51 ± 7	*43%*
		10		0.121	*-33%*	5.15	*-7%*	87 ± 9	*142%*
	Chlorine dioxide	1	0.2	0.161	*-9%*	5.61	*1%*	49 ± 8	*37%*
		4	0.7	0.131	*-26%*	5.41	*-2%*	77 ± 18	*114%*
		10	1.8	0.121	*-31%*	5.16	*-7%*	65 ± 0	*81%*
Arabian Sea	Chlorine	0		0.021		1.44		60 ±14	
		1		0.014	*-32%*	1.25	*-13%*	51 ± 13	*-15%*
		4		0.019	*-7%*	1.24	*-14%*	41 ± 13	*-32%*
		10		0.031	*51%*	1.22	*-15%*	58 ± 12	*-3%*
	Chlorine dioxide	1	0.7	0.016	*-22%*	1.40	*-3%*	51 ± 6	*-16%*
		4	2.8	0.016	*-22%*	1.26	*-13%*	10 ± 2	*-83%*
		10	6.9	0.030	*44%*	1.86	*29%*	2 ± 0	*-97%*

Chlorine demand is typically used in drinking water to evaluate the dose needed to maintain a residual in the distribution system after the disinfectant reacts with DOM, bacteria, and other substances that can deplete the residual. It is not surprising that the untreated water from Tampa Bay is highly reactive with chlorine and chlorine dioxide. Chlorine demand of TBSDP intake

water was 8 and 4 mg/L for chlorine dioxide. In comparison, Arabian Sea water had 80% less TOC and exhibited a demand less than 1.8 mg/L for both free chlorine and chlorine dioxide. WBMWD intake seawater had similar TOC levels to that from the Arabian Sea and exhibited a maximum chlorine demand of 2.5 mg/L when dosed with 15 mg/L chlorine. Arabian Sea chlorine demand was 1.8 mg/L. Demand from chlorine dioxide in WBMWD seawater was 3 mg/L; in Arabian Sea testing the demand was 1 mg/L.

3.4.3 Humic Acid Oxidation with Ozone

The results described in this section compare humic acid, a model organic compound, in a laboratory generated seawater matrix of similar conductivity to other environmental seawater matrices near the same TOC concentration (Table 17). UV_{254} decreased by an average of 27% throughout all the samples (n=12) and by an average of 47% in the solutions reacted with the maximum ozone dose of 3:1 ozone:TOC. Ozone reacts with the carbon-carbon double bonds in the complex humic acid structure and also reduces aromaticity to create more biodegradable organic carbon structures. The reduction in absorbance suggests that bonds in the carbon structure were broken through ozone oxidation. TOC increased at all concentrations tested at the higher ozone doses 3:1 and 2:1 ozone:TOC. TOC decreased at 0.7 dose ratio by an average of 21%, and at 0.3 dose ratio TOC decreased by 12%. AOC was mostly removed in the 0.7 to 3 dose ratios. The removal of AOC would result from mineralization of the background AOC in the control and a lack of BOM produced by the batch test. AOC consistently produced only at 0.3 dose ratio. AOC increased as much as 198% in the 1 mg/L humic acid solution. In freshwater, biodegradable organic carbon formation is maximized at ratios 1:1 and 0.5 ozone: TOC (von Gunten, 2003; van der Kooij, 1986). The ratios of AOC production were similar in our study at the 0.3 ozone:TOC ratio compared to the previously mentioned study although the complexity of humic substances in seawater makes a direct comparison difficult. In fact, humic matter exhibits different properties in

solutions of low ionic strength versus those of high ionic strength, such as seawater. For instance, humic matter is considered to be a conformation of molecules inherently hydrophobic and at high ionic strength the molecules become more densely packed, thereby enhancing electrostatic repulsion and hydrophobicity in solutions with higher concentrations of humic matter (Conte and Piccolo, 1999; Yu et al., 2010). This behavior might offer some explanation as to the difference in AOC production that occurred in the 0.3 dose ratio, where the percent of AOC production decreased in increased humic acid concentrations. It is possible that the concentration of humic acid at 5 mg/L was not as amenable to oxidation as humic acid at a lower concentration of 1 mg/L if the hydrophobicity of the structure increased because of stronger intermolecular and hydrophobic arrangements of the available organic material.

Ozonation is widely used in surface water treatment for drinking water but has not been thoroughly investigated in desalination. Some information exists from treatment of ballast water and brackish waters with ozone. Ozonation has not been applied in desalination pretreatment for drinking water because of the formation of byproducts including bromate, a carcinogen. Other impacts from the presence of bromide would include the formation of hypobromous acid and the hypobromide ion, which could react with DOM to form bromoform and other brominated byproducts. Residual oxidants produced from ozonation may also damage RO membranes if not removed in the feed. This study aimed to quantify whether AOC was formed at typical ozone:TOC dose ratios previously reported in freshwater literature. In the absence of adverse oxidation byproducts (such as bromate), breaking down high molecular weight and hydrophobic structures would be an option in seawater pretreatment. For instance, the hydrophobic nature and interactions between organic foulants and a hydrophobic membrane would exacerbate membrane fouling (Yuan & Zydney 1999; Yu et al. 2010). Advanced oxidation for reducing these issues has been introduced in the past few years. For instance applying AOP in seawater using UV and UV with hydrogen peroxide has been investigated in a seawater matrix (Penru et al., 2012) in order to

reduce aromaticity of humic matter and increase biodegradability. If treatment applications could be developed for seawater in which humic hydrophobicity is reduced and removed through biodegradation in a biological filter, minimizing bromate and other unwanted byproducts during pretreatment, AOPs could target both organic and biological fouling by removing the structures that lead to these issues.

Table 17 AOC formation (percent differences relative to the control) in humic acid solutions with variable ozone doses.

Dose ratio (mg:mg)	Humic acid (mg/L)	UV_{254} (cm^{-1})	TOC (mg/L)	AOC (µg/L)
3 O_3:TOC	0.3	-39%	8%	-98%
	0.5	-41%	35%	-97%
	1.3	-61%	35%	-98%
2 O_3:TOC	0.3	-29%	69%	-59%
	0.5	-27%	62%	-21%
	1.3	-42%	72%	6%
0.7 O_3:TOC	1.0	3%	-20%	-15%
	2.0	-8%	-19%	3%
	5.0	-20%	-24%	-42%
0.3 O_3:TOC	1.0	-12%	-8%	198%
	2.0	-17%	-12%	84%
	5.0	-33%	-15%	49%

For the 1 mg/L humic acid solutions, the full range of ozone doses from 0 to 3 $mg:mg^{-1}$ was compared (Figure 36 – Figure 38). UV_{254} and TOC were generally stable in all of the ozone tests with humic acid. AOC increased when ozone:TOC was 0.3; otherwise, AOC was nearly the same in reactors at 0.7 and 2 ozone:TOC (Figure 38).

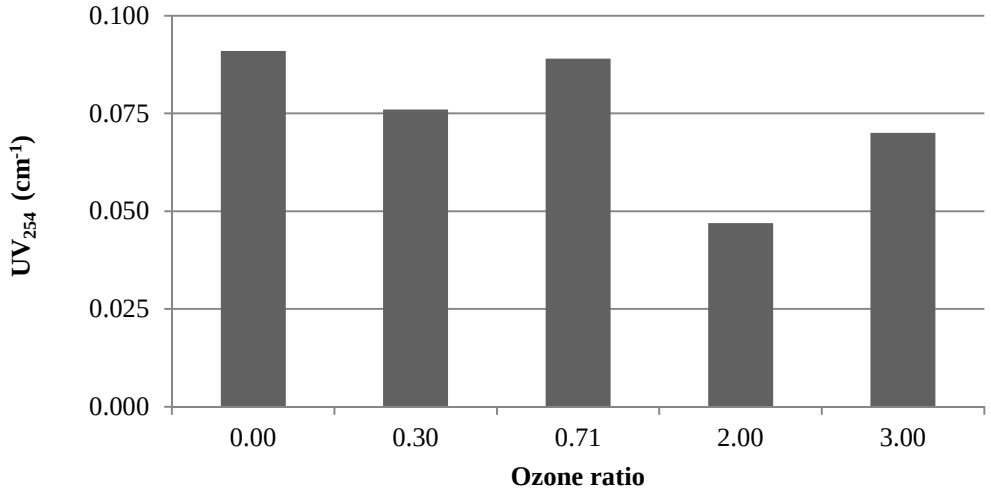

Figure 36 UV_{254} results from ozone:TOC dose ratios in 1 mg/L humic acid solutions.

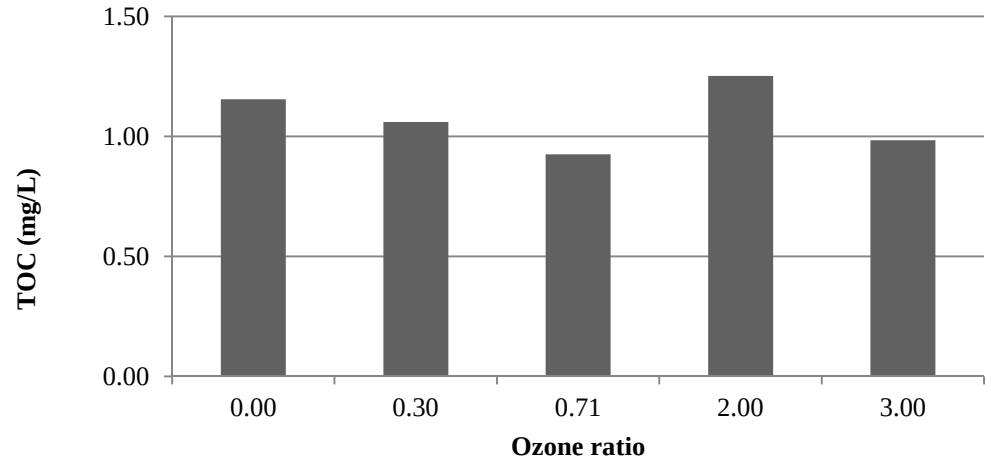

Figure 37 TOC results from ozone:TOC dose ratios in 1 mg/L humic acid solutions.

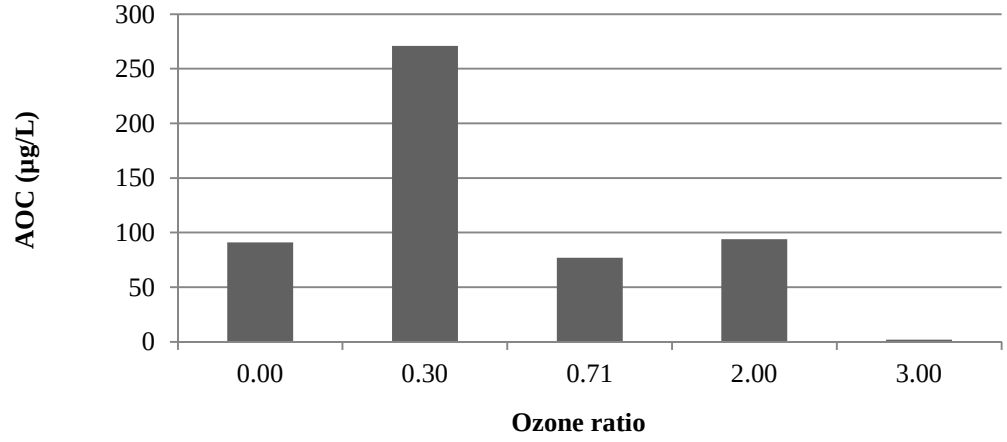

Figure 38 AOC results from ozone:TOC dose ratios in 1 mg/L humic acid solutions.

3.4.4 Seawater Oxidation with Ozone

Bulk seawater from Tampa Bay and the Arabian Sea was treated with 1:2 and 1:1 ozone:TOC to evaluate the impact of ozonation on environmental samples having a complex mixture of organic carbon (Table 18). Ozonated Arabian Sea water had nearly no change to UV_{254} or TOC (1.32 mg/L). UV_{254} was low at 0.01 cm^{-1}, suggesting that the inherent organic carbon was not high in aquatic humic matter (SUVA 1.0 L/mg-m). It is interesting to note that, although the content of the seawater had low organic carbon, ozonation increased AOC levels three-fold at 1:1 ozone:TOC dose ratio, and nearly six-fold at 1:2 ozone:TOC. These results are similar to the previous test with humic acid (Figure 39). The comparison reveals that increased ozone doses do not increase AOC by the same magnitude and also suggests that the organic matter in the seawater is a more complex mixture than the model organic, humic acid. Ozonated Tampa Bay seawater, which contained more TOC (5.95 mg/L), had nearly no change in AOC at a 1:2 dose ratio, but decreases were apparent for both UV_{254} and TOC.

Table 18 AOC formation in seawater with variable ozone doses.

	Ozone Dose (mg O_3:mg TOC)	**UV_{254} (cm^{-1})**	**% Diff Rel. to Control**	**TOC (mg/L)**	**% Diff Rel. to Control**	**AOC (µg/L)**	**% Diff Rel. to Control**
Tampa Bay	Control	0.171		5.95		57 ± 14	
	1:2	0.108	*-37%*	5.17	*-13%*	66 ± 25	*16%*
	1:1	0.079	*-54%*	4.19	*-30%*	19 ± 0	*-67%*
Arabian Sea	Control	0.014		1.32		13 ± 3	
	1:2	0.012	*-29%*	1.33	*1%*	69 ± 19	*431%*
	1:1	0.010	*-14%*	1.32	*-1%*	36 ± 2	*177%*

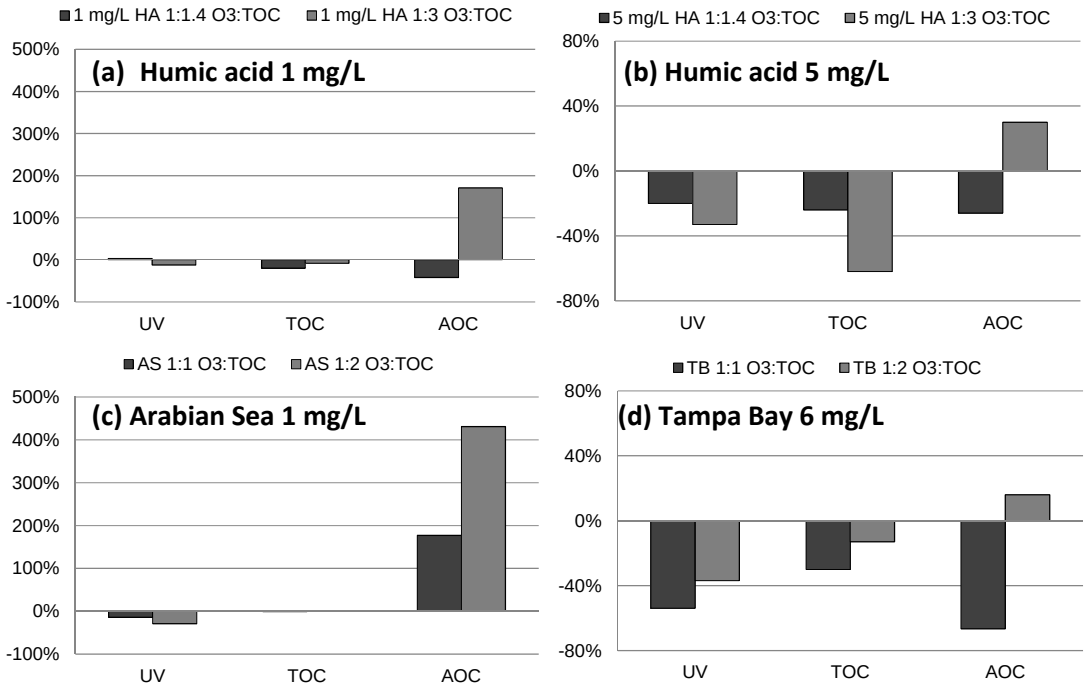

Figure 39 Comparison between organic carbon after ozonation of humic acid (a) 1 mg/L, (b) 5 mg/L and raw seawater from (c) Arabian Sea (AS; 1 mg/L) and (d) Tampa Bay (TB; 6 mg/L).

3.4.4 Chemical Grades and Impurities

Chemicals added during seawater RO desalination pretreatment may include a pH adjustor, antiscalant, and oxidant residual either alone or in combination. Chemicals such as citric acid, which may be used as part of a membrane cleaning or for pH adjustment, provide a readily biodegradable source of organic carbon and therefore an opportunity for unwanted bacterial proliferation on the RO membrane. In addition, comparisons between various chemical sources (e.g., sodium hexametaphosphate [SHMP]) indicated that impurities from different chemical grades and manufacturers may be an additional source of biodegradable carbon.

Four different manufactured sources of SHMP (SHMP A – D) were obtained to evaluate concentrations of organic carbon variability in solutions at two doses, 1 and 5 mg/L (Table 19). SHMP was used as a reliable chemical in RO pretreatment because of its ability to sequester and

prevent calcium from precipitating as a scale. Despite its use as an antiscalant, biofouling of RO membranes became a detrimental consequence (Alawadhi 1997; Voutchkov 2010). SHMP was selected for testing in this study to establish a baseline of biodegradable organic carbon from dosing a chemical known to cause biofouling. Chemical impurities have also been reported to cause biological fouling on RO membranes (Vrouwenvelder et al., 2001) and that potential side effect would not necessarily be detected in TOC (or even UV_{254}) measurements which are not specific to the biodegradability of the organic carbon. Three sources (SHMP B – D) provided an average of 100 µg/L AOC. The source with the lowest AOC (< 30 µg/L) was SHMP A but that had the greatest TOC concentration. AOC levels for SHMP D were similar for both solutions tested at 1 and 5 mg/L, which were 130 ± 10 and 100 ± 20 µg/L AOC, respectively. In all the samples UV_{254} was less than 0.01 cm^{-1}, which suggests that the impurities were not aromatic or carbon-carbon double bonds detected at that wavelength.

Only SHMP B showed a significant difference in AOC between the two doses; a 1 mg/L dose had 67 µg/L AOC and 5 mg/L had 141 µg/L AOC. SHMP-B is technical grade and therefore may have more impurities than the other chemicals, which were more expensive and of a higher grade. SHMP C and SHMP D concentrations also showed evidence of elevated organic carbon in higher dilutions; despite the fact that they were the same CAS number as SHMP A. SHMP B was also dosed at 1 mg/L into WBMWD intake seawater, with expected results: 164 µg/L AOC (control was 101 µg/L, SHMP 67 µg/L); however, neither UV_{254} nor TOC increased significantly. These results provide evidence that impurities in treatment chemicals may be sources of nutrients or a substrate for bacterial growth that may lead to biofouling. Furthermore, UV_{254}, and TOC are not effective methods for predicting the potential for bacterial growth, unlike the AOC test.

Polyphosphonates contain two or more phosphonate groups and may also be referred to as organophosphorus compounds because the structure contains at least one carbon. The simplest

structure that has been widely used in industry as an antiscalant and corrosion inhibitor is 1-hydroxy ethylidene-1,1-diphosphonic acid (HEDP). HEDP was tested at doses of 1 and 5 mg/L in a laboratory generated seawater matrix and in seawater from the intake at WBMWD (Table 20). The chemical was purchased neat and had variable AOC levels as high as 100 µg/L in seawater but less than 30 µg/L when tested in the buffer alone. A similar effect was seen in seawater for SHMP in that the AOC in the seawater test was increased by the amount of AOC in the laboratory generated matrix. Results reported are the average (and standard deviation) from two separate experiments in the WBMWD seawater.

Table 19 Organic carbon in solutions containing two doses of sodium hexametaphosphate (SHMP) from various manufacturers.

	Dose (mg/L)	UV_{254} (cm^{-1})	TOC (mg/L)	AOC (µg/L)
SHMP – A	1	0.004	1.0	27
	5	0.004	1.2	27
SHMP – B	1	0.004	0.6	67
	5	0.003	0.6	141
SHMP – C	1	0.003	0.7	101
	5	0.005	0.7	104
SHMP – D	1	0.001	< 0.25	130
	5	0.004	< 0.25	100
SHMP – B in seawater	Control	0.009	0.99	110
	1	0.010	1.06	164

Table 20 Organic carbon in solutions containing the polyphosphonate, 1-hydroxy ethylidene-1,1-diphosphonic acid (HEDP).

	Dose, mg/L	UV_{254} (cm^{-1})	TOC (mg/L)	AOC (µg/L)
HEDP	1	0.003	0.90	29
	5	0.003	1.80	20
HEDP in seawater	Control	0.009	0.99	110
	1	0.01	1.1	138 ± 47
	5	0.01	1.6	120 ± 7

The concentration of organic carbon was evaluated for linearity at increasing doses of antiscalants (Table 21). Active chemicals used for antiscalant applications in seawater RO are rarely identified specifically by the manufacturer and are a fraction of the concentration in the neat product sold. According to the MSDS assembled for this project, active concentration is generally 10 to 60% of the solution, averaging 35%. For dosing purposes, this is not taken into account and the manufacturers recommend calculating the dose based on 100% product concentration (or even super concentrates to facilitate easier shipping and storage with smaller volumes). Testing at elevated doses was planned to target only the active concentrate and thereby ascertain the potential for biodegradation of the neat chemical; however, testing using this approach prevented AOC measurement because the biocide and concentrated antiscalant prevented growth of the AOC test organism. TOC and UV_{254} were measured, and correlations were made at normal dosing ranges (< 10 mg/L) to the elevated range (40,000 mg/L).

The coefficient of determination indicated that the dose and resulting TOC showed a very strong correlation ($r^2 > 0.9$), partially because the range of concentrations spanned up to four magnitudes. For the antiscalant AWC A-104, there is a 1:1 relationship for dose versus TOC as indicated by the slope = 1.02. AWC A-104 is a polycarboxylate (inherently composed of organic carbon) with proprietary active ingredients, whereas the other chemicals are polyphosphonates without organic carbon as part of the proprietary formulation. At the lowest doses tested as recommended for the individual antiscalants, TOC increased 16 to 38% for phosphonates, and 19

to 60% for the polymer/polycarboxylates. Based on this information, organic carbon loading would occur from the addition of these chemicals. The potential for TOC to be broken down by oxidants into biodegradable carbon fractions could be significant depending on the treatment process, application, and dosing location. Furthermore, membrane fouling caused by elevated organic matter is a possibility if a treatment plant incorrectly doses antiscalant during pretreatment.

The polymer AWC A-104 had the greatest composition as TOC; the chemical is phosphorus-free, with an active concentration of a proprietary chemical. Depending on the dose (Table 22) TOC ranged from 50 to 100% of the composition of the antiscalant. AWC 102+, a polyphosphonate that contains phosphorus, not in phosphate form produced by the same manufacturer, was tested similarly. By comparison, the TOC composition of AWC 102+ was dose-dependent but ranged from 15 to 29%. A typical dosing rate for both chemicals is 1 mg/L for SWRO plants operating at 45 to 50% recovery.

AWC A-102+ and A-104 were dosed into seawater collected from the intake at WBMWD to evaluate the organic carbon levels in a seawater matrix. Targeted concentrations were 1 and 5 mg/L as outlined by the manufacturer. Two different tests were conducted (Table 22), and the results reported are the average (and standard deviation) from two separate experiments using the WBMWD seawater. In Test 1 the 5 mg/L dose seemed to be slightly lower than in Test 2 according to TOC concentrations. Inhibition by the bacteriostat in the 5 mg/L doses would explain the lower amount of AOC. By comparison with the 1 mg/L antiscalant doses in seawater, AOC levels are between 73 and 100 µg/L for the polymer A-104 and 109 to 163 µg/L for the polyphosphonate A-102 +. UV_{254} was generally within 20% of the seawater control.

Table 21 Correlations between organic carbon and antiscalant doses in typical and elevated ranges. Antiscalants were dosed with proprietary active ingredients into a laboratory generated seawater matrix.

		Typical range		Elevated range			
Poly-phosphate	**MDC 704 (mg/L)**	3	10	3800	40000	Slope	R^2
	TOC (mg/L)	0.59	0.79	40	144	0.003	0.966
	UV_{254} (cm^{-1})	0.01	0.01	0.01	0.01	9.6E-8	0.422
Polyphosphonate	**AWC 102+ (mg/L)**	1	10	100	500	Slope	R^2
	TOC (mg/L)	0.16	1.45	33	146	0.29	0.999
	UV_{254} (cm^{-1})	0.004	0.006	0.020	0.068	1.3E-04	0.997
	MDC 150 (mg/L)	3	10	3000	8500	Slope	R^2
	TOC (mg/L)	0.61	2.54	96	343	0.04	0.994
	UV_{254} (cm^{-1})	0.007	0.011	0.15	0.34	3.9E-05	0.994
	Vitec 3000 (mg/L)	2	7	3800	40000	Slope	R^2
	TOC (mg/L)	0.75	1.37	172	833	0.02	0.987
	UV_{254} (cm^{-1})	0.01	0.008	0.05	0.32	7.7E-06	0.999
Polycarboxylate/polymer	**AWC A-104 (mg/L)**	1	10	100	500	Slope	R^2
	TOC (mg/L)	0.60	4.86	107	508	1.02	0.9997
	UV_{254} (cm^{-1})	0.008	0.007	0.008	0.019	2.38E-05	0.971
	Flocon Plus N (mg/L)	3	10	3000	9000	Slope	R^2
	TOC (mg/L)	1.16	3.64	232	816	0.091	0.997
	UV_{254} (cm^{-1})	0.005	0.011	0.37	1.19	1.3E-04	0.999
	SpectraGuard™ SC	2	6	143000	275000	Slope	R^2
	TOC (mg/L)	0.37	0.37	1342	1860	0.007	0.962
	UV_{254} (cm^{-1})	0.001	0.001	0.285	0.511	1.9E-06	0.999

Table 22 Organic carbon in seawater from the WBMWD intake dosed with polyphosphonate and polymer antiscalants.

	Dose (mg/L)	UV_{254} (cm^{-1})	TOC (mg/L)	AOC (µg/L)
Seawater	Control	0.009	1.00	110 ± 21
AWC A-104	1	0.011 ± 0.001	1.47 ± 0.3	87 ± 19
	5	0.011 ± 0.003	3.86 ± 2.0	27 ± 16
AWC A-102 +	1	0.011 ± 0.002	1.12 ± 0.1	136 ± 38
	5	0.012 ± 0.001	1.76 ± 0.8	62 ± 65

Citric acid has been used for pretreatment in seawater RO, and has already been shown to be an assimilable food source for *V. harveyi* used in the AOC test (Weinrich et al., 2011). Understanding the chemical composition is an important part of predicting biological fouling potential. In some cases, such as citric acid, the actual chemical used for treatment can provide a food-source for microbial growth. There were two different tests conducted and the results reported are the average (and standard deviation) from two separate experiments in the WBMWD seawater (Table 23). Citric acid is used for membrane cleaning but also provides a nutrient source and increases the potential for biological growth in membranes. Tests of citric acid at concentrations of 1 and 5 mg/L in a laboratory generated seawater matrix resulted in AOC levels of 310 and 543 µg/L, respectively. In seawater, doses of 5 mg/L resulted in an average of 1020 µg/L. Citric acid is a known chemical food source for the marine AOC test organism; therefore, even if a high purity grade chemical is used, the inherent chemical component is easily assimilated. After cleaning, any residual citric acid that was not flushed or otherwise removed may cause increased AOC in the RO feed and additional nutrients for bacterial growth.

Table 23 Organic carbon in solutions dosed with the polycarboxylate, citric acid.

	Dose, mg/L	UV_{254} (cm^{-1})	TOC (mg/L)	AOC (µg/L)
Citric acid	1	0.003	1.50	310
	5	0.003	3.90	543
Citric acid in seawater	Control	0.009	0.99	110
	1	0.010 ± 0.001	1.38 ± 0.10	779 ± 510
	5	0.014 ± 0.004	3.45 ± 0.06	1020 ± 180

SBS was tested at doses of 1 and 5 mg/L (Table 24). SBS (alone or as a mixture of sodium metabisulfite) is applied during treatment to remove oxidant residual (e.g., chlorine) and protect membranes from oxidant damage. Many RO membrane warranties are contingent on keeping the ORP below a set point. Although UV_{254} and TOC levels were the same at both doses (UV_{254} = 0.003 cm^{-1} and TOC = 0.7 mg/L), AOC increased with increasing doses, from 58 µg/L in the 1 mg/L test solution to 116 µg/L for 5 mg/L SBS. SBS did not increase TOC or UV_{254} levels at the two doses tested but the amount of BOM measured by AOC increased.

Table 24 Organic carbon in seawater from WBMWD intake dosed with sodium bisulfite.

	Dose (mg/L)	UV_{254} (cm^{-1})	TOC (mg/L)	AOC (µg/L)
Sodium bisulfite	1	0.003	0.7	58
	5	0.004	0.6	116
Sodium bisulfite in seawater	Control	0.011	0.99	88
	5	0.012	0.97	102

3.4.5 Byproducts of Antiscalant and Chlorine Reactions

SBS is often the last chemical added before the RO membrane feed (i.e., after the cartridge filters), applied to reduce ORP, quench the disinfectant residual, and protect the membranes from the damaging effects of oxidants and disinfectants. Current pretreatment strategies often entail

antiscalant dosing prior to the addition of SBS; manufacturers recommend dosing antiscalant prior to the cartridge filters. In this scenario, the disinfectant residual (e.g., chlorine) would not have been quenched by SBS and would remain in the water during antiscalant addition. Because chlorine is a non-selective oxidant, the disinfectant would not only inactivate bacteria but also react with other components in the water including NOM and an antiscalant (if present). Byproducts from those reactions should be carefully considered. The following section discusses the potential for increased nutrient levels, for example AOC and phosphate that would occur following reactions between chlorine and frequently used antiscalants.

Antiscalant chemicals were tested from various manufacturers for each class: polyphosphates, polyphosphonates, and polycarboxylates. A total of 11 chemicals were tested at two doses each and the following results examine the changes to organic carbon and phosphate composition after reacting with free chlorine for 18 hours at 25°C. Polyphosphate had the greatest amount of AOC compared to the other chemical types (Table 25; 90 µg/L AOC at the 10 mg/L dose). Polyphosphonates and polycarboxylates generally had low AOC background levels (concentration before chlorination); AOC was only 10 µg/L higher than the control.

After reaction with chlorine, AOC increased by greater than 10 µg/L in seven of the solutions from five chemicals. Increases in AOC were not specific to a certain class of antiscalant; the results show that at least one chemical in each class had an increase in AOC after chlorination. The greatest increase was seen in the polyphosphonate chemical AWC A-102+ in the 10 mg/L solution, which increased AOC from 10 to 372 µg/L AOC, followed by an increase of 175 µg/L AOC in the 10 mg/L dose of polymer Acumer-Dow™ 2000 and an increase of 71 µg/L AOC in the 3 mg/L dose of polyphosphate Hypersperse™ MDC704. These and the other increases of biodegradable organic carbon are important considering that even a minor increase in AOC contributes to conditions where sufficient nutrients exist for bacteria to grow and

proliferate. For a few of the chemicals chlorination did not have an impact on AOC (i.e., ΔAOC was 0): HEDP, Acumer-DOW™ 2100, and AWC A-104.

Phosphate averaged 0.4 ± 0.6 mg/L, median 0.2 mg/L (n=22). Phosphate increased in all polyphosphate and polyphosphonate antiscalants after reaction with chlorine. This latter observation may be explained by an oxidation mechanism that breaks down one or two of the phosphonate groups from the carbon (Figure 40) to form orthophosphate. Although phosphate impurities in the polycarboxylate/polymer antiscalants averaged 0.4 mg/L, no increase was measured in the chlorinated solutions. No increase in phosphate was anticipated; the inherent makeup of polycarboxylate/polymers is not phosphate or phosphate-derivative based although the composition is proprietary.

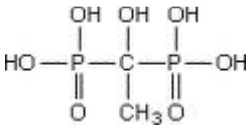

Figure 40 1-Hydroxy Ethylidene-1,1-Diphosphonic Acid (HEDP)

In the previous section, results were presented for the increase of TOC after addition of the antiscalant. Even at the minimum recommended doses, TOC increased by 0.5 and 2 mg/L in the minimum and maximum recommended doses, respectively. The range of changes in TOC was -0.3 to 0.3 mg/L. Although dosing the chemical increased TOC, changes to TOC were not detected after chlorination. For UV_{254} all levels were less than 0.01 cm^{-1}; these levels would be too low to practically identify impacts from treatment changes in an environmental seawater source. In fact, measurements for organic carbon including TOC and UV_{254} that are non-selective to BOM do not provide meaningful information regarding nutrients for bacterial growth and cannot be used as a BOM indicator measurement like AOC or even a direct phosphate nutrient measurement.

Chlorine demand was also monitored to evaluate the reactivity of the antiscalant; chlorine was measured after the 18 hour reaction time and subtracted from the residual in the matrix control. Chlorine demand was greatest in both Hypersperse™ MDC150 and Vitec® 3000 at 5.5 mg/L Cl_2. These chemicals are both polyphosphates; as such, the major byproduct did not appear to be AOC but rather phosphate. Phosphate increased by 3.3 and 3.4 mg/L in the post-chlorination solutions for Hypersperse™ MDC150 and Vitec® 3000, respectively.

Many of these antiscalants would react with chlorine to increase the amount of biodegradable carbon or other nutrients in the RO feed, which would create optimum conditions for biological growth on the membranes. Therefore, the treatment strategies could be amended to minimize additional AOC formation and phosphate liberation by removing the oxidant residual before the antiscalant is added. AOC and phosphate measurements both indicate the presence of necessary nutrients for bacterial growth and proliferation. A strategy to minimize nutrients would be useful for controlling RO membrane biofouling.

Table 25 Nutrient and organic carbon data for 11 antiscalants before and after reaction with chlorine in a laboratory generated seawater matrix.

				Baseline levels				Post-reaction with chlorine											
	Trade Name	Dose mg/L	pH	AOC (µg/L)	PO_4^{3-} (mg/L)	TOC (mg/L)	UV_{254} (cm^{-1})	Cl_2 demand (mg/L)	AOC (µg/L)	PO4 (mg/L)	TOC (mg/L)	UV_{254} (cm^{-1})	Δ AOC	Δ PO4	Δ TOC	Δ UV_{254}	% ΔAOC	% ΔPO4	% Δ TOC	% Δ UV_{254}
Poly-phosphate	Hypersperse™ MDC 704	3	8.8	76	1.2	0.55	0.001	2.9	147	1.5	0.39	0.001	71	0.4	-0.2	0.000	93%	32%	-29%	0%
		10	8.9	90	0.9	0.84	0.001	4.8	118	4.7	0.91	0.001	28	3.9	0.1	0.000	31%	446%	9%	0%
Polyphosphonate	AWC A102+	1	8.8	0	0.0	0.12	0.001	4.2	10	0.4	0.25	0.003	10	0.4	0.1	0.002	0%	0%	105%	200%
		10	8.8	10	0.0	1.41	0.001	4.5	372	5.0	1.51	0.005	362	5.0	0.1	0.004	3620%	0%	7%	400%
	HEDP	1	8.8	9	0.5	0.80	0.001	1.1	10	0.5	0.90	0.002	1	0.1	0.1	0.001	10%	18%	0%	100%
		5	8.6	10	0.1	1.70	0.001	1.6	10	1.2	1.80	0.009	0	1.1	0.1	0.008	0%	1892%	0%	800%
	Hypersperse™ MDC 150	3	8.7	10	0.3	0.57	0.001	4.2	58	2.8	0.61	0.007	48	2.6	0.0	0.006	480%	952%	8%	600%
		10	8.7	2	0.3	2.50	0.005	5.5	10	3.7	2.21	0.005	8	3.4	-0.3	0.000	342%	1107%	-12%	0%
	Vitec® 3000	2	8.9	5	0.0	0.71	0.004	4.2	50	2.5	0.44	0.004	45	2.5	-0.3	0.000	900%	0%	-38%	0%
		7	8.9	10	0.0	1.33	0.002	5.5	10	3.3	1.25	0.002	0	3.3	-0.1	0.000	0%	0%	-6%	0%
Polycarboxylate/polymer	Acumer-DOW™ 1035	1	8.7	7	2.8	0.15	0.001	0.5	10	0.0	0.22	0.005	3	-2.8	0.1	0.004	42%	-100%	43%	400%
		10	8.5	1	0.1	1.73	0.001	0.0	10	0.0	1.55	0.000	9	-0.1	-0.2	-0.001	688%	-100%	-10%	-100%
	Acumer-DOW™ 2000	1	8.6	10	0.4	0.28	0.001	0.5	12	0.0	0.50	0.003	2	-0.4	0.2	0.002	22%	-100%	81%	200%
		10	8.6	0	0.5	2.03	0.003	0.5	176	0.1	2.03	0.000	175	-0.4	0.0	-0.003	55340%	-85%	0%	-100%
	Acumer-DOW™ 2100	1	8.7	3	0.0	0.19	0.003	1.1	10	0.0	0.23	0.003	7	0.0	0.0	0.000	195%	0%	21%	0%
		10	8.7	10	0.0	1.66	0.003	0.8	10	0.0	1.74	0.003	0	0.0	0.1	0.000	0%	0%	5%	0%
	AWC A-104	1	8.8	1	0.0	0.56	0.002	0.7	10	0.0	0.68	0.005	9	0.0	0.1	0.003	890%	-100%	21%	150%
		10	8.8	10	0.3	4.82	0.001	0.0	10	0.0	4.79	0.008	0	-0.3	0.0	0.007	0%	-100%	-1%	700%
	FloCon+ N	3	8.6	10	0.1	1.12	0.001	0.2	10	0.0	1.26	0.004	0	-0.1	0.1	0.003	0%	-100%	12%	300%
		10	8.4	4	0.3	3.60	0.005	0.3	10	0.0	3.89	0.009	6	-0.3	0.3	0.004	150%	-100%	8%	80%
	SpectraGuard ™ SC	2	8.4	10	0.2	0.10	0.001	0.0	18	0.0	0.06	0.000	8	-0.2	0.0	-0.001	80%	-100%	-42%	-100%
		6	8.7	0	0.1	0.10	0.001	0.2	10	0.0	0.22	0.009	10	-0.1	0.1	0.008	6049%	-100%	108%	800%

CHAPTER 4: CONCLUSIONS AND FUTURE RESEARCH

4.1 Conclusions

This study was designed to investigate the hypothesis that biodegradable organic matter, specifically AOC contributes to biological fouling of RO membranes used for seawater desalination. The research results suggest that monitoring AOC is better than TOC or other parameters commonly used in the industry. Evaluating AOC after various stages in pretreatment would provide the operator with the information needed to institute a control strategy for minimizing biofouling potential within the plant and before the RO membranes.

4.1.1 Objective 1 Summary

Through the investigation of relationships among biofouling potential, chemical dosing, operational data, and AOC in full scale SWRO desalination plants, it was revealed that pretreatment processes were not typically effective for removal of organic carbon. Predictor variables were modeled to determine the impact of water quality on differential pressure and specific flux; SDI was not a significant predictor despite routine monitoring at the plant. The addition of SBS increased AOC and biofouling potential.

The removal of TOC by the pretreatment process at TBSDP ranged between 3 and 6%, and UV_{254} was not reduced by more than 16% to a minimum of 0.11 cm^{-1}. TOC was greater than 5 mg/L in the RO feed (around 5 – 6 mg/L at the intake). AOC within the TBSDP pretreatment steps was generally low in the diatomaceous earth filtrate but increased in the post-cartridge filter sampling point (i.e., RO feed). Chemical addition of SBS accounted for the increase in AOC. AOC in the RO feed led to biological growth and subsequent RO membrane fouling; at TBSDP, fouling was observed as elevated differential pressure in November 2012 and a decrease in specific flux over the time period investigated.

During the collection periods at WBMWD, membrane changes and hybrid configurations were being evaluated. The changing operations challenged meaningful interpretations of the impact on differential pressure. The plant had reported challenges in the past with biological fouling of the RO membranes. From the data modeling, decreased specific flux had the strongest correlation to AOC levels at the plant. Other operational observations indicated that chemical dosing accounted for higher AOC levels upstream of the RO membranes, even when the seawater at the intake had the lowest organic carbon content compared to the other sampling events. The trends were comparable by observing increases in AOC from cleaning agent residuals and the addition of SBS; the increased biodegradable organic carbon was not observed in the TOC measurement alone.

Operational data from the Al Zawrah plant were limited because the staff was not using normalization software for record keeping. The absence of RO operating information limited the evaluation of water quality impacts on the RO system, but changes in differential pressure at the cartridge filter provided information about their condition and evidence that biological growth may have occurred. The data showed a very strong positive correlation for differential pressure of the cartridge filters and AOC in the RO feed ($r = 0.984$, $p < 0.01$, $n = 48$). UV_{254} also had a strong relationship to the data cartridge filter data. This plant was the only facility of the three in this project that had potential for AOC removal through DMF; however, AOC removal across the filters was not consistent. If AOC is monitored and pretreatment is optimized for the removal of organic carbon, biological fouling on both cartridge filters and ultimately on RO membranes could be minimized.

Full-scale SWRO treatment plants generally had poor or inconsistent TOC removal. AOC was present in the RO feed at all locations from 10 to 180 µg/L. In most cases, neither TOC nor UV_{254} had a statistically significant relationship to AOC. Increases, in RO membrane differential

pressure, and decreases in specific flux, were two operational changes that were most consistent with the effects of fouling on the RO membranes. Poor organic carbon removal and inconsistent operations are widespread challenges in SWRO. The positive and strong relationships determined from investigating AOC as a predictor variable for biological growth confirms the presence of biodegradable organic carbon and the resulting adverse impact on operations. Based on the results from TBSDP, a threshold between 30 and 60 µg/L AOC would increase the potential for biofouling. Other SWRO plants should evaluate their systems to identify impacts of chemical addition on the presence of AOC and determine the thresholds at which the system would experience increased biofouling potential and operational changes.

4.1.2 Objective 2 Summary

The influence of AOC on biological fouling in bench- and pilot-scale RO membrane testing was investigated. Changes to differential pressure were monitored in pretreated TBSDP water under constant flux conditions in a pilot unit. Increased differential pressure was associated with RO membrane biological fouling when the median AOC concentration naturally present in TBSDP was 50 µg/L and permeate flux was constant. Even with a constant setting, flux decline occurred from biological fouling, and membrane pores were blocked by biofilm growth. AOC was more significant than TOC for predicting changes to differential pressure. A regression model with AOC and TOC combined was significant for predicting differential pressure; however, UV_{254} was not a significant predictor variable.

Using a crossflow RO membrane test cell, RO feed that contained 1000 µg/L acetate carbon was used to evaluate whether increased AOC loading would affect RO membrane fouling as compared to the 30 µg/L AOC baseline. The extreme difference in AOC concentrations was used to increase the fouling occurrence and monitor the effect in a shorter time period. Permeate flux decline was associated with RO membrane biological fouling when AOC was elevated and

other conditions were constant, including operating pressure and water quality. Flux decline under the same operational conditions was greater in the test where the RO feed contained more AOC from additional biofilm formation and organic fouling. Biofilm and bacterial deposits were apparent from the SEM imaging. Fouling was detected on more portions of the RO membrane when AOC was higher.

4.1.3 Objective 3 Summary

AOC formation and other organic carbon changes were evaluated in seawater treated with three commonly used oxidants: chlorine, chlorine dioxide, and ozone. Laboratory generated seawater solutions containing humic acid and environmental seawater was tested in a series of bench-scale oxidation tests using chlorine, chlorine dioxide, and ozone to observe the impacts of these oxidants on BOM formation. AOC was formed as a byproduct of reactions with these disinfectants commonly used in water treatment. In many of the treatments, the biodegradability of the water increased; in full-scale applications, these effects would generate conditions amenable to bacterial proliferation and subsequent biological fouling. AOC was increased as much as 70% in seawater with 1 mg/L humic acid and a chlorine dose of 0.5 mg/L Cl_2; changes to UV_{254} and TOC were minimal (2% and -4%, respectively). Higher concentrations of humic acid did not produce additional AOC, most likely because of the high ionic strength of the seawater matrix and internal hydrophobic molecular interactions of humic acid that have been reported to inhibit expansion of the molecule. Implications from these results suggest that even plants with low TOC (e.g., 1 mg/L) would be vulnerable to reaction with the oxidant and subsequent increased RO feed biodegradability. Chlorine dioxide reacts slowly with humic acid and did not significantly change UV_{254}, TOC, or AOC in testing with a 4-hour contact time. Longer contact times or greater chlorine dioxide doses may have a different effect. The reactivity between oxidants and environmental seawater sources varied. Except for the intake seawater from WBMWD, UV_{254} decreased or remained unchanged in all the water tested. Decreases in UV_{254}

are usually from the breakdown of aromatic and double carbon bonds in humic structures. UV_{254} increased in the seawater collected from WBMWD when chlorine or chlorine dioxide was applied. Increases are not as clearly understood but may have resulted from the breakdown or lysis of microbial components (e.g., algae) that released intracellular organic material. When the AOC and therefore inherent biodegradability of the seawater increased after treatment, TOC did not follow the same trend. In test solutions with either chlorine or chlorine dioxide that exhibited increases in UV_{254} (West Basin) and AOC (Tampa Bay), TOC changes averaged 3% and -2%, respectively. TOC does not provide insight into the changes to the biodegradability of the water. Unfortunately, TOC is often the only organic carbon parameter used in SWRO water quality monitoring, although it is not an informative tool for the plant operators to predict biofouling potential.

4.1.4 Objective 4 Summary

Pretreatment chemicals, including antiscaling, membrane cleaning and dechlorinating agents were tested for AOC formation and other organic carbon changes following chlorination. Chemical impurities in treatment chemicals were shown to increase AOC concentrations (e.g., SBS increased AOC at a baseline level of 58 µg/L for 1 mg/L of SBS) that were otherwise undetected by UV_{254} and TOC measurements. Antiscalants increase organic carbon concentration linearly by dosing the neat chemical. Antiscalants often contain a bacteriostat to inhibit bacterial growth during storage. If the solution is underdosed, the biocide will be diluted and inherent nutrients or chemical impurities have been shown to increase AOC during bench-scale testing. Phosphate and AOC are byproducts of reactions between antiscalants and chlorine. The byproducts could lead to biological fouling on the RO membrane because of the increased assimilable nutrient loading and potentially decrease effectiveness of the antiscalant. Better operational practices that include removing the chlorine residual prior to dosing the antiscalant would alleviate the adverse effect of AOC byproducts.

4.1.5 Recommendations

SWRO plant managers would benefit from exploring more efficient techniques for the removal of organic carbon during treatment. TOC removal efficiency is typically very poor and pretreatment impacts on AOC levels should be understood and controlled in SWRO plants that have biological fouling problems. Personnel should investigate the sources of AOC during pretreatment since certain pretreatment chemicals were shown to increase AOC if present along with a disinfectant residual. Minor pretreatment adjustments may help control AOC levels in the RO feed. Despite impacts to water quality at the intake (e.g. algal blooms), this report has shown that antiscaling, membrane cleaning, and dechlorinating agents could be wholly responsible for increasing AOC in the RO feed. Monitoring chemical supplies for impurities is one option for AOC control. Furthermore, it would be useful if the water industry was provided with specifications and additional information on antiscalant and chemical dosing in the form of a guidance manual from the American Water Works Foundation or other national organizations an unbiased source of information. At the moment, most information on dosing is directly from the manufacturer without a larger oversight for other implications at the plant. Changing the configuration to reduce the ORP before addition of antiscalant would reduce the contact time between the disinfectant and the antiscalant, which may breakdown the parent compound and produce AOC as a byproduct.

Pretreatment applications have largely been focused on physical separation. Membrane pretreatment, for example, using micro- or ultrafiltration membranes can be effective for particulate removal, and even some removal of TOC. However, low molecular weight organic molecules can readily pass through those membranes. These molecules typically compose the AOC fraction of water. Therefore, membrane pretreatment systems would still be vulnerable to biological fouling on the RO membranes unless the AOC fraction was controlled. Further development of biological treatment to reduce nutrients in the RO feed would be valuable.

Evaluating pretreatment impacts using new methods such as the bioluminescent AOC test will facilitate control measures to optimize chemical addition and achieve reduced biodegradable nutrients loading and fouling rates. Additional focus on information collection for data modeling applications and real-time monitoring is recommended. Other quantitative and qualitative techniques for monitoring water quality and microbiology of seawater intakes and during pretreatment will aid current and future SWRO applications. Additional SWRO research and development are crucial for the efficiency of this growing industry.

Biological filtration and other pretreatment management options should be investigated for removal of biodegradable byproducts to minimize AOC and subsequent biological fouling. This research shows that AOC was a significant predictor variable for biological fouling impacts on increased differential pressure or permeate flux decline in bench-, pilot-, and full-scale studies. SWRO plant managers interested in minimizing these adverse operational effects and biofouling occurrence in SWRO should consider the following scenarios:

- Measuring the water quality at the intake and the RO feed would be a first step in determining the effectiveness of pretreatment on AOC removal.
- Systems that use oxidants (e.g. hypochlorite, chlorine dioxide) should monitor AOC after typical and extreme dosing scenarios.
- Systems that use antiscalants should first reduce ORP first (e.g. with SBS/sodium metabisulfite) to maintain antiscalant effectiveness and minimize formation of AOC. SBS solutions may also contain impurities that increase AOC, so dosing should be carefully considered.
- Chemical dosing should be evaluated through bench-scale tests to minimize AOC, maximize desired outcome, and optimize the treatment process for better operational control.

- Fluctuating water quality at the intake should be tracked to correlate sources of AOC increases (algae, increased organic loading, rain events) so that operations may be adjusted to account for changes in AOC and minimize biofouling potential.

Future studies should be conducted at individual treatment plants to evaluate the maximum AOC threshold for controlling biological fouling based on water quality and the process train. Plant managers may thereby institute measures to control the nutrients entering the RO feed; pretreatment adjustment by maximizing organic carbon removal or minimizing chemicals that may exacerbate the biodegradability of the RO feed would be efficient preliminary approaches. Identifying the locations during pretreatment in a specific system where AOC is formed or increased would be the first step to control biofouling occurrence and minimize its potential and associated adverse effects on SWRO plant operations.

ACRONYMS

AOC	assimilable organic carbon
ATMP	amino trimethylene phosphonic acid
BOM	biodegradable organic matter
CAS	Chemical Abstract Service
CIP	clean in place
DE	diatomaceous earth
DMF	dual media filter
DOC	dissolved organic carbon
DOM	dissolved organic matter
g	gram
gpm	gallons per minute
gpd	gallons per day
HEDP	1-hydroxy ethylidene-1,1-diphosphonic acid
L	liter
Lpm	liters per minute
Lmh/bar	liters per square meter per hour per bar of applied pressure
M	molarity
MCL	maximum contaminant level
MGD	million gallons per day
min	minutes
mL	milliliter
mm	millimeter
mV	millivolt unit for oxidation reduction potential; microvolt for zeta potential
nm	nanometer
NDP	net driving pressure

O_3	ozone
O&M	operation and maintenance
ORP	oxidation reduction potential
PBTC	2-phosphonobutane-1,2,4-tricarboxylic acid
ppm	parts per million
psi	pounds per square inch
RLCA	reaction-limited colloid aggregation
RO	reverse osmosis
SDI	silt density index
SHMP	sodium hexametaphosphate
SEM	scanning electron microscopy
SS	stainless steel
SWRO	seawater reverse osmosis
TBSDP	Tampa Bay Seawater Desalination Plant
TFC	thin film composite
TOC	total organic carbon
UF	ultrafiltration
WBMWD	West Basin Municipal Water District

LIST OF REFERENCES

Alawadhi, A. A. Pretreatment plant design – key to a successful reverse osmosis desalination plant. *Desal*., **1997**, *110 (1–2),* 1–10.

American Public Health Association. 2005. Standard Methods for the Examination of Water and Wastewater. 21st Edition.

Amy, G. L.; Rodriguez, S. G. S.; Kennedy, M. D.; Schippers, J. C.; Rapenne, S.; Remize, P.-J.; Barbe, C.; de O. Manes, C. L.; West, N. J.; Lebaron, P.; van der Kooij, D.; Veenendaal, H.; Schaule, G.; Petrowski, K.; Huber, S.; Sim, L. N.; Ye, Y.; Chen, V.; Fane, A. G. **2011** Chapter 1. Water quality assessment tools. *Membrane-Based Desalination: An Integrated Approach (MEDINA)*. (Drioli, E., Criscuoli, A. & Macedonio, F. eds.) IWA Publishing, London.

Antony, A., Low, J. H., Gray, S., Childress, A. E., Le-Clech, P., Leslie, G. Scale formation and control in high pressure membrane water treatment systems: A review. *J. of Mem. Sci*., **2011**. *383*(1-2): 1-16.

Bae, H., Kim, H., Jeong, S., Lee, S. Changes in the relative abundance of biofilm-forming bacteria by conventional sand-filtration and microfiltration as pretreatments for seawater reverse osmosis desalination. *Desal.* **2011**, *273*(2), 258-266.

Benner, R., Biddanda, B., Black, B., McCarthy, M. Abundance, size distribution, and stable carbon and nitrogen isotopic compositions of marine organic matter isolated by tangential-flow ultrafiltration. *Mar. Chem.* **1997,** *57*(3–4), 243–263.

Cai, Z. & Benjamin, M. M. NOM fractionation and fouling of low-pressure membranes in microgranular adsorptive filtration. *Environ. Sci. Technol*. **2011,** *45*(20), 8935–8940.

Caron, D. A., Garneau, M. È., Seubert, E., Howard, M. D., Darjany, L., Schnetzer, A., ... & Trussell, S. Harmful algae and their potential impacts on desalination operations off southern California. *Wat. Res*. **2010**, *44*(2), 385-416.

Carter, N. T. 2011 *Desalination: Technologies, Use, and Congressional Issues.* 7-5700. Congressional Research Service, Washington DC.

Chong, T.H., Wong, F.S., Fane, A.G. The effect of imposed flux on biofouling in reverse osmosis: role of concentration polarisation and biofilm enhanced osmotic pressure phenomena. *J. Mem. Sci*., **2008**. *325*(2), 840-50.

Conte, P., & Piccolo, A. Conformational arrangement of dissolved humic substances. Influence of solution composition on association of humic molecules. *Env. Sci. & Tech.*,**1999,** *33*, 1680–1690.

Cornelissen, E. R., Vrouwenvelder, J. S., Heijman, S. G. J., Viallefont, X. D., Van Der Kooij, D., Wessels, L. P. Periodic air/water cleaning for control of biofouling in spiral wound membrane elements. *J. Mem. Sci.*, **2007**, *287*(1), 94-101.

Demadis, K.D., R.G. Raptis, and P. Baran, Chemistry of Organophosphonate Scale Growth Inhibitors: 2. Structural Aspects of 2-Phosphonobutane-1,2,4-Tricarboxylic Acid Monohydrate (PBTC.H2O). *Bioinorg. Chem. and App.*, **2005**. *3*(3-4): 119-134.

Drew, R., Desalination in Florida: Technology, Implementation, and Environmental Issues. 2010: Tallahassee, FL. http://www.dep.state.fl.us/water/docs/desalination-in-florida-report.pdf. 2014.

Duranceau, S. J. 2007 *Use of Membrane Forensics for Solving Operational Problems in Desalting Facilities.* International Desalination Association World Congress of Desalination and Water Reuse, Maspalomas, Gran Canaria.

Ebrahim, S., Abdel-Jawad, M., Bou-Hamad, S., Safar, M. Fifteen years of R&D program in seawater desalination at KISR Part I. Pretreatment technologies for RO systems. *Desal*., **2001**, *135*(1), 141-153.

Edzwald, J. K. & Haarhoff, J. Seawater pretreatment for reverse osmosis: chemistry, contaminants, and coagulation. *Water Res.* **2011,** *45 (17),* 5428–5440.

Flemming, H. C.; Schaule, G.; Griebe, T.; Schmitt, J.; Tamachkiarowa, A. Biofouling - the Achilles heel of membrane processes. *Desal*. **1997,** *113,* 215–225.

Fujiwara, N.; Matsuyama, H. Elimination of biological fouling in seawater reverse osmosis desalination plants. *Desal.* **2008,** *227,* 295–305.

Gasson, C (Ed.), C. Gonzalez-Manchon, F. Alvarado-Revilla 2010. Desalination Markets 2010: Global Forecast and Analysis. Global Water Intelligence.

Glaze, W.H. and H. Weinberg, *Identification and Occurrence of Ozonation By-Products in Drinking Water*. 1993, American Water Works Association (Water Research Foundation): Denver, CO.

GWI DesalData. Desalination Tracker. Global Water Intelligence. 2012. http://www.globalwaterintel.com

Griebe, T. & Flemming, H. C. Biocide-free antifouling strategy to protect RO membranes from biofouling. *Desal.* **1998,** *118,* 153–156.

Hambsch, B. & Werner, P. Control of bacterial regrowth in drinking-water treatment plants and distribution system. *Water Supply.* **1993,** *11*, 299–308.

Hammes, F.; Salhi, E.; Köster, O.; Kaiser, H.P.; Egli, T.; von Gunten, U. Mechanistic and kinetic evaluation of organic disinfection by-product and assimilable organic carbon (AOC) formation during the ozonation of drinking water. *Water Res*. **2006,** *40*, 2275–2286.

Hammes, F.; Meylan, S.; Salhi, E.; Köster, O.; Egli, T.; von Gunten, U. Formation of assimilable organic carbon (AOC) and specific natural organic matter (NOM) fractions during ozonation of phytoplankton, *Water Res*. **2007,** *41*, 1447–1454.

Hausman, R., Gullinkala, T., & Escobar, I. C. Development of copper-charged polypropylene feedspacers for biofouling control. *J. Mem. Sci*, **2010**, *358*(1), 114-121.

Herzberg, M. and Elimelech, M. Biofouling of reverse osmosis membranes: Role of biofilm-enhanced osmotic pressure. *J. Mem. Sci*., **2007**. *295*(1-2): 11-20.

Hilal, N., Al Abri, M., Al Hinai, H. Enhanced Membrane Pre Treatment Processes using Macromolecular Adsorption and Coagulation in Desalination Plants: A Review. *Sep. Sci. and Tech*., **2006**. *41*(3): 403-453.

Hilal, N., Al-Zoubi, H., Darwish, N. A., Mohamma, A. W., Abu Arabi, M. A comprehensive review of nanofiltration membranes: Treatment, pretreatment, modelling, and atomic force microscopy. *Desal*., **2004**, *170*(3), 281-308.

Huang, J.; Su, Z.; Xu, Y. The evolution of microbial phosphonate degradative pathways. *J. Mol. Evol.* **2005,** *61*(5), 682–690.

Kumar, M.; Adham, S. S.; Pearce, W. R. Investigation of seawater reverse osmosis fouling and its relationship to pretreatment type. *Environ. Sci. Technol.* **2006,** *40*, 2037–2044.

Ladner, D. A.; Litia, E.; Seng, C. M.; Clark, M. M. *Membrane Fouling by Marine Algae in Seawater Desalination*. **2010.** Report of the Water Research Foundation, Arsenic Water Technology Partnership, WERC.

LeChevallier, M. W.; Becker, W. C.; Schorr, P.; Lee, R. G. Evaluating the performance of biologically active rapid filters. *J. AWWA* **1992,** *84*(4), 136–140.

LeChevallier, M. W.; Shaw, N. E.; Kaplan, L. A.; Bott, T. L. Development of a rapid assimilable organic carbon method for water. *Appl. Environ. Microb.* **1993,** *59*(5), 1526–1531.

Lee, J., Jung, J. Y., Kim, S., Chang, I. S., Mitra, S. S., Kim, I. S. Selection of the most problematic biofoulant in fouled RO membrane and the seawater intake to develop biosensors for membrane biofouling. *Desal.* **2009**. *247*, 125-136.

Lenntech B.V. 2008-2014 © http://www.lenntech.com/processes/desalination/reverse-osmosis/general/reverse-osmosis-desalination-process.htm#Spiral_Wound_Seawater_Reverse_Osmosis_modules. 2014.

Lyster, E. and Y. Cohen, Numerical study of concentration polarization in a rectangular reverse osmosis membrane channel: Permeate flux variation and hydrodynamic end effects. *J. Mem. Sci.*, **2007**. *303*(1-2): 140-153.

Mansouri, J., Harrisson, S., Chen, V. Strategies for controlling biofouling in membrane filtration systems: challenges and opportunities. *J. Mat. Chem.*, **2010**. *20*(22): 4567-4586.

Matin, A., Khan, Z., Zaidi, S. M. J., Boyce, M. C. Biofouling in reverse osmosis membranes for seawater desalination: phenomena and prevention. *Desal.*, **2011**, *281*, 1-16.

McDonogh, R., G. Schaule, H.-C. Flemming. The permeability of biofouling layers on membranes. **1994**. Amsterdam, Netherlands: Publ. by Elsevier Science Publishers B.V.

Miltner, R. J.; Shukairy, H. M.; Summers, S. Disinfection by-product formation and control by ozonation and biotreatment. *J. AWWA* **1992,** *84*(11), 53–62.

Musale, D. A.; Yao, B.; Lopes, S.; Urmenyi, A.; Fazel, M.; Lohokare, H.; Yeleswarapu, R.; Hallsby, A.; Sheikh, A. A new phosphorus-free antiscalant for membrane desalination. *Desal. Water Treat.* **2011,** *31*, 279–284.

Naidu, G.; Jeong, S.;, Vigneswaran, S.; & Rice, S. A. Microbial activity in biofilter used as a pretreatment for seawater desalination. *Desal.*, **2013,** *309*, 254–260.

National Research Council. Desalination: A National Perspective. Washington, DC: The National Academies Press, **2008**.

Ong, S. L.; Hu, J. Y.; Ng, W. J.; Wang, L.; Phua, E. T. An investigation on biological stability of product water generated by lab-scale and pilot-scale distillation systems. *Environ. Mon. Assess.* **2002,** *77*, 243–254.

Pang, C. M.; Hong, P.; Guo, H.; Liu, W.-T. Biofilm formation characteristics of bacterial isolates retrieved from a reverse osmosis membrane. *Environ. Sci. Technol.* **2005,** *39*(19), 7541–7550.

Panglisch, S., et al., Chapter 7. *Optimization and modelling of seawater and brackish water reverse osmosis desalination membranes* in *Membrane-Based Desalination: An*

Integrated Approach (MEDINA), E. Drioli, A. Criscuoli, and F. Macedonio, Editors. 2011, IWA Publishing: London, UK.

Penru, Y.; Guastalli, A. R.; Esplugas, S.; Baig, S. Application of UV and UV/H2O2 to seawater: Disinfection and natural organic matter removal. *J. of Photochem. & Photobiology A: Chemistry*. **2012,** *233*, 40–45,

Picioreanu, C., Vrouwenvelder, J.S., van Loosdrecht, M.C.M. Three-dimensional modeling of biofouling and fluid dynamics in feed spacer channels of membrane devices. *J. Mem. Sci.*, **2009**. *345*(1-2): 340-54.

Pontié, M., et al., Tools for membrane autopsies and antifouling strategies in seawater feeds: a review. *Desal*., **2005**. *181*(1-3): 75-90.

Radu, A. I., Vrouwenvelder, J. S., Van Loosdrecht, M. C. M., Picioreanu, C. Modeling the effect of biofilm formation on reverse osmosis performance: Flux, feed channel pressure drop and solute passage *J. Mem. Sci.*, **2010**. *365*(1-2): 1-15.

Reckhow, D.A., Singer, P.C.; Malcolm, R.L. Chlorination of Humic Materials: Byproduct Formation and Chemical Interpretations. *Env. Sci. & Tech*, **1990,** *24:11*, 1655–1664.

Resosudarmo, A., Ye, Y., Le-Clech, P., Chen, V. Analysis of UF membrane fouling mechanisms caused by organic interactions in seawater. *Wat. Res*., **2013**, *47*(2), 911-921.

Saeed, M. O., Al-Otaibi, G. F., Ozair, G., & Jamaluddin, A. T. **2004**. Boifouling <sic> Potential In Open Sea And Adjacent Beach Well Intake Systems. In Report of International Conf. on Water Resources & Arid Environment.

Schechter, D. S. & Singer, P. C. Formation of aldehydes during ozonation. *Ozone Sci. Eng.* **1995,** *17*(1), 53–69.

Schneider, O., *et al*., *Investigation of Organic Matter Removal in Saline Waters by Pretreament*. 2011, Water Research Foundation: Denver, CO.

Schneider, O. D.; Weinrich, L. A.; Giraldo, E.; LeChevallier, M. W. Impacts of salt type and concentration on coagulation of humic acid and silica. *J. of Water Supply*. **2013,** *62(6)*, 339–349.

Schneider, R. P.; Ferreira, L. M.; Binder, P.; Bejarano, P. M.; Goes, K. P.; Machado, C. R.; Rosa, G. M. Z. Dynamics of organic carbon and of bacterial populations in a conventional pretreatment train of a reverse osmosis unit experiencing severe biofouling. *J. Mem. Sci.* **2005,** *266*(1–2), 18–29.

Shih, W.-Y.; Albrecht, K.; Glater, J.; Cohen, Y. A dual-probe approach for evaluation of gypsum crystallization in response to antiscalant treatment. *Desal.* **2004,** *169*(3), 213–221.

Siddiqui, M. S.; Amy, G. L.; Murphy, B. D. Ozone enhanced removal of natural organic matter from drinking water sources. *Water Res.* **1997,** *31*(12), 3098–3106.

Sobana, S. and Panda, R. Review on modelling and control of desalination system using reverse osmosis. *Rev. in Env. Sci. and Biotech.* **2011**. *10*(2): 139-150.

Subramani, A., Kim, S., Hoek, E.M.V. Pressure, flow, and concentration profiles in open and spacer-filled membrane channels. *J. Mem. Sci.*, **2006**. *277*(1-2): 7-17.

Sweity, A.; Oren, Y.; Ronen, Z.; Herzberg, M. The influence of antiscalants on biofouling of RO membranes in seawater desalination. *Water Res.* **2013,** *47(10)*, 3389–3398.

Świetlik, J.; Dąbrowska A.; Raczyk-Stanisławiak U.; Nawrocki, J. Reactivity of natural organic matter fractions with chlorine dioxide and ozone. *Water Res.* **2004,** *38,* 547–558

Tang, C.Y.; Chong, T.H.; Fane, A.G. Colloidal interactions and fouling of NF and RO membranes: A review. *Advances in Colloid and Interface Science*, **2011**, *164*, 126-143.

Tansakul, C., S. Laborie, and C. Cabassud, Adsorption combined with ultrafiltration to remove organic matter from seawater. *Water Res.* **2011,** *45* (19), 6362-6372..

Taylor, J. S. & Weisner, M. 1999 Chapter 11. Membranes. *Water Quality and Treatment. A Handbook of Community Water Supplies.* Letterman, R. D. ed. McGraw-Hill, New York.

Van Der Kooij, D. Effect of Treatment on Assimilable Organic Carbon in Drinking Water in Second National Conference on Drinking Water. 1986. Edmonton, Canada Pergamon Press.

Veza, J. M., Ortiz, M., Sadhwani, J. J., Gonzalez, J. E., Santana, F. J. Measurement of biofouling in seawater: some practical tests. *Desal*., **2008**, *220*(1), 326-334.

Veerapaneni, S. V.; Klayman, B.; Wang, S., Bond, R. *Desalination Facility Design and Operation for Maximum Efficiency*. 2011, Water Research Foundation: Denver, CO.

von Gunten, U. Ozonation of drinking water: Part I. Oxidation kinetics and product formation. *Wat. Res.* **2003,** *37(7):* 1443–1467.

Voutchkov, N. *Seawater Pretreatment*. Water Treatment Academy, Bangkok, 2010.

Vrouwenvelder, J.S.; Manolarakis, S.A.; Veenendaal,, H.R.; van der Kooij, D. Biofouling potential of chemicals used for scale control in RO and NF membranes. *Desal*, **2000**, *132(1–3),* 1–10.

Vrouwenvelder, J. S. & Van Der Kooij, D. Diagnosis, prediction and prevention of biofouling of NF and RO membranes. *Desalination.* **2001,** *139,* 65–71.

WateReuse Association. 2011 *Seawater Desalination Costs*. White paper of the WateReuse Association. WateReuse Association, Alexandria, VA.

Weinberg, H., Glaze, W., Krasner, S., Sclimenti, M. Formation and removal of aldehydes in plants that use ozonation. *Journal* AWWA. **1993**, *85,* 72-85.

Weinrich, L. A.; Giraldo, E.; LeChevallier, M. W. Development and application of a bioluminescence-based test for assimilable organic carbon in reclaimed waters. *App. Env. Microb*. **2009,** *75,* 7385–7390.

Weinrich, L.A.; Haas, C. N., LeChevallier, M. W. Recent advances in measuring and modeling reverse osmosis membrane fouling in seawater desalination: a review. *J. of Water Reuse and Desal*. **2013**, *3*(2), 85-101.

Weinrich, L.A.; Schneider, O.D.; LeChevallier, M.W. Bioluminescence-based method for measuring assimilable organic carbon in pretreatment water for reverse osmosis membrane desalination. *App. Env. Microb*. **2011**, *77*, 1148–1150.

Wells, M. L., & Goldberg, E. D. Colloid aggregation in seawater. *Marine Chemistry*, **1993**. *41*(4), 353-358.

Wells, M.L. & Goldberg, E. D. Occurrence of small colloids in sea water. *Nature*. **1991**. *353*(6342): 342-344.

Yang, H.-L., J.C.-T. Lin, and C. Huang, Application of nanosilver surface modification to RO membrane and spacer for mitigating biofouling in seawater desalination. *Wat. Res*., **2009**. *43*(15): 3777-3786.

Yu, Y.; Lee, S.; Hong, S. Effect of solution chemistry on organic fouling of reverse osmosis membranes in seawater desalination. *J. of Mem. Science*. **2010,** *351, 205–213.*

Yuan, W. & Zydney, A. L. Effects of solution environment on humic acid fouling during microfiltration. *Desal.* **1999,** *122(1),* 63–76.

Zhang, M., et al., Composition and variability of biofouling organisms in seawater reverse osmosis desalination plants. *App. Env. Microb.* **2011**. *77*(13): 4390-4398.

Zhu, X. & Elimelech, M. Fouling of reverse osmosis membranes by aluminum oxide colloids. *J. Environ. Eng.* **1995,** *121***,** 884–892.

APPENDIX A

AOC PROCEDURE

The seawater assimilable organic carbon (AOC) test was published in Applied and Environmental Microbiology, 2011, pp. 1148–1150 (doi:10.1128/AEM.01829-10). The following summary of the materials and procedures is provided for an overview with particular focus on preparation of the standard curve solutions for operations and laboratory staff interested in using the application for monitoring AOC in their facilities.

Principle: The biological fouling potential of seawater was evaluated through the application of a predictive tool, the seawater AOC test in which the maximum biomass density of an inoculum is measured in a pasteurized water sample. Pasteurization inactivates native microflora so nutrients are not depleted by other organisms. The test organism is a heterotrophic, nutritionally diverse, bioluminescent marine organism, *Vibrio harveyi*. *V. harveyi* exhibits constitutive luminescence, an attribute that facilitates a proportional relationship between light produced and biomass; in which biomass results in assimilation of available substrate, (i.e., AOC). The growth of *V. harveyi* follows Monod bacterial growth kinetics, and maximum growth (N_{max}) occurs during the stationary phase when maximum biomass is produced following depletion of available substrate. Standard curves are used to convert N_{max} luminescence units into µg acetate carbon equivalents per L (µg C/L). A series of standard curves are prepared to confirm reproducibility in the laboratory. Once established, blank, yield, and growth controls may be used for quality control per set of analyses. Minimizing carbon carryover or bacterial contamination should be carefully controlled. Laboratories equipped with clean preparation areas and a laminar flow hood would facilitate appropriate contamination control. If not available, additional procedural controls to reduce and monitor contamination will be necessary.

Apparatus

1. Luminometer: programmable, photon-counting microplate reader such as SpectraMax L (Molecular Devices, LLC, Sunnyvale, CA) operated using SoftMax® Pro software v5.4. Readings were reported in relative light units, defined as the integral of the photon count versus the time-reaction curve. Units were considered to be relative because the formula can be modified manually, which added to the ease of data monitoring and reporting. The software was programmed for automated reading of the samples in the microplate wells with a chamber temperature of 30°C. Settings were adjusted for fast kinetic integration (1 second) over 30 second intervals. Data analysis and automated calculations were adjusted by the user from SOFTMax® Pro exports in spreadsheet processing software. The average luminescence values for replicates were monitored until maximum growth was reached (further description under the standard curve section).

2. 96-Well plates: Microlite™ 1+ Flat bottom (Thermo Milford, MA, part number 7571) or similar 96-well opaque, white, polystyrene microplates with very-low cross talk. Plates were covered using an adhesive sealing film during analysis.

3. Sampling vessels: Organic carbon-free borosilicate glass vials (45 mL capacity) with tetrafluoroethylene-lined silicone septa. Vials were rendered free of organic-carbon through washes with 2% Citrajet® (Alconox, White Plains, NY), drying, and muffling at 550°C in a furnace for 6 hours. Closures were detergent washed, then soaked overnight in 10% hydrochloric acid (American Chemical Society Grade, EMD Chemicals, Gibbstown, NJ) and rinsed three times with Milli-Q water, dried, then autoclaved. Optional: AOC-free, precleaned sub-sample vials (Scientific Specialties Inc., 2000 class, part number 276720).

4. Stock preparation vessel: Screw thread, graduated, borosilicate glass bottles (250 mL capacity) were used for the preparation of the reagents and the *V. harveyi* culture. Caps were

black polypropylene welded to a polytetrafluoroethylene (PTFE) /silicone liner (Kimble Chase Supplier No. 61110P-250). The PTFE/silicone liner eliminates the possibility of glue contamination to bottle contents.

5. Hot water bath capable of achieving and holding 70°C.

6. Micropipettes: adjustable volume, capable of delivering volumes between 10 to100 µL and 100 to 1000 µL.

***Vibrio harveyi* stock and reagent solutions**

1. *V. harveyi*: ATCC® 700106™; American Type Culture Collection, Manassas, VA. Stock was propagated according to product sheet directions. A reference stock was stored at -80°C in marine broth and 10% glycerol. From the reference stock, a refrigerated inoculum stock was prepared for each analysis set and enumerated before sample testing. Enumeration was conducted by spreading 0.1 mL of the refrigerated stock onto marine agar plates. Dilutions were necessary to achieve plate counts in the 30 to 300 cfu range. Typical stock solutions were 1 x 10^7 cfu/mL.

a. Refrigerated inoculum stock was prepared by streaking the frozen stock onto a marine agar plate incubated at 30°C (overnight, ~18 hours). A single colony was then inoculated into a sterile saline buffer containing acetate-carbon (1X M9 salts [BD and Co., Sparks, MD] in 1000 mL laboratory grade water with 2% sodium chloride, 0.1 mM $CaCl_2$, and 1.0 mM $MgSO_4$ and adjusted to pH 7.2, fortified with 2 mg of acetate-carbon/L) and incubated at 30°C. The stock was then enumerated and stored in the refrigerator for the inoculation of water samples. Stocks were stable up to 1 month.

b. Marine agar plates (for enumerating *V. harveyi* stock) prepared by dissolving the following in laboratory grade water (per liter): 10 g peptone, 5 g yeast extract, 15 g agar (BD and Co., Sparks, MD), and 20 g sodium chloride (EMD Chemicals, Gibbstown, NJ). The agar was

heated with frequent agitation, boiled for 1 minute to completely dissolve the additives, and then autoclaved at 121°C for 15 minutes, cooled to 50°C, and poured into petri dishes; as an alternative, premade plates may be used.

Standard Curve:

Approach: Using 40-mL, carbon-free sampling vessels, 20 mL of the saline buffer was fortified with acetate-carbon working solution (20 mg/L) and then inoculated with 10^3 cfu/mL of *V. harveyi* stock inoculum. Solutions were mixed to distribute cells and 300 µL was then immediately transferred into replicate wells in the microplate. The microplate was covered with adhesive film and put into the luminometer. Luminescence is measured immediately and then at predetermined intervals until maximum growth during the stationary-growth phase is reached (Figure A1). The regression line produced for acetate-carbon concentration versus maximum luminescence was used for converting environmental sample luminescence into acetate carbon equivalents (Figure A2). Depending on the frequency of readings, an average of the stationary growth phase readings may be used for construction of the standard curve. As an alternative, the Monod model may be applied to determine substrate maximum and growth rates.

b. A 2000-mg/L stock solution of acetate-carbon was prepared by adding 113 mg of sodium acetate (ACS grade; Mallinckrodt, Paris, KY) to 100 mL of Milli-Q water. The acetate carbon stock was then sterile filtered into an autoclaved borosilicate bottle by using an Acrodisc syringe filter 0.2- µm HT Tuffryn membrane (PALL, East Hills, NY) and a 10-mL Luer-Lock-tip syringe (BD, Franklin Lakes, NJ). This stock was stored up to 6 months at 4°C and used for preparing standard curves and positive controls.

c. Standard curve test solutions were prepared by adding the requisite volume of acetate stock to sterile saline buffer (1X M9 salts in 1000 mL laboratory grade water with 2% sodium chloride, 0.1 mM $CaCl_2$, and 1.0 mM $MgSO_4$ and adjusted to pH 7.2) at concentrations ranging

from 10 to 1000 µg acetate-C/L. Instead of this saline buffer, alternative solutions such as a seawater or marine mix for aquarium applications may be used, although these sources may have impurities that should be considered.

Sample analysis

a. Samples were collected in 40 mL vials and pasteurized for 30 minutes once the temperature of the proxy reached 70°C. After pasteurization, the cooled samples were analyzed as soon as possible; in some cases, samples were stored at 4°C for no longer than 1 week. Half of the aliquot from the collection vessel was reserved (20 mL) and inoculated with 10^3 cfu/mL *V. harveyi* from the refrigerated inoculum stock. Solutions were mixed to distribute cells, and 300 µL was then immediately transferred into replicate wells in the microplate. Once all were transferred, the microplate was covered with adhesive film, and luminescence was measured immediately and then at predetermined and programmed intervals (e.g., 4 hours) until maximum growth during the stationary-growth phase is reached.

b. Quality control: Because the method produces a bacterial growth curve, sample toxicity is readily apparent from very low or decreasing luminescence over time in the inoculated samples. For confirmation of bacterial activity per set of analyses, controls are to be analyzed in the same manner described in the procedure section. Negative controls should show little or no luminescence increase over time. Positive controls containing 100 µg acetate/L will have the appropriate luminescence response.

Figure A2 Luminescence during Vibrio harveyi growth phases measured on SpectraMax L (Molecular Devices, LLC).

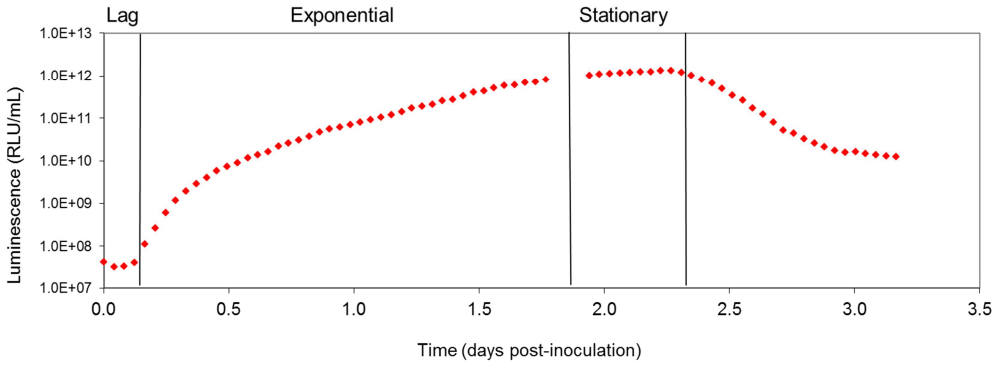

Figure A3 Standard curve of maximum stationary phase luminescence for *V. harveyi* for acetate-carbon concentrations.

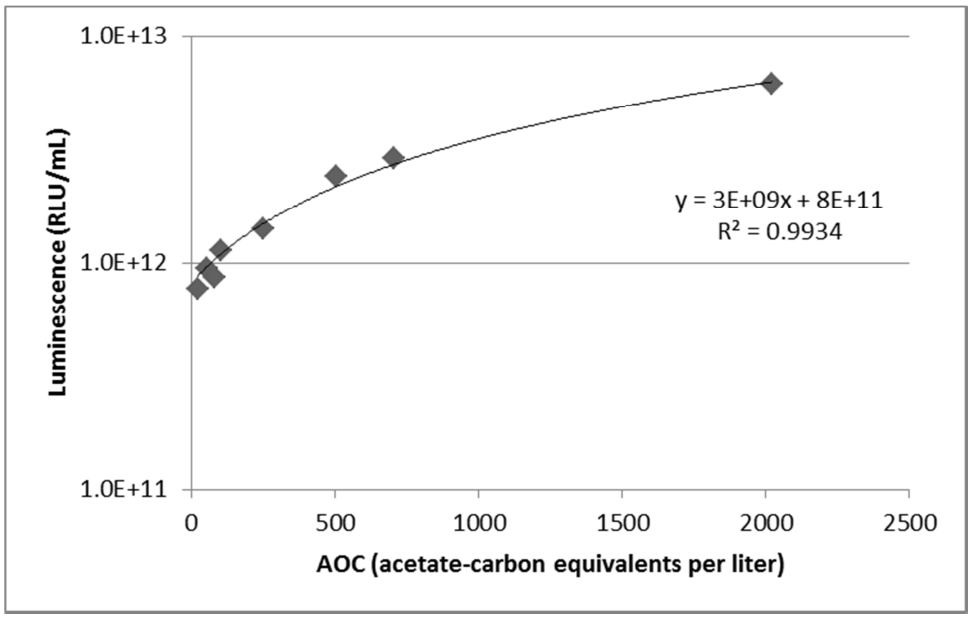

VITA

Lauren Ann Weinrich grew up in Pennsylvania in a suburb of Philadelphia where her interest in nature was cultivated from an early age. She was a Clare Boothe Luce scholar at Marymount University in Arlington, Virginia and majored in Biology with a concentration in Environmental Science. She graduated in 2002 with her Bachelor of Science (B.S.) degree. She was drawn to the challenges and rewards of research and continued her education at the University of North Carolina - Chapel Hill. She graduated in 2005 with a Master of Science (M.S.) in Environmental Science and Engineering; her research focused on disinfection byproducts in drinking water and analytical chemistry. In 2005 she returned to the Northeast and began her career at American Water. For 10 years she has continued her passion for researching drinking water challenges in the Innovation and Environmental Stewardship Department. She began the pursuit of a Doctor of Philosophy (Ph.D.) degree in Environmental Engineering at Drexel University, Philadelphia in 2010. Her research quantified the assimilable organic carbon fraction partially responsible for biological fouling on seawater reverse osmosis membranes and was funded through the WateReuse Research Foundation (WRRF-11-07).

Professional Activities and Publications

2013 – 2016, Council member for Philadelphia Chemists Committee, American Chemical Society.
2012 – Present, Organizer of Water Quality Symposia, PittCon Conference & Exposition.
2011 – Present, Chair of Standard Methods Joint Task Group; Section 9217 Assimilable Organic Carbon.
2011 – Present, Delegation president Water Management; German-American Chamber of Commerce.
2005 – Present, Member of American Chemical Society (ACS).
2003 – Present, Member of American Water Works Association (AWWA).

Weinrich, L.A., C. N. Haas and M.W. LeChevallier. 2013. “Recent advances in measuring and modeling reverse osmosis membrane fouling in seawater desalination: a review” Journal of Water Reuse and Desalination. 03.2: 85 – 101.
Weinrich, L. A., O. Schneider, E. Giraldo, and M. W. LeChevallier. 2011. Bioluminescence-based method for measuring assimilable organic carbon in pretreatment water for reverse osmosis membrane desalination. Applied and Environmental Microbiology. 77:1148 – 1150.
Weinrich, L.A., P.K. Jjemba, E. Giraldo, and M.W. LeChevallier. 2010. Implications of organic carbon in the deterioration of water quality in reclaimed water distribution systems. Water Research. 44: 5367 – 5375.
Weinrich, L.A., E. Giraldo, and M.W. LeChevallier. 2009. Development and application of a bioluminescence-based test for assimilable organic carbon in reclaimed waters. Applied and Environmental Microbiology. 75:7385-7390.